

Hydrogen / deuterium exchange reactions: small variations for heavy changes

Cumulative Dissertation

to acquire the academic degree
doctor rerum naturalium (Dr. rer. nat.)
of the Faculty of Mathematics and Natural Sciences
at the University of Rostock

Submitted by Florian Bourriquen, born on 3rd June 1995 in Paris XII

Rostock, 12.12.2022

The present work was accomplished at the Leibniz-Institute for Catalysis e.V. at the University of Rostock, at the chair for Applied Catalysis in the research group of Prof. Dr. Matthias Beller during the period from January 2020 to December 2022.

Reviewer #1: Prof. Dr. Matthias Beller

Leibniz-Institut für Katalyse e.V.
Angewandte Homogenkatalyse
Albert-Einstein-Straße 29a
18059 Rostock

Reviewer #2: Prof. Dr. Manuel van Gemmeren

Christian-Albrechts-Universität zu Kiel
Room 322
Otto-Hahn-Platz 4
24118 Kiel

Year of the submission to the faculty: 2022

Year of the oral defence: 2023

Statement of Authorship

I hereby affirm that I have written the present work by myself without outside assistance. No other resources were utilised than stated. All references as well as verbatim extracts were quoted, and all sources of information were specifically acknowledged.

Ich versichere hiermit an Eides statt, dass ich die vorliegende Arbeit selbstständig angefertigt und ohne fremde Hilfe verfasst habe. Dazu habe ich keine außer den von mir angegebenen Hilfsmitteln und Quellen verwendet und die den benutzten Werken inhaltlich und wörtlich entnommenen Stellen habe ich als solche kenntlich gemacht.

Rostock,

Florian Bourriquen

Acknowledgments

First and foremost, I would like to thank my supervisor **Prof. Matthias Beller** for welcoming me in his group. Thank you for the opportunity to thrive in remarkable working conditions, for your guidance on the numerous and diverse topics you allowed me to work on. Your prompt replies and your constant enthusiasm were always sources of motivation.

Thank you to **Dr. Kathrin Junge** for accepting me in the Redox Group and for providing me with a place to work for the past three years. I am grateful for the pleasant atmosphere while sharing your office and for your advice in and out of the lab.

The financial support from the European Union through the **FLIX** project which funded my PhD has to be recognised, as I would not have been in Rostock and could not have done any of this work without it. Similarly, thank you to everyone at LIKAT who made everything possible: the analytical, purchasing, and technical teams, as well as the secretariat.

I also would like to acknowledge **Dr. Wu Li** for guiding me in the lab when I started. Thank you so much for teaching me about heterogeneous catalysis and letting me join your challenging projects starting from day one. Thank you as well for your contribution to the review! Speaking of the writers of the review, it is impossible not to mention **Dr. Sara Kopf**. Our discussions on isotopic labelling were always fruitful, and so was the renowned Deuteration Newsletter, thank you for that!

My next thanks go to my other lab-mates Svenja, Helen, Niklas, Katja, Andrea, Peter, and Jannik. Thank you for all the laughs, good mood and good times in the office and the lab. I am going to miss our Friday-afternoon playlist. An extended recognition to all the members of the Redox Group (and neighbouring labs), namely, Shuxin, Johannes, Caro, Sebastian, Dennis, Veronica, Thomas, David, Leandro, Pavel, Ruiyang, Julien, Haifeng, Zupeng. Thank you for the support, discussions, and pleasant lunches and cake breaks together.

A special appreciation to the readers of my thesis, Prof. Matthias Beller, Dr. Kathrin Junge, Dr. Peter McNeice, Dr. Sara Kopf and (soon to be Dr.) Shuxin Mao.

Lastly, I wish to thank my family and all the friends I made along the way. En particulier, un immense merci à mes parents, Sabrya et Pascal, ainsi qu'à mon frère Yanis. Merci d'avoir été là pour moi, de m'avoir toujours soutenu et de m'avoir donné l'opportunité d'arriver où je suis aujourd'hui. Tout cela n'aurait pas été possible sans vous.

Summary

This dissertation reports the development of new catalytic methodologies for deuterium incorporation into organic molecules. In a first part, the use of a simple Lewis acid is reported for the isotopic labelling of electron-rich (hetero)arenes. Next, two original heterogeneous catalysts are presented for the labelling of comparable compounds: a first-generation iron-based system and a follow-up work using manganese. Both materials are easily prepared and fully characterised. Additionally, investigations were performed to gain insight on the mechanisms. In particular, all of these systems rely on base metals, which are of key interest due to their high abundances, low prices and minimal toxicity in comparison to noble metals. Furthermore, for all these methodologies, deuterium oxide (D_2O), the most affordable and easy-to-handle deuterium source was used.

Zusammenfassung

Diese Dissertation befasst sich mit der Entwicklung neuartiger katalytischer Methoden zur Deuterierung organischer Moleküle. Im ersten Teil wird der Gebrauch einer einfachen Lewis-Säure zur Isotopenmarkierung elektronenreicher (Hetero)arene behandelt. Anschließend werden zwei heterogene Katalysatoren zur Isotopenmarkierung vergleichbarer Verbindungen vorgestellt: ein System der ersten Generation auf Eisenbasis sowie eine Folgearbeit unter der Verwendung von Mangan. Beide Materialien sind einfach herzustellen und wurden vollständig charakterisiert. Weiterhin wurden Untersuchungen zu den jeweiligen Reaktionsmechanismen durchgeführt. Alle vorgestellten Katalysatorsysteme basieren auf unedlen Metallen, welche aufgrund ihrer hohen Verfügbarkeit, ihres niedrigen Preises sowie ihrer im Vergleich zu Edelmetallen geringen Toxizität von besonderem Interesse sind. Darüber hinaus wurde für alle diese Methoden Deuteriumoxid (D_2O), die günstigste und am einfachsten zu handhabende Deuteriumquelle, verwendet.

Table of contents

1. Introduction	1
1.1. Interests in, and uses of deuterated compounds	2
1.2. Methodologies for the deuterium labelling of organic molecules.....	3
1.2.1. Deuterated building blocks and common reagents	6
1.2.2. Homogeneous catalysis	6
1.2.2.1. Reductive deuteration.....	7
1.2.2.2. Acid/base + Lewis acid catalysis	9
1.2.2.3. Aromatic metal-catalysed HIE.....	10
1.2.2.4. Aliphatic metal-catalysed HIE	13
1.2.3. Heterogeneous catalysis	15
1.2.3.1. Acid/Base catalysis.....	15
1.2.3.2. Reductive deuteration.....	15
1.2.3.3. Noble Metals	16
1.2.3.4. Non noble metals.....	21
2. Objectives of this work	23
3. Summary of publications.....	24
3.1. Recent developments for the deuterium and tritium labeling of organic molecules	24
3.2. Homogenous iron-catalysed deuteration of electron-rich arenes and heteroarenes ..	25
3.3. Scalable and selective deuteration of (hetero)arenes.....	29
3.4. Manganese-catalysed deuterium labelling of anilines and electron-rich (hetero)arenes	34
4. Conclusion and perspectives	40
5. References	41
6. Selected publications	53
7. Appendix.....	77
7.1. Further publications.....	77
7.2. List of publications	78
7.3. Conference participations	78

Table of figures

Figure 1. Number of publications referenced in the search engine SciFinder containing the word “deuterium” per year between 1931 and 2021.....	1
Figure 2. Illustration of the uses of deuterated organic compounds.	2
Figure 3. Timeline of methodologies for deuterium incorporation.	24
Figure 4. Evaluation of various Lewis acids for the deuterium labelling of 1,2,3,4-tetrahydroquinoline.	25
Figure 5. Kinetic profile for the deuterium labelling of 1,2,3,4-tetrahydroquinoline.....	27
Figure 6. High resolution ABF-STEM (left) and HAADF-STEM (right) images of an Fe particle of Fe@Cellulose-1000.	30
Figure 7. Recycling experiments of Fe@Cellulose-1000 under hydrogen and nitrogen atmospheres.....	32
Figure 8. Screening of metals using starch as carbon source for the labelling of <i>para</i> -anisidine.	35
Figure 9. Left: HAADF-STEM images of freshly prepared Mn@Starch-1000 (a, b) and used Mn@Starch-1000 after one run of deuteration of <i>para</i> -anisidine (c, d). Right: XPS Mn 3s spectra of the fresh (e) and recycled catalyst (f).....	36

Table of schemes

Scheme 1. Main approaches for isotopic labelling.	4
Scheme 2. Synthesis of β -ionone- d_6 , acylation and reduction with deuterated reagents.	7
Scheme 3. Selected examples of photo- and electrocatalysis.....	8
Scheme 4. Selected examples of deuterodehalogenation.....	9
Scheme 5. Brønsted acid, superbasic, and Lewis acid catalysis for deuterium labelling.	10
Scheme 6. Crabtree, Kerr, and Tamm catalyst families for HIE. Typical reaction conditions and directing groups are shown.....	11
Scheme 7. Template-directed <i>meta</i> -labelling.	12
Scheme 8. Iron complexes for undirected labelling.	13
Scheme 9. Aliphatic labelling via transfer hydrogenation.	14
Scheme 10. Aliphatic labelling <i>via</i> photocatalysis.	14
Scheme 11. Reductive deuteration of Br ₂ -DPA-714.	16
Scheme 12. Porous CdSe for photocatalytic deuteration.	16
Scheme 13. Pt/C and Pd/C for deuterium labelling.	17
Scheme 14. Benzylic deuteration with PdNp@PVP.	18
Scheme 15. Ru/C for deuterium labelling.....	18

Scheme 16. Tuned reactivity of Ru/C for deuterium labelling.	19
Scheme 17. RuNp@PVP for isotopic labelling.	19
Scheme 18. Heterogeneous iridium for isotopic labelling.	20
Scheme 19. Heterogeneous rhodium for isotopic labelling.	20
Scheme 20. Mixed ruthenium:iridium nanoparticles for isotopic labelling.	21
Scheme 21. Heterogeneous nickel for isotopic labelling.	22
Scheme 22. Summary of this work.	23
Scheme 23. Selected scope entries for the iron triflate-mediated labelling methodology.	28
Scheme 24. Synthesis and HIE application of Fe@Cellulose-1000.	29
Scheme 25. Proposed catalytic cycle for the Fe@Cellulose-1000 methodology.	31
Scheme 26. Selected scope entries for the Fe@Cellulose-1000 methodology.	33
Scheme 27. Control experiments – Kinetic isotope effect.	38
Scheme 28. Selected scope entries of the Mn@Starch-1000 methodology.	39

Table of tables

Table 1. Prices of common deuterium sources.	5
Table 2. Comparison of homogeneous and heterogeneous transition metal catalysis.	6
Table 3. Variation of the catalyst loading and D ₂ O amount.	26
Table 4. Deuterium labelling at higher temperature.	27
Table 5. Design of quality experiments for the labelling of 4-phenylmorpholine.	31
Table 6. Catalyst screening for the deuteration of <i>para</i> -anisidine as model substrate.	34
Table 7. Optimisation of reaction conditions for the labelling of <i>para</i> -anisidine with Mn@Starch-1000.	37

List of abbreviations

4CzIPN	1,2,3,5-Tetrakis(carbazol-9-yl)-4,6-dicyanobenzene
ABF	Annular Bright Field
Ac	Acyl
acac	Acetylacetone
Ad	Adamantyl
ADME	Absorption Distribution Metabolism Excretion
Ar	Aryl
BAr^{F-}	Tetrakis(3,5-bis(trifluoromethyl)phenyl)borate
Boc	<i>tert</i> -Butyloxycarbonyl

Bu	Butyl
COD	Cycloocta-1,5-diene
Cy	Cyclohexyl
D	Deuterium
DCM	Dichloromethane
DG	Directing Group
DIPEA	<i>N,N</i> -Diisopropylethylamine
DMA	Dimethylacetamide
DMF	Dimethylformamide
DMPO	5,5-Dimethyl-1-pyrroline <i>N</i> -oxide
DMSO	Dimethylsulfoxide
e.g.,	Example
EELS	Electron Energy Loss Spectroscopy
EPR	Electron Paramagnetic Resonance
eq.	Equivalent(s)
Et	Ethyl
FLPs	Frustrated Lewis Pairs
Gly	Glycine
h	hour
HAADF	High-Angle Annular Dark Field
HAT	Hydrogen Atom Transfer
HIE	Hydrogen Isotope Exchange
<i>i</i>	<i>iso</i>
ICP	Inductively Coupled Plasma
KIE	Kinetic Isotope Effect
LA	Lewis acid
LC	Liquid Chromatography
m	milli
Me	Methyl
MeOH	Methanol
Mes	Mesityl
mL	Millilitre
mmol	Millimole
MS	Mass Spectrometry
MTBE	Methyl <i>tert</i> -butyl ether
<i>n</i>	normal
NADH	Nicotinamide Adenine Dinucleotide Hydride

NHC	N-Heterocyclic Carbene
NMR	Nuclear Magnetic Resonance
NP	Nanoparticle
Np	Nanoparticles
NTf₂	Bis(trifluoromethane)sulfonimide
NWAs	Nanowire Arrays
OLED	Organic Light Emitting Diode
OTf	Trifluoromethanesulfonate
<i>p</i>-	<i>para</i>
PC	Photocatalysis
Ph	Phenyl
PMDETA	<i>N,N,N',N'',N'''</i> -Pentamethyldiethylenetriamine
PPh₃	Triphenylphosphine
ppm	parts-per-million
Pr	Propyl
PVP	Polyvinylpyrrolidone
py^tbpx	1,2-bis((<i>tert</i> -butyl(pyridin-2-yl)phosphanyl)methyl)benzene
R	Organic rest
RDS	Rate Determining Step
rt	room temperature
SD	Standard Deviation
SILS	Stable Isotope Labelled internal Standard
STEM	Scanning Transmission Electron Microscopy
<i>t</i>	<i>tert</i>
TBAI	Tetra- <i>n</i> -butylammonium iodide
TEMPO	2,2,6,6-Tetramethylpiperidinyloxy
THF	Tetrahydrofuran
TMP	2,2,6,6-Tetramethylpiperidide
u	Atomic mass unit
XAS	X-ray Absorption Spectroscopy
XPS	X-ray Photoelectron Spectroscopy
XRD	X-Ray Diffraction
μW	Microwave irradiation

Units of measurement

The International System of Units (SI) is utilised throughout this work to measure experimental or theoretical quantities. All derived units and their expression in terms of the SI base units are given below.

Quantity	Unit	Name	Conversion to SI base units
Temperature	°C	degree Celsius	$T/K = T/^\circ\text{C} - 273.15$
Volume	mL	millilitre	$1 \text{ mL} = 1 \text{ cm}^3 = 10^{-6} \text{ m}^3$
Energy	J	joule	$1 \text{ J} = 1 \text{ m}^2 \cdot \text{kg} \cdot \text{s}^{-2}$
	eV	electronvolt	$1 \text{ eV} = 1.602 \cdot 10^{-19} \text{ J}$
Time	h	hour	$1 \text{ h} = 3600 \text{ s}$
	min	minute	$1 \text{ min} = 60 \text{ s}$
Pressure	Pa	pascal	$1 \text{ Pa} = 1 \text{ kg} \cdot \text{m}^{-1} \cdot \text{s}^{-2}$
	bar	bar	$1 \text{ bar} = 10^5 \text{ Pa}$
Capacitance	F	farad	$1 \text{ F} = \text{kg}^{-1} \cdot \text{m}^{-2} \cdot \text{s}^4 \cdot \text{A}^2$

1. Introduction

Hydrogen is the lightest chemical element constituted simply of one proton and one electron. It is the most abundant in the universe, estimated to represent 90% of all atoms.^[1] Differing by an additional neutron, a hydrogen isotope of mass number 2 was discovered in 1931 and named “deuterium” by Harold C. Urey.^[2] Highlighting the importance of this discovery, Urey was awarded the Nobel Prize in chemistry in 1934 “for his discovery of heavy hydrogen”.^[3] Clearly, the fundamental difference between protium^[4] and its rare isotope (0.015% abundance) deuterium is the atomic mass.^[5] In fact, with almost a 100% increase from 1.008 u to 2.014 u, the mass difference between hydrogen isotopes is greater than those of any other elements. This leads to vastly different properties in compounds containing deuterium rather than protium. The change is particularly striking when the lowered vibrational frequencies of carbon-deuterium bonds vs. carbon-protium bonds are observed.^[6] Consequently, bonds involving a deuterium atom exhibit lower zero-point energy (by 1.2–1.5 kcal/mol), thus, more energy is necessary to cleave C–D bonds compared to C–H bonds.^[7-8] This is referred to as the primary kinetic isotope effect (KIE) and rationalises numerous applications of deuterium-labelled compounds.

Research dealing with this isotope has been constantly increasing since Urey’s discovery, as illustrated in Figure 1. One particular field, and the topic of this thesis, is the incorporation of deuterium atoms into organic molecules in order to tune their properties.

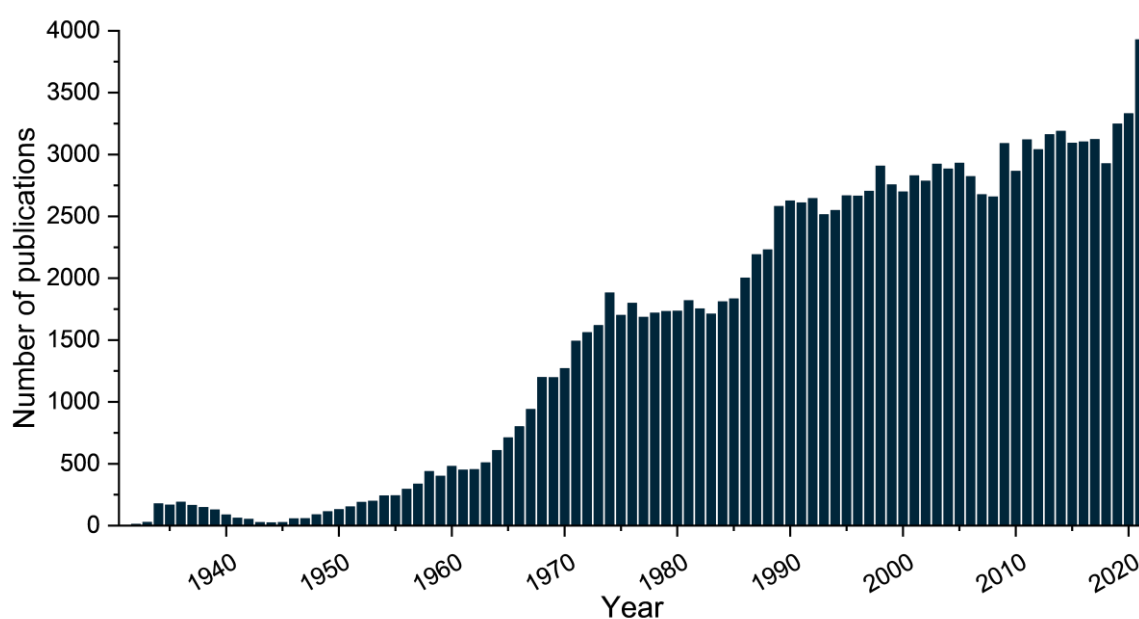


Figure 1. Number of publications referenced in the search engine SciFinder containing the word “deuterium” per year between 1931 and 2021.

1.1. Interests in, and uses of deuterated compounds

The main advantage of isotopically labelled organic molecules, is that small structural modifications can have a major impact upon the physical properties and biological activities.^[9] For example, assuming enough isotopes are incorporated (typically more than four), Stable Isotope Labelled internal Standards (SILSs) can be prepared, which are of paramount importance for LC-MS/MS applications.^[10-11] Indeed, the use of SILSs is a key technique for pharmacokinetics and metabolites investigations,^[12-17] as well as food and environment quantitative analyses.^[18-24] Furthermore, hydrogen/deuterium exchange mass spectrometry allows the investigations of more challenging biological systems. Here, examining the exchange rate of amide hydrogens in protein backbones permits the determination of high-order structures and systems dynamics.^[25-28] As hydrogen bonding significantly slows the exchange rate of backbone

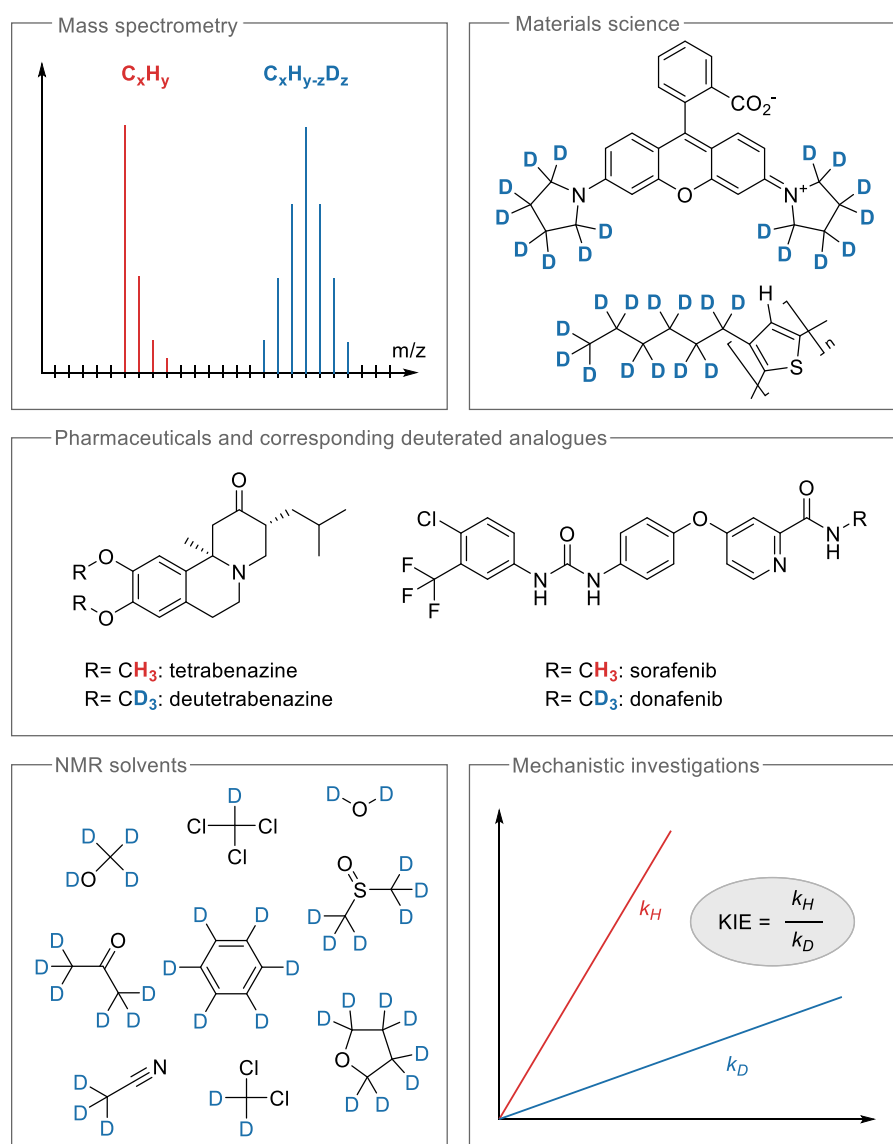


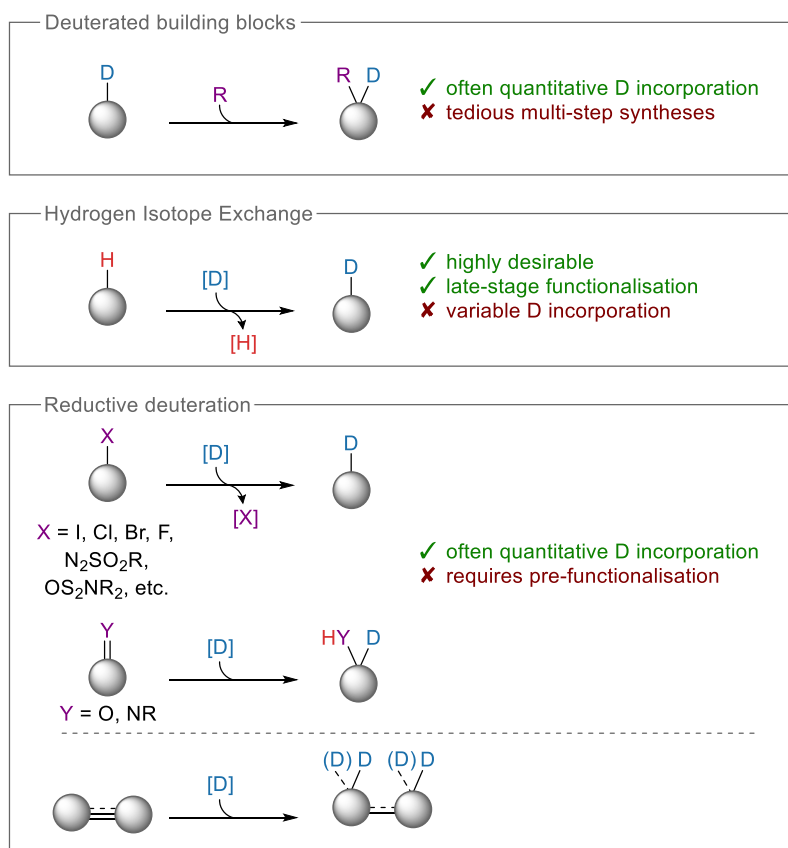
Figure 2. Illustration of the uses of deuterated organic compounds.

amide hydrogens, their analysis provides insight into the structure, hydrogen bonding strength, and conformational mobility of proteins. Taking advantage of the KIE, deuterium-labelled compounds are often applied to investigate reaction mechanisms: it is common to run chemical reactions with substrates labelled at positions susceptible to be involved in Rate-Determining Steps (RDSs), then monitor and compare the kinetic profiles of labelled vs. unlabelled compounds.^[29-31] Similarly, isotope-labelled substrates or reagents are utilised to track the position of deuterium incorporation in products (e.g. crossover experiments), thus providing further insights on reaction pathways.^[32-35]

Conversely to these analytical applications, deuterium-containing compounds are also end-products. For instance, perdeuterated molecules are routinely used by chemists as solvents for NMR spectroscopy. Besides, taking advantage of the KIE, deuterated compounds are a field of research in materials science, leading to OLEDs^[36-43], fluorophores^[44-46], or conducting polymers^[47-48] with tuned properties. Besides this, “*the most fruitful basis for the discovery of a new drug is to start with an old drug*” claimed the 1988 Nobel Prize laureate in medicine James Whyte Black.^[49] This approach is particularly true in the case of isotopic labelling, as replacing hydrogen atoms with deuterium ones can generate more metabolically stable pharmaceuticals. Indeed, due to the KIE, the absorption, distribution, metabolism, and excretion (ADME) properties of drugs and drug candidates can be adjusted.^[50-52] This is for example the case for drugs approved for human use like deutetrabenazine^[53] and donafenib^[54-55] (Figure 2). In fact, in the case of (deu)tetrabenazine, one key metabolic step involves the cleavage of (trideuterio)methoxy groups leading to inactive metabolites.^[56] This “simple” change of protiums for deuteriums allows for a less frequent daily dosing (two times a day instead of three) as well as a more favourable side effects profile.^[57-58]

1.2. Methodologies for the deuterium labelling of organic molecules

Due to the high demand for deuterated compounds, a broad “toolkit” of methodologies to incorporate deuterium atoms into organic molecules has been developed.^[59-74] Such approaches can be divided into three main categories. First, classic stoichiometric organic syntheses taking advantage of deuterated analogues of common organic reagents is possible. Here, the main advantage is the high deuterium content already present in the reagents (usually >99%) (Scheme 1, top). Yet, not only can such compounds be expensive, but one main drawback of this approach is the common loss of deuterium-labelled products during multi-step syntheses, especially if the label is incorporated in the early stages of a synthesis. To circumvent these limitations, Hydrogen Isotope Exchange (HIE) is the methodology of choice. In this late-stage functionalisation technique, protium atoms are (selectively) exchanged with deuterium ones.



Scheme 1. Main approaches for isotopic labelling.

This strategy is usually preferable as HIE can theoretically be implemented at any stage of a process, or even directly on a final compound, although it often requires specific optimisation as chemo- and regioselectivities can be challenging. Furthermore, HIE reactions often rely on reasonably priced isotope sources in comparison to deuterated building blocks. The deuterium incorporation obtained by HIE methodologies is however highly variable. Plus, starting materials and products are virtually impossible to separate, thus, the labelling is provided as the percentage of exchange. The third principal method is reductive deuteration, typically resulting in quantitative deuterium incorporations inherent to the mechanisms of such reactions. Although reductive deuteration of functional groups such as carbonyls, alkenes, and alkynes is observed, deuterodehalogenation is more frequently encountered. Substrate availability is the primary restriction for such reactions: even though aryl and alkyl halides are widely accessible as simple building blocks, pre-functionalisation steps (namely, the introduction of a halide) may be necessary for some complex compounds (Scheme 1).

As an illustration, Table 1^[31] presents a selection of deuterium sources and their corresponding prices. It should be mentioned that deuterium oxide (D₂O), being the parent of all the other, is the most affordable source of deuterium and hence the most desirable to use in HIE approaches to develop cost-efficient methodologies for the incorporation of this isotope.

Table 1. Prices of common deuterium sources.

Deuterium source	Price / mol (approximative) [€]
D ₂ O	15
CH ₃ OD	53
AcOD	75
DMSO- <i>d</i> ₆	100
CD ₃ OD	115
Acetone- <i>d</i> ₆	120
DCl (35% in D ₂ O)	200
D ₂	230
AcOH- <i>d</i> ₄	310
KOD (40 mol% in D ₂ O)	770
CD ₃ I	1020
NaBD ₄	1240
Ac ₂ O- <i>d</i> ₆	3000
LiAlD ₄	6720

The majority of the HIE methodologies are in fact catalysed reactions. In this field, both homogeneous (reaction mixture present in one phase) and heterogeneous (at least two phases) catalyses are equally important. A general comparison of these approaches is given in Table 2.^[75] From an industrial point of view, heterogeneous catalysis is usually preferred due to the facile separation of catalysts from reaction mixtures and potential recycling, although homogeneous catalysis often allows for a better selectivity. However, one should be cautious with these differentiations as for example some extremely selective heterogeneous catalysts are reported in HIE and other fields of chemistry. The following sections will discuss state-of-the-art methodologies for deuterium incorporation into organic molecules. As this thesis presents results of both heterogeneous and homogeneous catalyses for HIE, important developments of each will be shown. In the interest of completeness, some applications of deuterated building blocks are briefly presented.

Table 2. Comparison of homogeneous and heterogeneous transition metal catalysis.

Criteria	Heterogeneous catalysis	Homogeneous catalysis
Active centres	Only the surface atoms	All the metal atoms
Catalyst activity	Variable	High
Catalyst reproducibility	Difficult	Very high
Catalyst selectivity	Poor	High
Catalyst stoichiometry	Undefined	Defined
Catalyst structure	Undefined	Defined
Catalyst variability	Little	High
Conditions	Harsh	Mild
Deactivation through poisoning	Common	Rare
Diffusion problems	Present	Rare
Mechanism knowledge	Very little	Known
Separation and recycling	Simple	Difficult

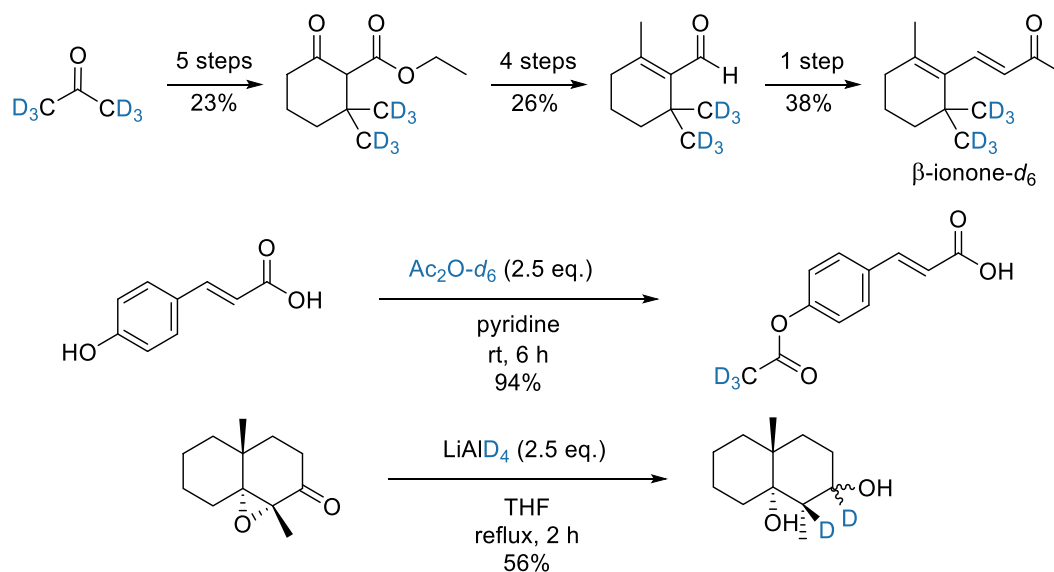
1.2.1. Deuterated building blocks and common reagents

As mentioned above, the use of deuterated starting materials is scarce in comparison to HIE reactions. Nevertheless, such reports exist when a specific target is necessary, often for SILSs applications. As an illustration, the preparation of β -ionone- d_6 is feasible starting from the NMR solvent acetone- d_6 .^[76] With an overall yield of 2% for 10 steps, it is clear that most of the initial deuterium atoms are lost during the synthesis (Scheme 2, top). In a similar vein, CD_3I ,^[77-80] CD_3Li ,^[81] $LiAlD_4$,^[82-85] $NaBD_4$,^[86-88] $NaBD_3CN$,^[89] CD_2O ,^[87, 89-91] DCO_2H ,^[92] Ac_2O-d_6 ,^[93] etc. are reported as labelled analogues of organic reagents (Scheme 2, bottom). Comparably, it is evident that using the Wilkinson catalyst for olefin hydrogenation in the presence of D_2 gas will provide the corresponding deuterated alkane.^[94] However, one should bear in mind that such reagents are not only severely expensive (e.g., 6720 €/mol of $LiAlD_4$, see Table 1), but it should also be mentioned that deuterated analogues are not available for every chemical compound, hence the necessity of supplementary methodologies for deuterium incorporation. A selection of approaches is presented in the next chapters to provide an overview of the available techniques, their uses, and limitations.

1.2.2. Homogeneous catalysis

This section focuses on the methodologies for deuterium incorporation relying on homogeneous catalytic systems. In practice, homogeneous methodologies occupy the vast majority of

the available HIE techniques. Accordingly, for clarity it is easier to partition them into subcategories, namely reductive deuteration, acid/base and Lewis acid catalyses, aromatic metal-catalysed and aliphatic metal-catalysed HIE.

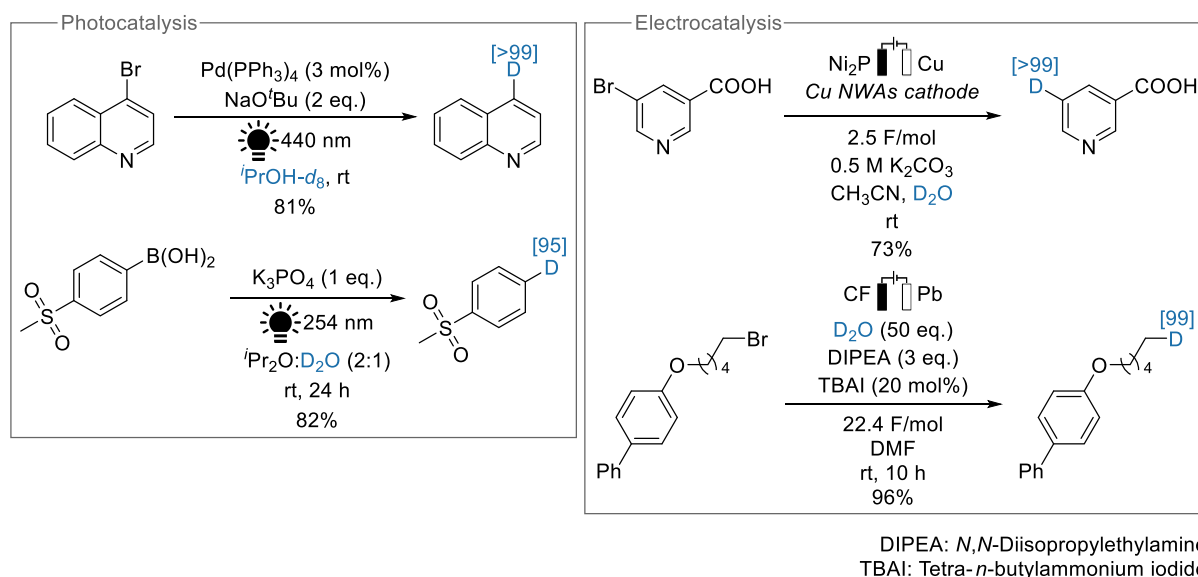


Scheme 2. Synthesis of β -ionone- d_6 , acylation and reduction with deuterated reagents.

1.2.2.1. Reductive deuteration

As mentioned in the introduction, reductive deuteration reactions usually induce quantitative deuterium incorporation. Reports of deuterodehalogenation, as well as reductive deuteration of functional groups and multiple bonds will be presented here.

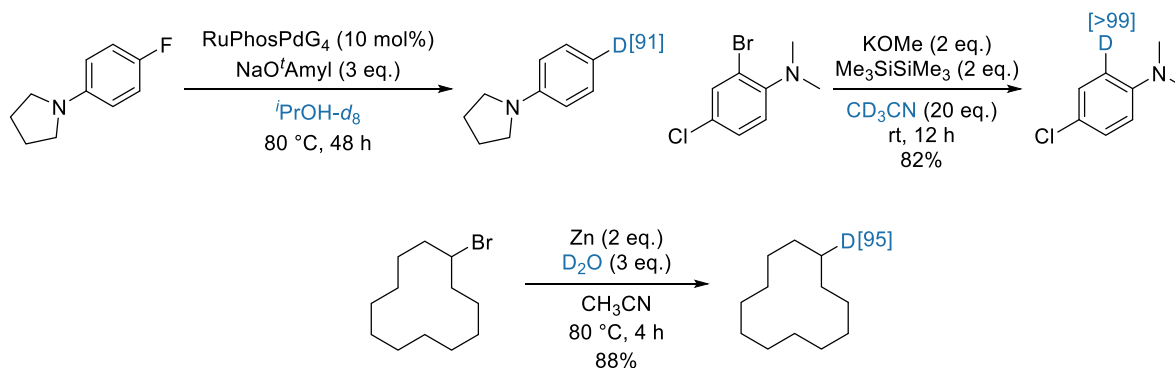
Popular approaches in this field are photocatalysis and electrocatalysis, allowing mild reaction conditions and excellent selectivities (Scheme 3). For the former, in most cases the solvent plays the role of isotope source. As an example, in Pd- or Ni-catalysed reactions, the reduction of aryl bromides and subsequent dissociation of the bromide atom led to aryl radicals that abstract deuterium atoms from the solvents.^[95-96] Similarly, in addition to haloaryls, vinyl bromides are efficiently reduced with organic photocatalysts.^[97] Other metal-free procedures deal with the reductive deuteration of aryldiazonium tetrafluoroborates^[98], arylazosulfones^[99] or arylboronic acids.^[100] Regarding the photoredox deuteration of aliphatic halides, enantioselective deuteration of azaarenes is reported *via* a carbanion intermediate which further reacts with a chiral phosphoric acid.^[101] In addition, 1-bromo-2-acetoxy sugars lead to a deuterium incorporation at the C2 position *via* a spin-centre shift.^[102] In terms of electrocatalysis, pioneering works from the 1970s, although using D_2O as isotope source, relied on toxic mercury electrodes, operated under harsh reaction conditions, and presented limited substrate scopes.^[103-105] Yet, with the progress of materials science resulting in new electrodes, such reactions were facilitated. In general, deuterium incorporation takes place with either the formation of a radical



Scheme 3. Selected examples of photo- and electrocatalysis.

followed by deuterium atom transfer from the isotope source, or further reduction to a carbanion which reacts with D^+ .^[106-107] Recent developments for instance make use of a palladium catalyst to generate electrophilic deuterides for deuteriobromination.^[108] In addition, a copper nanowire array cathode permitted the labelling of brominated and iodinated aryls.^[109] This report was complemented by another catalyst-free methodology earlier this year, this time focused on deuterium incorporation at more challenging unactivated aliphatic positions.^[110] Going away from photo- or electrocatalysis, further reactions make use of palladium-borane for the deuteriodechlorination of aryl substrates,^[111] copper for the monodeuteration of allylic chlorides,^[112] palladium for deuteriodefluorination,^[113] etc. Importantly, even though organic halides are commonly used as substrates (Scheme 4), possibly due to their broad availability, other reducible or leaving groups are reported to introduce deuterium atoms, for example the sulfamate^[114] and the pinacolborane moieties.^[115] In addition to these aromatic examples, cobalt catalysis allows the deuterioboronation of aryl and vinyl boronates.^[116] As an alternative for catalytic reactions, organohalides can be converted to the corresponding organometallic compounds (organozinc, organomagnesium) which can be further hydrolysed with deuterium oxide.^[117] Also without the aid of a metal catalyst, electron-rich and neutral (hetero)aryl iodides and bromides were dehalogenated in a practical and simple fashion using potassium methoxide and disilane in deuterated acetonitrile.^[118] Similarly, excellent yields of deuterated compounds are obtained from a phenalenyl potassium complex and $DMSO-d_6$.^[119]

Conversely, reductive deuteration can theoretically involve any reducible chemical function, not just halogens. Several papers, for example, deal with the transformation of carbonyl compounds into isotopically labelled groups. Bouveault–Blanc-type Single Electron Transfer reduction of esters in the presence of D_2O yielded α -deuterated alcohols. In this context, super



Scheme 4. Selected examples of deuterodehalogenation.

stoichiometric amounts of sodium dispersions or Kagan's reagent (SmI_2) afforded the desired products.^[120-122] These reductants were further applied for the reductive deuteration of amides,^[123] nitriles^[124-125] and oximes^[126]. Evidently, carbonyl reductions are feasible using catalytic methods, although reports are far less frequent. Notable results for deoxygenative deuteration of ketones take use of iridium catalysts with concomitant HIE at aromatic positions (see below for more details on homogeneous Ir-catalysed HIE),^[127] or simple palladium diacetate.^[128]

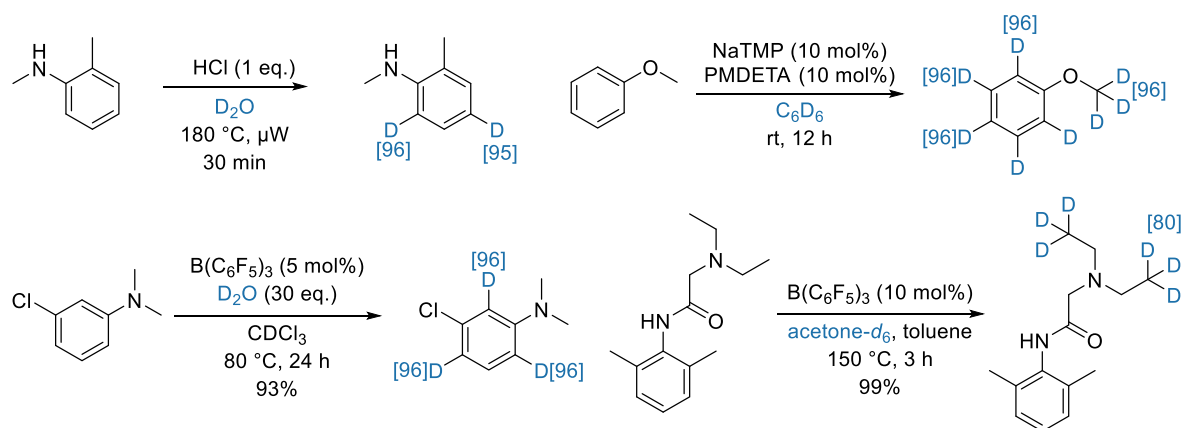
Instead of using D_2 as the isotope source, transfer deuteration from D_2O is reported with cobalt, although quantitative amounts of zinc were used as a reductant.^[129] With water-soluble ruthenium catalysts, ketones were reduced in aqueous media^[130] whereas imines required a biphasic (D_2O -toluene) system.^[131] To prepare deuterated *N*-tosylamines enantioselectively, a nickel-based system was used with the common Binapine ligand and isopropanol- d_8 as isotope source.^[132] In this case, the electron-withdrawing tosyl substituent was crucial to prevent imine tautomerism and achieve a high selectivity.

The reductive deuteration of olefins easily takes place in the presence of the Wilkinson catalyst and D_2 gas, as mentioned previously. Nevertheless, as avoiding the use of noble metals is a key interest in chemistry nowadays, the majority of the new reports deal with base-metals: copper,^[133] nickel,^[134] and iron,^[135] or boron.^[136-137] In terms of biocatalysis, the judicious choice of NADH-dependant reductases in the presence of adequate deuterated buffers is reported for highly chemoselective reductive deuterations: for instance benzylideneacetone was selectively deuterated either at the ketone or at the olefin position.^[138]

1.2.2.2. Acid/base + Lewis acid catalysis

Acid/base deuterium labelling requires either the substrate bearing acidic or basic positions or the use of an acid/basic catalyst (Scheme 5). For instance, in the case of substrates with acidic positions (typically aliphatic methylenes alpha to carbonyl groups) HIE takes place in refluxing D_2O even in the absence of catalysts. Multiple runs might however be necessary to attain high

isotopic enrichment. Strong Brønsted acids like HCl (or DCl),^[139-140] D₂SO₄,^[141] D₃PO₄,^[142] and HClO₄^[143] or strong bases such as NaOH,^[144] or ^tBuOK^[145] can also catalyse H/D exchange in arenes, although often high reaction temperatures, or microwave irradiation are required. On the contrary, so called “superbasic”^[146] or “superelectrophilic”^[147] species permit hydrogen/deuterium exchange at room temperature.



TMP: 2,2,6,6-tetramethylpiperidine
PMDETA: *N,N,N',N',N''*-pentamethyldiethylenetriamine

Scheme 5. Brønsted acid, superbasic, and Lewis acid catalysis for deuterium labelling.

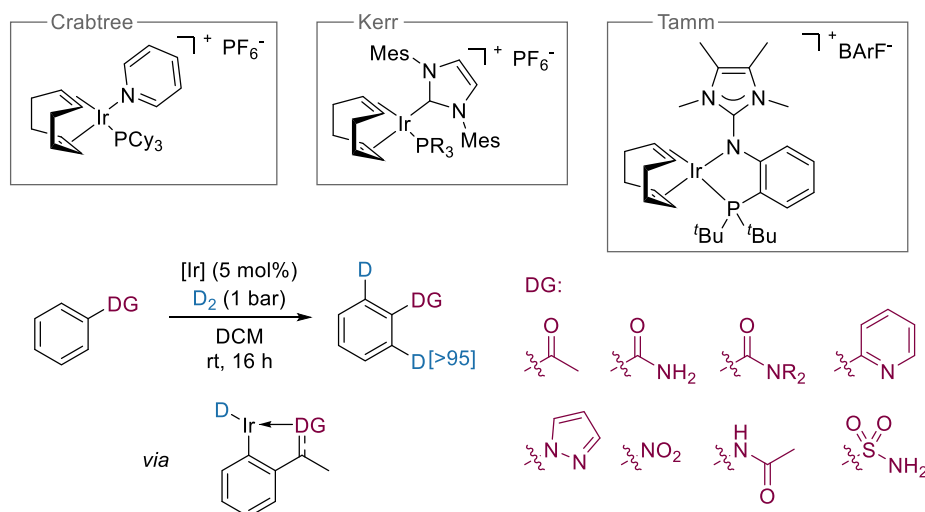
A broad variety of Lewis acids (LA) is also frequently used for HIE reactions. For nonpolar arenes, EtAlCl₂ is highly reactive, affording quantitative D incorporation from benzene-*d*₆ at room temperature.^[148] In fact, in 1975, a parallel was made between arene halogenating agents and potential HIE LA catalysts, leading to studies of elemental halides as catalysts.^[149-151] Yet the potential toxicity and instability of these reagents called for more accessible catalysts. For instance, it is known that the coordination of water to a LA weakens the O–H bond,^[152] hence, employing LAs in the presence of D₂O could generate an acidic D⁺. This approach was applied to the labelling of electron-rich arenes under B(C₆F₅)₃^[153] or silver catalysis.^[154] In combination with a Brønsted basic *N*-alkylamines and acetone-*d*₆, B(C₆F₅)₃ has also been reported for amine β-labelling *via* a deuterated ammonium intermediate.^[155]

1.2.2.3. Aromatic metal-catalysed HIE

First and foremost, it should be mentioned that aromatic HIE is arguably the more active research field for deuterium labelling, hence the existence of a plethora of methodologies to achieve diverse selectivities. In fact, approaches developed for C–H activation are often transferred to HIE, and the following examples represent only a small selection of the available methodologies.

Ortho selectivity. Homogeneous transition-metal catalysed hydrogen-isotope exchange has been a topic of interest since the early days of HIE.^[156-159] In particular, an efficient and easy

approach to direct HIE (and more generally C–H activation) processes is to exploit the Lewis basic ability of functional groups present on a substrate. These so-called directing groups (DG) will coordinate to a metal centre, orienting reactivity to neighbouring positions. *Ortho*-selective HIE reports are dominated by iridium catalysts, with the initial use of the Crabtree catalyst,^[160-162] where often times (super-)stoichiometric amounts of the complex were required, as well as long reaction times. Since then, two main classes of iridium catalysts were developed, affording systems operating in extremely mild conditions: room temperature, short reaction time, and absence of additives (Scheme 6). On the one hand, a group of electron-rich catalysts featuring sterically demanding N-heterocyclic carbene (NHC) ligands and either a phosphine in the case of cationic catalysts,^[163-168] or a chloride for neutral ones,^[169] was developed by Kerr. On the other hand, the Tamm group designed P,N-ligands with electron-rich coordinating nitrogen atoms.^[170] In both cases, D₂ is the isotope source and a dihydrogen hydride is the key intermediate. Similarly, these systems make use of a variety of directing groups – such as carbonyl, pyridine, azoles, nitro, Boc protecting groups, sulfones, etc. – which validates the relevance of those methodologies.

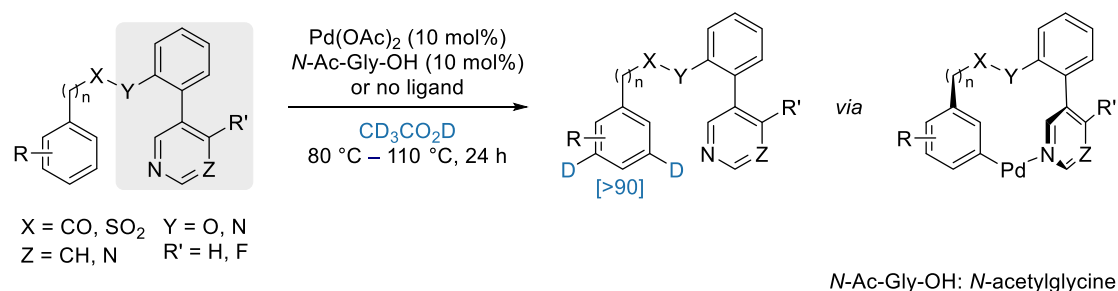


Scheme 6. Crabtree, Kerr, and Tamm catalyst families for HIE. Typical reaction conditions and directing groups are shown.

It should be mentioned that catalysts have to be selected depending on the substrates, as not all directing groups can be of use with both catalyst families. The commercially available Burgess catalyst for the labelling of aromatic sulfonamides and ketones,^[171-172] or a mesoionic carbene complex for aniline deuteration^[173] are further examples of iridium-catalysed HIE. When moving to other noble metals, alternate deuterium sources are reported for HIE, due to the distinct mechanism of each metal. For instance, rhodium-olefin complexes allow H/D exchanges in C₆D₆,^[174] whilst Pd(OAc)₂ is active for the labelling of benzoic acid derivatives with AcOH-*d*₄ as solvent.^[175] These substrates are also labelled under ruthenium catalysis in a dioxane-D₂O mixture.^[176]

On the contrary to the use of iridium, ruthenium or palladium, reports of non-noble metals for *ortho*-directed HIE are scarce. A notable example is indole deuteration at the C2 position under cobalt catalysis.^[177] Another remarkable report, relies on the use of a transient directing group, where imines are generated *in situ* from aromatic aldehydes using catalytic amounts of amines.^[178] With D₂O acting as the isotope source for this manganese-based methodology, the transient imines are hydrolysed during the course of the reaction and the corresponding aldehydes are recovered.

Meta selectivity. Without being able to use coordinating groups to form the 5-membered metal-lacycles usually responsible for high *ortho*-selectivity, it is apparent that the development of methodologies for *meta*-HIE is more challenging. One approach is the use of large template groups pre-installed on the substrates *via* an ester, amide, or sulfonyl ester for palladium-catalysed HIE (Scheme 7). Pyrimidines^[179-180], or pyridine^[181] are thus auxiliaries for Pd-catalysed deuteration, again using AcOH-*d*₄ as D-source.

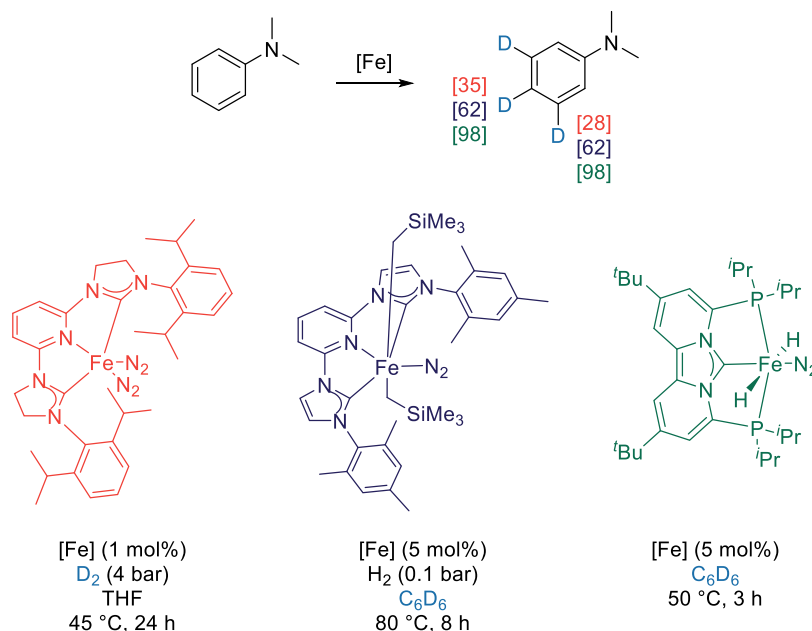


Scheme 7. Template-directed *meta*-labelling.

Undirected labelling. Further HIE tactics do not depend on directing groups. While this is mostly a domain of heterogeneous catalysis (see part 1.2.3.3), homogeneous examples also exist, usually opening access to an orthogonal selectivity with regard to classical Ir catalysis. The first breakthrough in this field is from the Chirik group with the use of an iron complex under D₂ atmosphere. Labelling takes place at the more accessible, and preferentially (but not limited to) electron-poor positions.^[182] Mechanistic investigations suggested iron hydrides as the catalytically active species, which led to a second generation precatalyst, this time more stable and easy-to-handle, and importantly relying on benzene-*d*₆ as the isotope source.^[183] However, low H₂ pressure was required to generate the active iron(II) dideuteride species. Alternatively, a static vacuum could be applied with the trade-off of drastically elongated reaction time being required. In parallel, another iron dinitrogen complex, this time a PC_{NHCP}, was reported for a similar reaction.^[184] Owing to the greater stability of the dideuteride intermediate, the reaction is feasible without a hydrogen atmosphere (Scheme 8).

A series of nickel dimer complexes also plays a crucial role in undirected labelling. The first system was limited to the labelling of strongly σ -donating electron-deficient heteroarenes such

as azines.^[185] In fact, a Ni–N interaction was necessary to dissociate the robust dimeric pre-catalyst to generate the active species. Hence, a second generation of a more labile dimer was designed, affording a superior HIE performance for a broader scope of electron-deficient and electron-rich substrates.^[186]



Scheme 8. Iron complexes for undirected labelling.

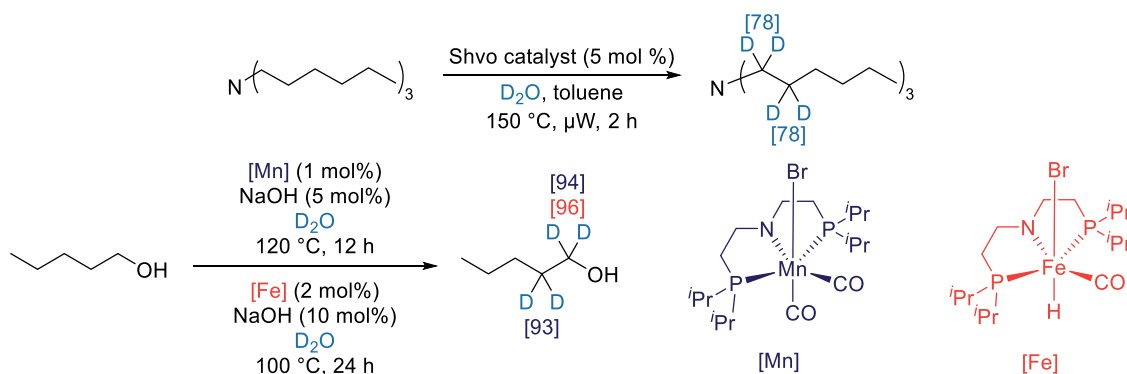
Additional fine-tuning of the abovementioned systems allowed two cobalt-based methodologies: on the one hand, an α -diimine ligand permits the enantioselective HIE at benzylic positions in the presence of D_2 .^[187] Concomitant labelling of *meta*- and *para*- $C(sp^2)$ -H positions suggests a mechanism similar to the iron-based methodologies might additionally take place. On the other hand, earlier this year a bis(silylene)pyridine cobalt(III) dihydride boryl complex was reported, which could deuterate arenes using C_6D_6 as the isotope source.^[188] In contrast to the iron dimers, the main advantage of this approach is that catalyst activation does not require H_2 .

Other undirected approaches rely, for example, on ruthenium pincer catalysts, either *via* a ruthenium-deuteride,^[189] or ruthenium-deuteroxo intermediate in basic medium.^[190] Besides, a palladium-based methodology using dual ligand catalysis is a technique for the undirected labelling of a tremendous number of substrates.^[191] Even though the mechanism was initially unclear, extensive investigations revealed the (multiple) roles of the (required) pyridine and *N*-acyl amino acid derived as ligands in a concerted metalation deprotonation step.^[192]

1.2.2.4. Aliphatic metal-catalysed HIE

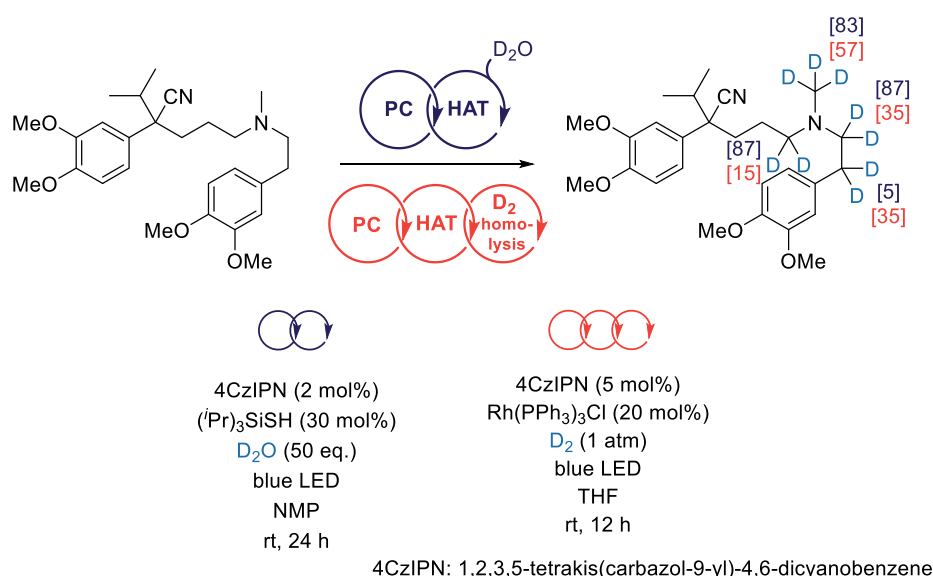
Aliphatic HIE often takes place adjacent to heteroatoms, with the majority of the reports dealing with α - and/or β -labelling of alcohols and amines (Scheme 9). In this case, progress in transfer

hydrogenation chemistry were judiciously applied to the labelling of these substrates. For instance, amines were initially labelled using the commercially available Shvo catalyst^[193] or



Scheme 9 Aliphatic labelling via transfer hydrogenation.

$[\text{Ru}(\rho\text{-cymene})\text{Cl}_2]_2$.^[194] Advancements in pincer chemistry allowed further improvements in the reactivity, namely, a reduced reaction temperature and the possibility to deuterate chiral amines in a stereoretentive manner due to the high binding affinity of imine intermediates to metal centres.^[195] Notably, even though these reports use D_2O as the isotope source, all of them rely on ruthenium, whereas from a green chemistry point of view the use of base metals such as iron and manganese would be preferable. In comparison to amines, the dehydrogenation of alcohols is simpler. Hence, not only is their labelling reported using ruthenium catalysis (Ru_{PNN} pincer complex^[196] or Ru-MACHO ^[197]), but it is also feasible with Mn or Fe pincer complexes.^[198]



Scheme 10. Aliphatic labelling *via* photocatalysis.

A breakthrough for highly selective labelling α to amines was presented by MacMillan and co-workers in 2017 by merging two radical reactivity modes: the photocatalysed oxidation of alkylamines and hydrogen atom transfer (HAT). Extremely mild reaction conditions and the

tolerance of a broad range of functional groups are key justifications for its application to the labelling of pharmaceutical compounds with D_2O .^[199] Adding a third type of catalysis, namely D_2 homolysis, a comparable reactivity is achieved in the presence of rhodium (Scheme 10).^[200] Although the interest might be limited for deuterium labelling, it is of tremendous importance in terms of tritium labelling where T_2 is the isotope source of choice.

Last but not least, despite being mainly applied for aromatic labelling, Kerr-class catalysts are highly active for aliphatic labelling, especially in activated positions of tertiary amines with the aid of N-heterocycles as directing groups.^[201]

1.2.3. Heterogeneous catalysis

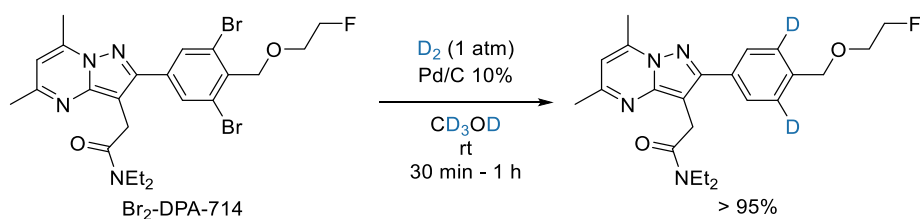
As mentioned above, it is clear that heterogeneous catalysis possesses advantages in comparison with homogeneous catalysis, especially the separation of the active catalyst from reaction mixture and its potential recycling, which are critical parameters for potential industrial applications. Yet surprisingly, their reports are less frequent than those dealing with homogeneous catalysis, possibly due to the difficulty in generating active heterogeneous catalysts for deuterium incorporation. Nevertheless, applications of such materials are presented in the following sections.

1.2.3.1. Acid/Base catalysis

In contrast to homogeneous acids, the variety of supported equivalents is rather limited. Nevertheless, activated positions of phenols are labelled using Nafion^[202] or Amberlyst^[203] as supported acid catalysts in D_2O . Similarly, aromatic hydrocarbons were labelled in supercritical D_2O in the presence of deloxan resin.^[204]

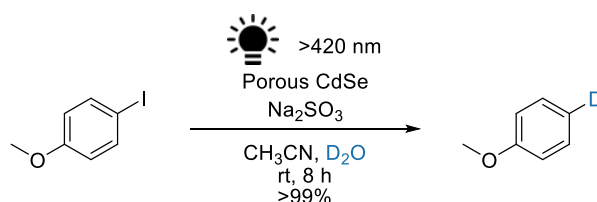
1.2.3.2. Reductive deuteration

Arguably one of the most commonly applied processes to incorporate deuterium atoms into organic molecules relies on commercially available Pd/C following well-known hydrodehalogenation chemistry, and replacing H_2 gas with D_2 gas. This is a practical and powerful method to obtain quantitative D content at a specific position in numerous building blocks, given the broad availability of simple halogenated compounds, or pre-functionalised molecules (Scheme 11).^[205-208] The chemoselectivity of such reactions can however be challenging, especially in the presence of alkenes that are typically reduced under these conditions. Notably, the necessary D_2 can be generated *in situ* from D_2O ,^[209] and this approach can also be of use for tritium labelling.^[207, 210] In contrast, converting olefins to the corresponding deuterated alkanes is smoothly achieved using the same catalyst.^[211]



Scheme 11. Reductive deuteration of Br₂-DPA-714.

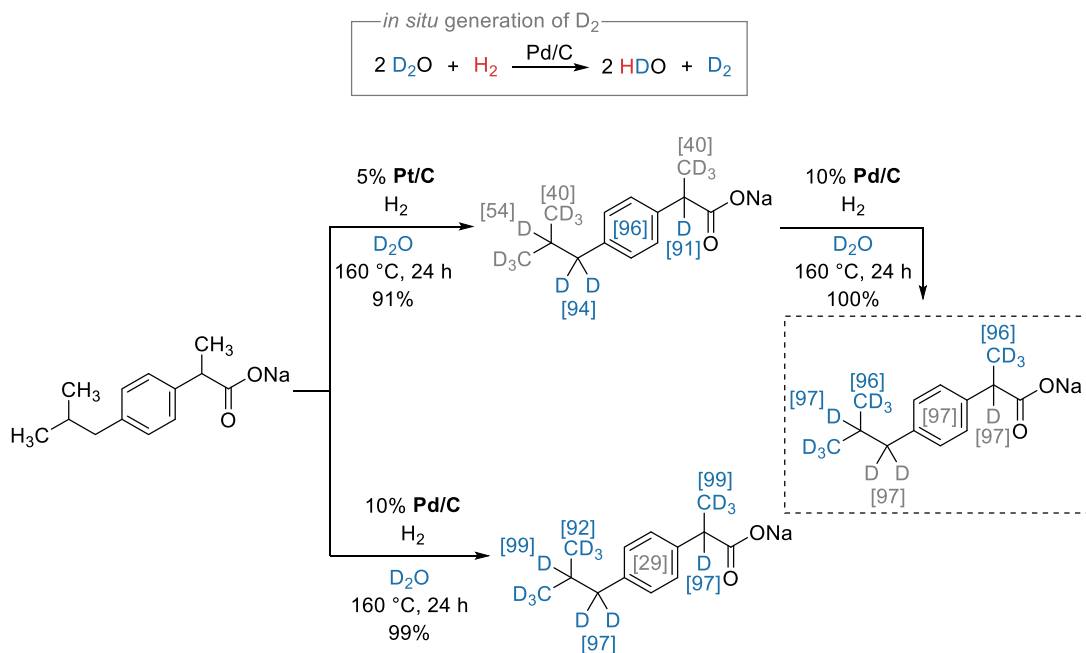
To limit the use of D₂, the trend in recent years is to use D₂O or other practical and easy-to-handle isotope sources. In terms of reductive deuteration, this could be a problem as electrophilic deuterides are often necessary, and these are not broadly available. Solutions to address this issue again rely on electrochemical^[212] or photochemical^[73, 213] catalysis, where D₂O and milder reaction conditions can be used. For instance, Loh and co-workers showed the efficiency of easily synthesised porous CdSe nanosheets acting as selective photocatalysts for the dehalogenation of a variety of substrates.^[214] This methodology seemed however mostly applicable to iodo substrates, which on the one hand can be a limitation, but on the other hand can enable further functionalisation for substrates bearing multiple halogen atoms. Here, irradiation causes electron-hole pairs to form on the catalyst surface. Given the defective sites, the electrons are trapped and transferred to the halogenated substrates and/or D₂O. Thus, the deuterated products are formed by the combination of the two radicals. A sacrificial agent, Na₂SO₃, is used for the catalyst to return to its ground state (Scheme 12).



Scheme 12. Porous CdSe for photocatalytic deuteration.

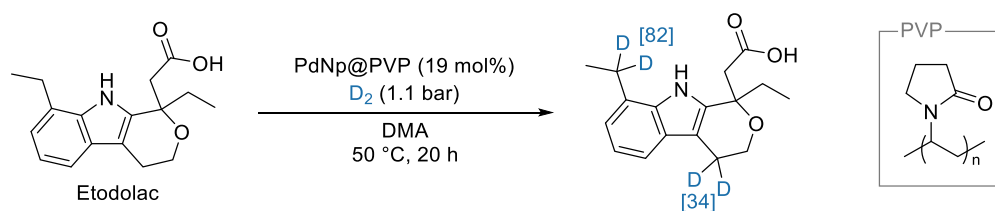
1.2.3.3. Noble Metals

Palladium and platinum. A considerable amount of literature has been published on supported noble metals for HIE reactions, especially commercially available supported platinum and palladium. Numerous historical reports make advantage of the Adam's catalyst (PtO₂) for the labelling of aliphatic amines and amino acids,^[215] nucleosides and nucleotides,^[216] or polystyrene^[217] under hydrothermal conditions, or of Pd/C under D₂ pressure.^[218] In addition, Pt/C and Pd/C were thoroughly investigated by Sajiki and co-workers for the labelling of a broad range of substrates.^[219-229] Here, D₂ is generated *in situ* from D₂O. In general, aromatic and benzylic positions are exchanged with platinum, whereas for palladium aliphatic protons are favoured. As highlighted in Scheme 13 for the deuteration of ibuprofen,^[230] it is thus feasible to reach global labelling using sequenced reactions (or a combination) of these two catalysts.^[231]



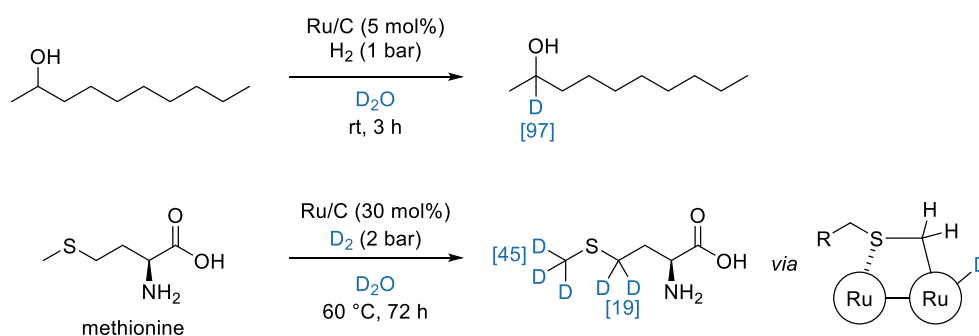
These reactions often require high temperatures (160 °C and above) when D₂O is used as the sole solvent. To operate under milder conditions, it is possible to add carefully selected solvents. A cyclohexane-isopropanol mixture^[232] or isopropanol^[233] reduced the necessary reaction temperature (to 100 °C and rt, respectively). Other reports present NaBD₄ to activate these supported catalysts under microwave irradiation.^[234] It should be mentioned here that even though this Pt–D₂O–H₂ system was reported almost 20 years ago, it attracts continuous interest. For example, it has been reported earlier this year for the selective labelling of allylic alcohols in the presence of amylamine.^[235]

In addition to commercially available heterogeneous catalysts, it is clear that more selective, tailor-made ones are desirable to improve selectivities. Therefore, an emerging trend in heterogeneous HIE reactions relies on metals supported on PVP (polyvinylpyrrolidone, *vide infra* for additional examples) and stabilised by carbene ligands. Accordingly, an active PdNp@PVP material was synthesised by researchers from Boehringer Ingelheim and applied to the selective labelling of the benzylic positions of multiple model substrates, pharmaceutical candidates in development, and commercial drugs.^[236] Here, D₂ was used as the isotope source, and this methodology could be expanded to tritium labelling (Scheme 14). Counterintuitively, higher reaction rates were observed when a lower amount of D₂ gas was used. Assuming the active species are metallic nanoparticles with adsorbed deuterides, the authors suggest the inverse pressure dependence activity is directly linked with the higher mobility of fewer deuterides on the palladium surface. Possibly, under a higher gas pressure more binding sites are occupied by deuterides, and substrate coordination becomes more challenging.

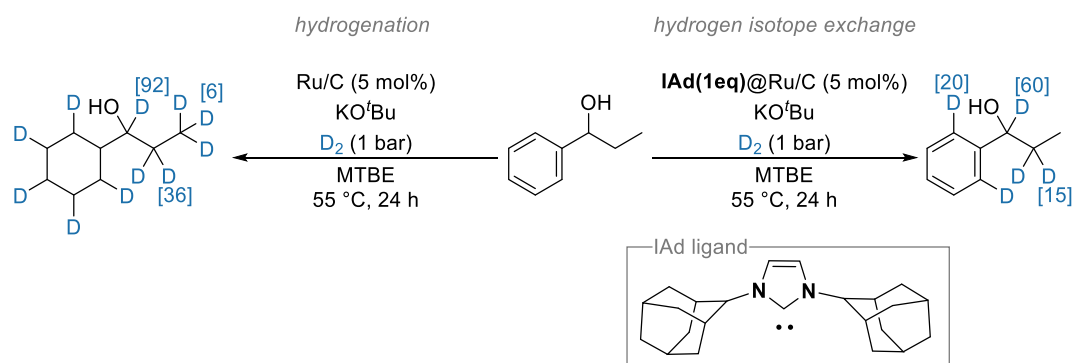


Scheme 14. Benzylic deuteration with PdNp@PVP.

Ruthenium. In addition to Pd and Pt, another metal frequently studied for heterogeneous HIE is ruthenium. Commercial Ru/C (Scheme 15) allows, for example, the α -labelling of alcohols in D₂O.^[237] Racemisation is observed when chiral alcohols are used as substrates, and traces of ketones are detected during the course of this reaction, which suggests dehydrogenation followed by reduction of the ketone is likely to take place here. However, a direct C–H activation mechanism cannot entirely be ruled out. The same catalyst enables deuterium incorporation at the α -position of sulphur atoms.^[238] A four-membered dimetallacycle is proposed as a key intermediate that favours C–H activation at this specific position. Evidently, supported ruthenium materials are prime catalysts for arene hydrogenation. As a consequence, it is challenging to use such catalysts for HIE in the presence of arenes, especially when using of H₂ or D₂ gas. The reactivity on arene rings can however be tuned by the addition of sterically demanding N-heterocyclic ligands. Strong NHC coordination at the surface of the Ru catalyst prevents π -coordination of aromatic rings of the substrates, but not side-on approaches and coordination of oxygen and nitrogen atoms, thereby orienting C–H activation (Scheme 16). More specifically, Ru/C bearing the bulky IAd ligand completely suppressed the hydrogenation process in favour of HIE.^[239]

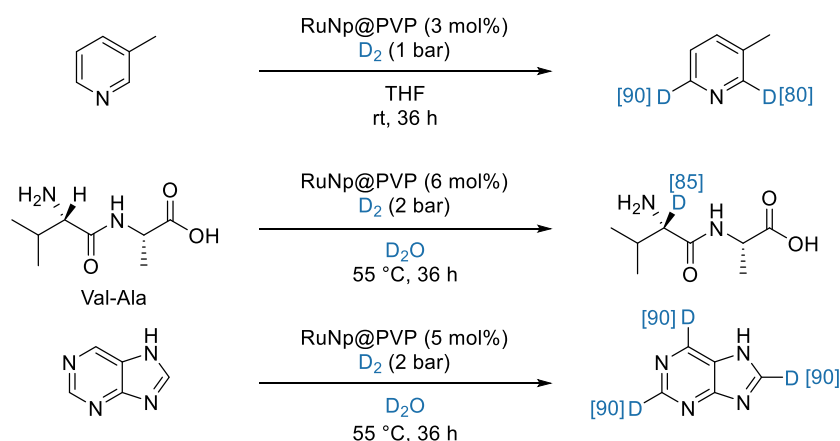


Scheme 15. Ru/C for deuterium labelling.



Scheme 16. Tuned reactivity of Ru/C for deuterium labelling.

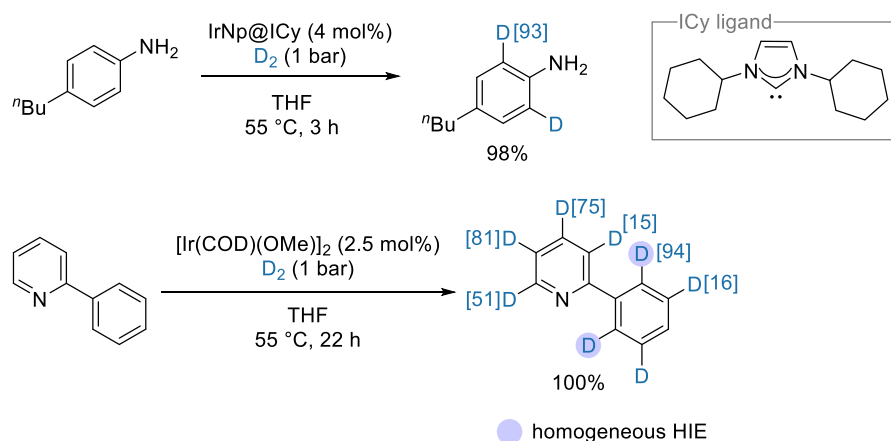
Similarly, PVP-stabilized ruthenium particles were applied to label a variety of nitrogen-containing compounds, including pyridines, quinolines, indoles, and primary, secondary, and tertiary alkyl amines.^[240-242] The high selectivity for the exchange adjacent to the nitrogen atom points towards nitrogen-ruthenium coordination followed by cleavage of the C–H bond and deuteride addition (Scheme 17). Further research demonstrated the enantiospecificity of this catalyst in the labelling of chiral amines, as well as its performance in the deuteration and tritiation of nucleobases.



Scheme 17. RuNp@PVP for isotopic labelling.

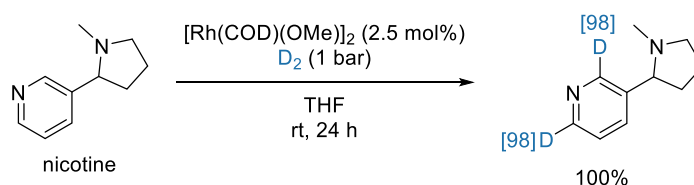
Iridium. As discussed previously, there is rich iridium chemistry for homogeneous HIE reactions. Furthermore, heterogeneous iridium catalysts are less susceptible to hydrogenate arenes than ruthenium ones. For these two reasons, Chaudret, Derdau, Pieters, and co-workers designed metallic iridium nanoparticles using similar NHC ligands they reported for ruthenium nanoparticles.^[243] In this work, IrNp@ICy proved to be a potent material for the deuteration and tritiation of a broad range of anilines (Scheme 18, top). Intriguingly, the authors showed that not only D_2 is the active isotope source, as reactivity is observed solely in its presence, but also that D_2O can act as a reservoir of deuterium and regenerate consumed D_2 in the gas phase. In fact, exchange between D_2O and the catalyst to generate D_2 is assumed to be faster than between substrates and the deuterides at the catalyst surface. Furthermore,

this material also allows HIE between H_2 and D_2O , rendering this methodology feasible without D_2 gas. During the course of these investigations, the authors discovered the iridium precatalyst $[Ir(COD)(OMe)]_2$ decomposed into 2 nm nanoparticles in THF under a D_2 atmosphere. Even more interestingly, these nanoparticles were capable of HIE at $C(sp^2)$ -H positions.^[244] The authors suggest that this methodology is however not purely heterogeneous, and the deuteration of positions typically labelled with homogeneous HIE catalysis is detected. However, its strength relies in the commercial availability and easy access to this precatalyst and broad substrate scope (Scheme 18, bottom).



Scheme 18. Heterogeneous iridium for isotopic labelling.

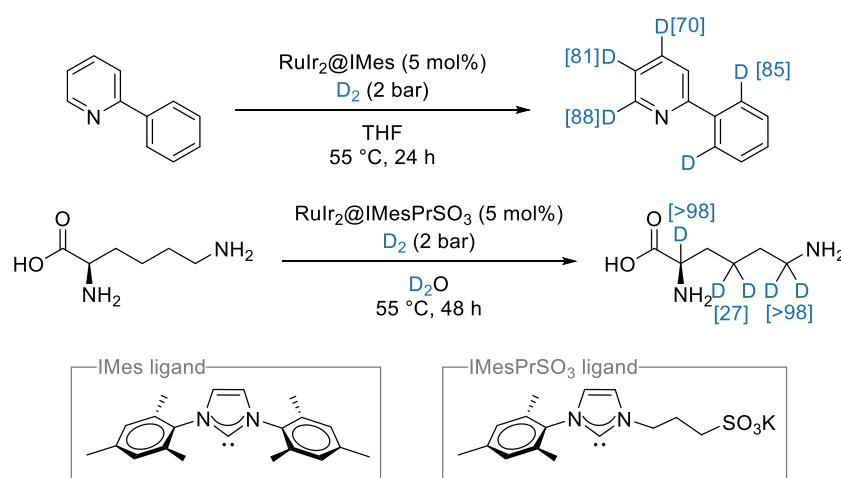
Rhodium. Heterogeneous methodologies involving rhodium catalysis for HIE are scarce. Rh/C was mentioned as a catalyst for HIE reactions at aliphatic positions, although the reaction outcome proved to be highly dependent on the commercial source.^[245] Plus, either substrate decomposition and hydrogenation took place concomitantly.^[246] Nonetheless, $[Rh(COD)(OMe)]_2$ has recently been reported for HIE in N-heterocycles, alkylamines, and benzylic positions, following the decomposition procedure aforementioned with iridium. Here, rhodium particles of various aggregation states, but with a consistent diameter of 3 nm acted as catalysts under D_2 or T_2 pressure (Scheme 19). To limit hydrogenation side reactions, the nanoparticles can again be stabilised with NHC ligands.



Scheme 19. Heterogeneous rhodium for isotopic labelling.

Mixed metals. While the previous sections focus on one metal at a time, the synergies between ruthenium (high HIE activity yet possible arene hydrogenation side reactions), iridium (moderate HIE activity yet limited arene hydrogenation tendency), PVP as support, and NHCs as

stabilisers have recently been evaluated.^[247] Critical to create active and selective catalysts are the ruthenium:iridium 1:2 molar ratio and the increased electronic density on the nanoparticles induced by NHC ligands (Scheme 20, top). In fact, with RuIr₂@IMes being more active than RuIr₂@PVP, the improved catalytic activity seemed directly linked to the electron-enriching properties of the IMes ligand, as previously reported for ruthenium nanoparticles.^[248] Water-soluble particles bearing the IMesPrSO₃ ligand were similarly synthesised and applied for the labelling of the amino acid L-Lysine, although here, no major difference was observed between the different metal ratios (Scheme 20, bottom). Nevertheless, this impressive work is an addition to the toolbox for the labelling of biological compounds, as the nanoparticles operate at milder pH conditions than reported before for such substrates (9.2 vs. 13).

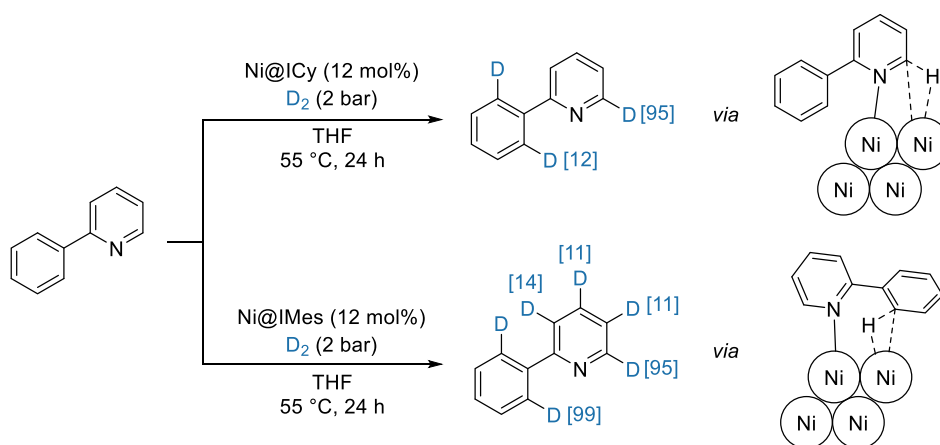


Scheme 20. Mixed ruthenium:iridium nanoparticles for isotopic labelling.

1.2.3.4. Non noble metals

Compared to homogeneous HIE reactions, where an increasing number of methodologies rely on non-noble metals, their heterogeneous counterparts are less common. Raney Nickel was reported in 1954 for aniline deuteration,^[249] which was applied a decade later to phenols and pyridine derivatives,^[250] and more recently reported for a broader range of substrates, including carbohydrates.^[251] After a period dominated by more active noble metals, the revival of nickel-catalysed HIE took place with the NHC-ligand stabilisation strategy for the α -heteroatom deuteration of heterocycles.^[252] The key point of this report is the tuneable concurrent labelling at the *ortho* position of neighbouring rings, which can be turned on or off depending on the bulkiness of the ligand. In this regard, steric hindrance induced by the ICy ligand preferentially allows substrates to approach the Ni surface end-on *via* the pyridine ring (Scheme 21, top). When a greater space is available on the catalyst surface (Ni@IMes, Scheme 21, bottom), side-on or even flat coordination of the aromatic rings is feasible, hence the supplementary deuterium incorporation. It should also be mentioned that for this methodology a higher catalyst

loading than for most of the noble metal-based methodologies is necessary (12 mol%). Apart from nickel, cobalt catalysis is reported, for instance in an aluminium alloy for the enantioselective labelling of benzylic positions.^[253]



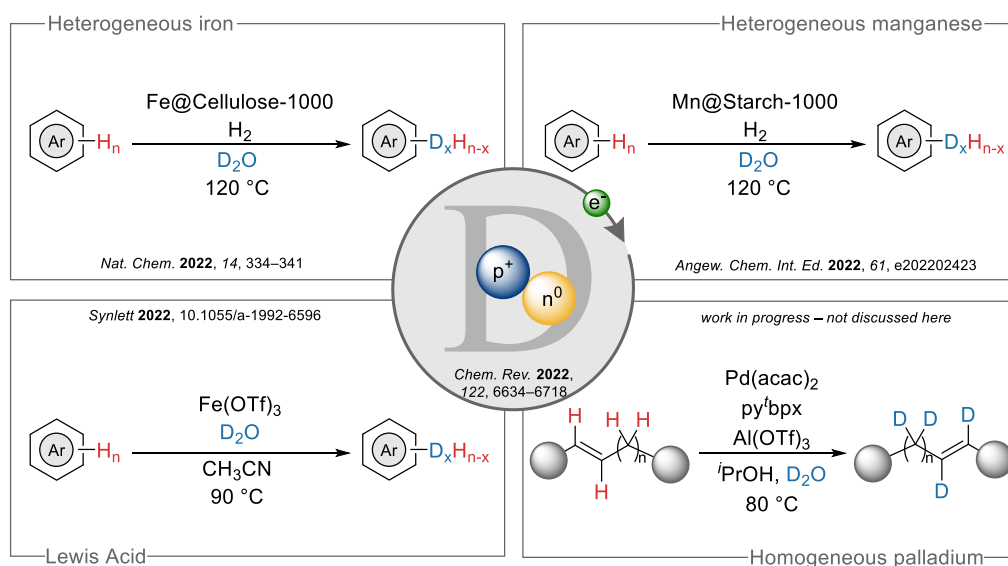
Scheme 21. Heterogeneous nickel for isotopic labelling.

2. Objectives of this work

Primary reports dealing with deuterium incorporation into organic molecules were already published decades ago. Nonetheless, these initial works either aimed towards academic purposes, with industrial applications not the primary objective, or the outcomes were insufficient for “real life” applications.^[206, 254-255] Nowadays, the situation has switched as the demand for labelled compounds, especially in industry, is peaking. SILS are for instance applied in various fields such as mass spectrometry, medicinal chemistry, material sciences and others, new methods are needed for their preparation.

To access such compounds in an efficient and accessible manner, we were interested in the development of new methodologies for the deuterium labelling of organic compounds using catalytic systems (Scheme 22). Here, our main objectives were to:

- complement the current state-of-the-art methodologies for the late-stage labelling of aromatic as well as aliphatic positions,
- preferentially establish methodologies relying on deuterium oxide as the most available and affordable source of this isotope, keeping in mind the disparate prices of the deuterium sources available,
- preferably develop catalytic systems based on non-noble metals.



Scheme 22. Summary of this work.

3. Summary of publications

This section highlights the summary of new iron- and manganese-based heterogeneous catalysts for deuterium labelling. Moreover, a methodology taking advantage of a simple Lewis acid will be presented.

3.1. Recent developments for the deuterium and tritium labelling of organic molecules

The interest in deuterium- and tritium-labelled compounds was discussed in the introduction, and representative methodologies for their synthesis were examined. Unequivocally, this field is a “hot topic” in chemical research, with numerous novel methodologies published in recent years. To our surprise, the most up-to-date general literature review dealing with deuterium labelling was published in 2017,^[63] thus, we saw the need for an updated one to collect the – numerous – most recent publications dealing not only with deuterium, but also tritium labelling (Figure 3). Furthermore, applications of such compounds were also discussed, mainly in the case of medicinal chemistry. Methodologies for isotopic enrichment were presented based on the approaches used by the authors (i.e. HIE, reductive deuteration, and other miscellaneous reactions).^[31]

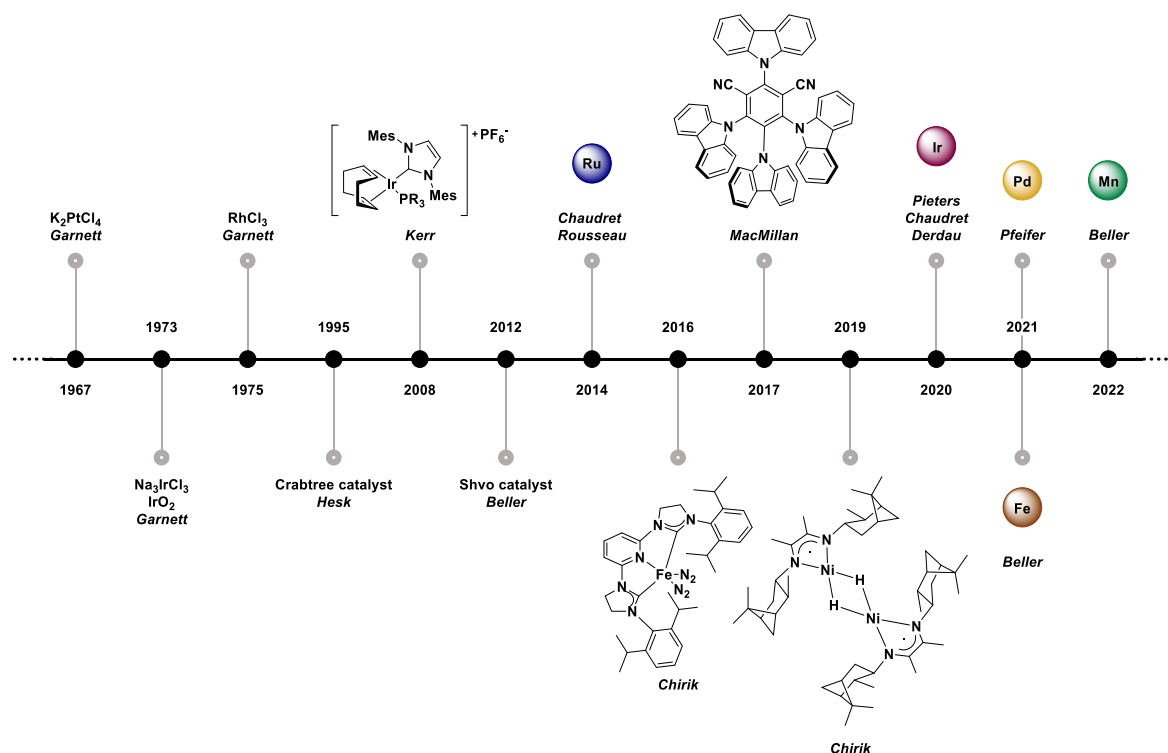
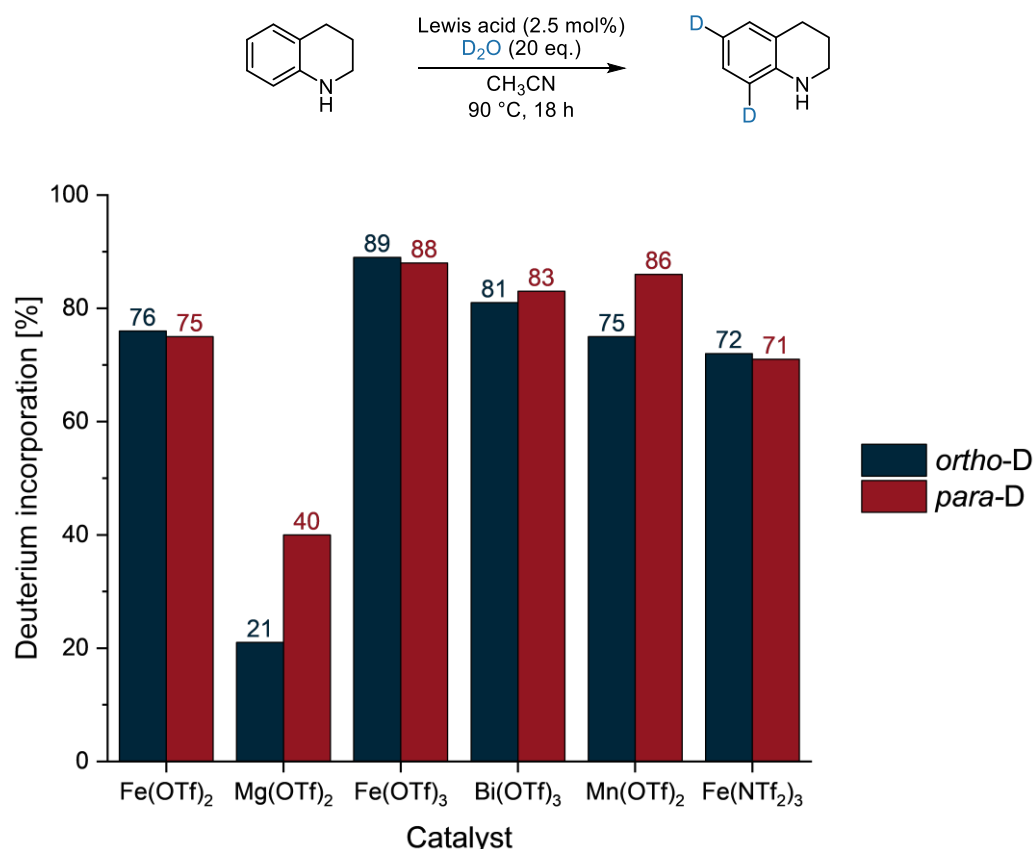


Figure 3. Timeline of methodologies for deuterium incorporation.

3.2. Homogenous iron-catalysed deuteration of electron-rich arenes and heteroarenes

As stated in the introduction, one trend in HIE reactions is the introduction of deuterium in electron-rich arenes and heteroarenes employing Frustrated Lewis Pairs (FLP) and Lewis acids. To do so, reported methodologies often make use of CDCl_3 and D_2O as a solvent combination and isotope source. We were interested in developing alternative Lewis-acid-based approaches for deuterium labelling and targeted a system relying on D_2O .

We initiated our investigations with the screening of various Lewis acids for the labelling of 1,2,3,4-tetrahydroquinoline as the model substrate. Under our reaction conditions, $\text{Fe}(\text{OTf})_3$ was identified as the most active catalyst (Figure 4). It should be mentioned that the reactivity here is not only due to the formed triflic acid. If this was the case, for instance $\text{Fe}(\text{OTf})_2$ and $\text{Mg}(\text{OTf})_2$ should induce comparable deuterium enrichments yet clear differences are observed.

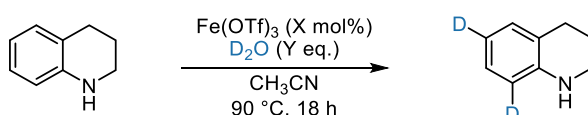


Reaction conditions: 1,2,3,4-tetrahydroquinoline (0.5 mmol), Lewis acid (2.5 mol%), D_2O (20 eq.), CH_3CN (1 mL), 90°C , 18 h.

Figure 4. Evaluation of various Lewis acids for the deuterium labelling of 1,2,3,4-tetrahydroquinoline.

We eventually studied the effects of reaction temperature and solvent for this methodology. Acetonitrile provided the best results, and a temperature of 90 °C was necessary to induce high deuterium content.^[256] Further investigations of catalyst loading and D₂O equivalents are depicted in Table 3. Remarkably, using a catalyst loading higher than 0.5 mol% does not greatly improve the deuterium enrichment. Furthermore, merely 20 eq. of D₂O were sufficient to induce a labelling >90%. In fact, an excess of D₂O proved to be detrimental, and performing the reaction in D₂O as the sole solvent significantly reduced the deuterium incorporation

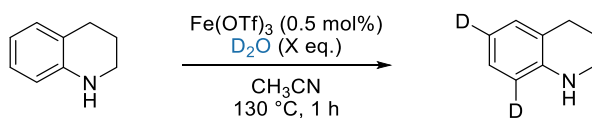
Table 3. Variation of the catalyst loading and D₂O amount.



Entry	Fe(OTf) ₃ [X mol%]	D ₂ O [Y eq.]	<i>ortho</i> -D [%]	<i>para</i> -D [%]
1	2.5	10	83	84
2	2.5	20	90	90
3	2.5	50	95	96
4	1.25	10	81	81
5	1.25	20	90	90
6	1.25	50	95	96
7	0.5	10	83	84
8	0.5	20	92	93
9	0.5	50	65	90
10 ^[a]	0.5	solvent	27	41
11	0.1	20	33	57
12	0.1	50	25	45
13	0.1	100	30	54
14 ^[a]	0.1	solvent	5	16

Reaction conditions: 1,2,3,4-tetrahydroquinoline (0.5 mmol), Fe(OTf)₃ (2.5 – 0.1 mol%), CH₃CN (1 mL), 90 °C, 18 h.
^[a] D₂O (1 mL) instead of CH₃CN.

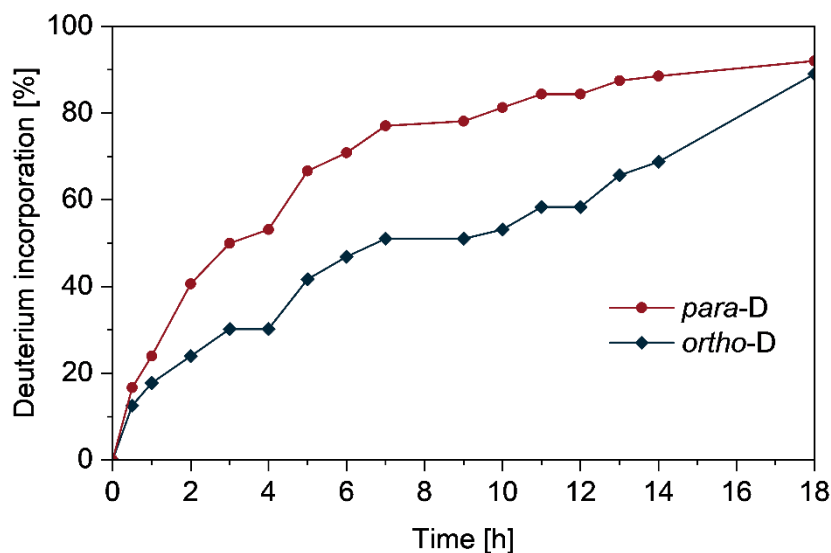
Conversely to lengthy although “mild” reactions, attention is also given to rapid ones. Fast reactions are preferable for tritium labelling as operating with a limited exposure time of radioactive isotopes is highly desirable to minimise hazards and ensure safety. In this regard, we performed our model reaction at higher temperature (130 °C) for one hour with reduced D₂O amounts (Table 4). Gratifyingly, only 2 equivalents of D₂O were sufficient to induce a labelling superior to 50%, and 5 equivalents provided a D content above 70%.

Table 4. Deuterium labelling at higher temperature.

Entry	D ₂ O [X eq.]	<i>ortho</i> -D [%]	<i>para</i> -D [%]
1	20	80	89
2	10	75	85
3	5	71	74
4	2	53	54
5	1	33	36

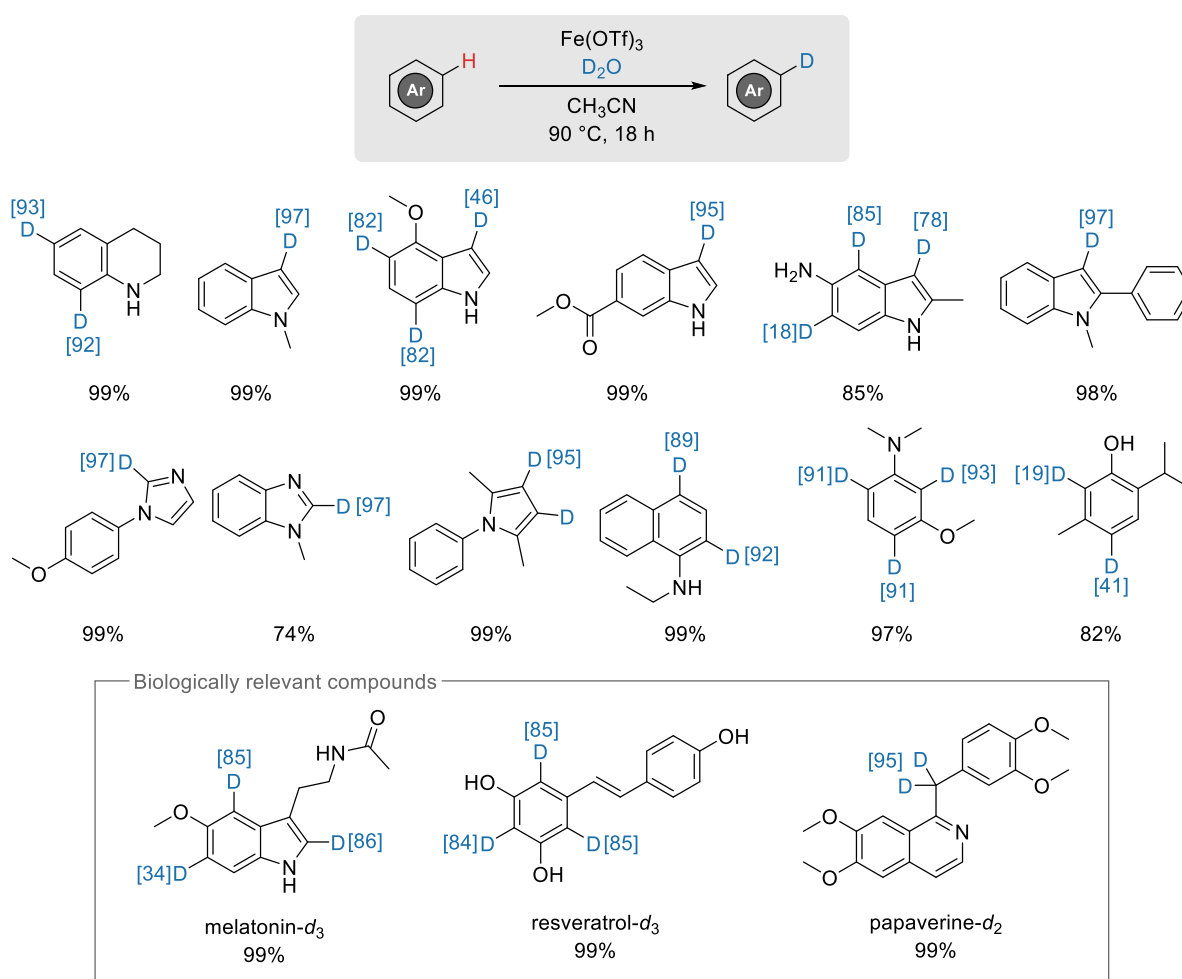
Reaction conditions: 1,2,3,4-tetrahydroquinoline (0.5 mmol), Fe(OTf)₃ (0.5 mol%), CH₃CN (1 mL), D₂O (X eq.), 130 °C, 1 h.

During these experiments, we also noticed that the deuterium content at the *para*-position was often higher than at the *ortho*. Hence, we monitored a kinetic profile of our model reaction (using conditions from Table 3, entry 8) which clearly indicated that *para*-labelling takes place more rapidly (Figure 5). This behaviour could be explained by the greater stability of Wheland intermediates at the *para*-position in aromatic amines in comparison with the *ortho*-position.^[257]

**Figure 5.** Kinetic profile for the deuterium labelling of 1,2,3,4-tetrahydroquinoline.

Selected scope entries under our optimised reaction conditions are depicted in Scheme 23. As can be seen, the methodology is efficient for the labelling of a variety of electron-rich compounds, notably heteroarenes. For instance, indoles are deuterated preferentially at the more reactive C3 position, but also on the aromatic ring. In fact, the labelling is highly dependent on the nature of the substituents: an electron-donating one such as methoxy at the C4 position

will permit labelling at other positions (C5 and C7) whereas electron-neutral or electron-withdrawing ones will restrict the reactivity. Other heteroarenes such as imidazole, benzimidazole and pyrrole were also efficiently labelled, with a deuterium content above 95%. Similarly, deuteration of a 1-naphthylamine representative took place with 92% D and 89% D at the *ortho*- and *para*- positions, respectively. All the electron rich positions of 3-(dimethylamino)anisole were deuterated. In terms of phenols, the deuterium incorporation is limited. This could be explained by the reduced electron-donating ability of phenols in comparison with anilines. Nevertheless, deuterium incorporation in the natural terpenoid thymol was 19% in the *ortho* position and 41% in the *para* position with respect to the hydroxy group. As disclosed in the introduction, the deuterium incorporation in biologically relevant compounds is of key interest. Thus, melatonin, bearing an indole scaffold was a candidate of choice for this methodology, and pleasingly, 99% melatonin-*d*₃ was obtained. In a similar fashion, we isolated resveratrol-*d*₃ quantitatively. In the case of the alkaloid papaverine, aromatic labelling did not take place. Instead, deuterium atoms were detected on the methylene group alpha to the nitrogen, which was previously reported in Lewis acid-based deuteration methodologies.

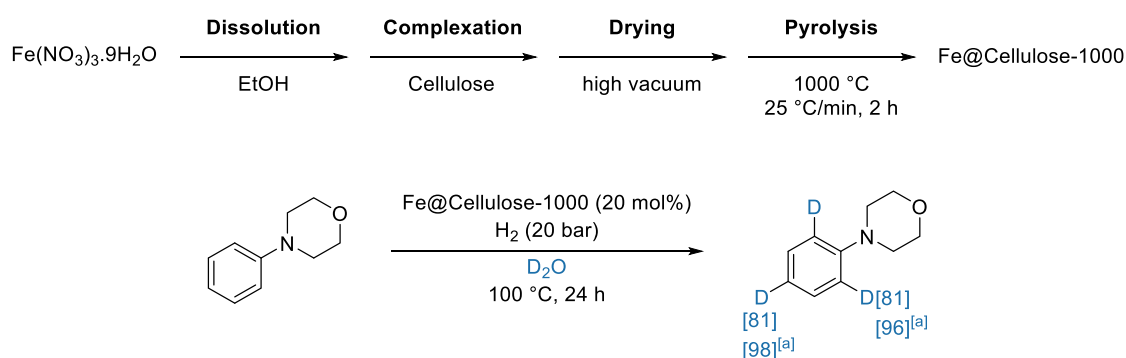


Scheme 23. Selected scope entries for the iron triflate-mediated labelling methodology.

3.3. Scalable and selective deuteration of (hetero)arenes

Heterogeneous catalysis possesses advantages compared to homogeneous, notably catalyst separation and potential recycling. Furthermore, due to their broader availabilities and lower prices, non-noble metals should be used in preference to noble ones. However, despite being a topic of research in both industry and academia, to the best of our knowledge all non-noble metal based heterogeneous catalysts previous to our works relied on either nickel or cobalt. In this regard, we were interested in the development of heterogeneous systems relying on other environmentally benign metals, and iron appeared to us as the metal of choice.

Based on our group's expertise in the development and application of nanoparticles for several catalytic reactions, we synthesised a variety of heterogeneous catalysts *via* a simple impregnation method: first, the iron precursor was heated in ethanol, then a support was added, and stirring was continued overnight. The obtained mixtures were dried *in vacuo* and the remaining solid was pyrolysed at high temperatures (800 – 1000 °C) under argon. In general, at such high temperatures organic-based supports decompose to carbon matrixes, and in our specific case this happens with the metals embedded. Here, cellulose, the most abundant biopolymer, was utilised as support (Scheme 24, top), and the obtained materials were applied for hydrogen deuterium exchange reactions in D₂O using 4-phenylmorpholine as substrate. The highest deuterium incorporation was observed using Fe@Cellulose-1000,^[258] with 81% D at the *ortho* and *para* positions, and this deuterium incorporation could be further increased by raising the reaction temperature from 100 °C to 120 °C (Scheme 24, bottom).



Scheme 24. Synthesis and HIE application of Fe@Cellulose-1000.

Fe@Cellulose-1000 was comprehensively characterised with XRD (X-Ray Diffraction), XPS (X-Ray Photoelectron Spectroscopy), STEM (Scanning Transmission Electron Microscopy) and XAS (X-Ray Absorption Spectroscopy) to understand its structure. These analyses revealed that the fresh catalyst consists of 20 – 50 nm Fe/Fe₃C particles surrounded by a 6 – 10 nm shell of up to 30 graphene layers embedded in a carbon matrix (Figure 6). Notably, the iron content at the surface is rather low (around 0.1 atom%). Furthermore, no oxygen could be

detected at the Fe surface by Electron Energy Loss Spectroscopy (EELS), and the XPS measurement showed a sharp peak at around 707.0 eV, which is characteristic of zerovalent iron. However, these features were different in the used catalyst. The catalyst shell largely disappeared, and instead, the particles – even though of comparable size and distribution in the carbon matrix – were covered by iron oxide which is likely formed by exposure of the used catalyst to ambient air. In addition, the relative intensity of the peaks corresponding to Fe₃C decreased in the XRD spectra of used materials. With these results, we postulate the following: (i) the carbon matrix prevents the aggregation of the particles, (ii) during the course of the reaction, the graphene layer is partly removed which permits the contact of the substrate and the iron surface, and (iii) Fe₃C is in part converted to Fe⁰ which is considered the active site of this reaction.

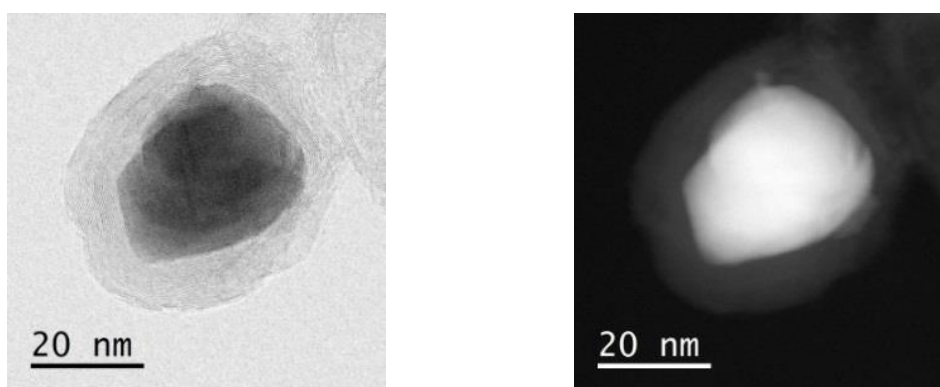
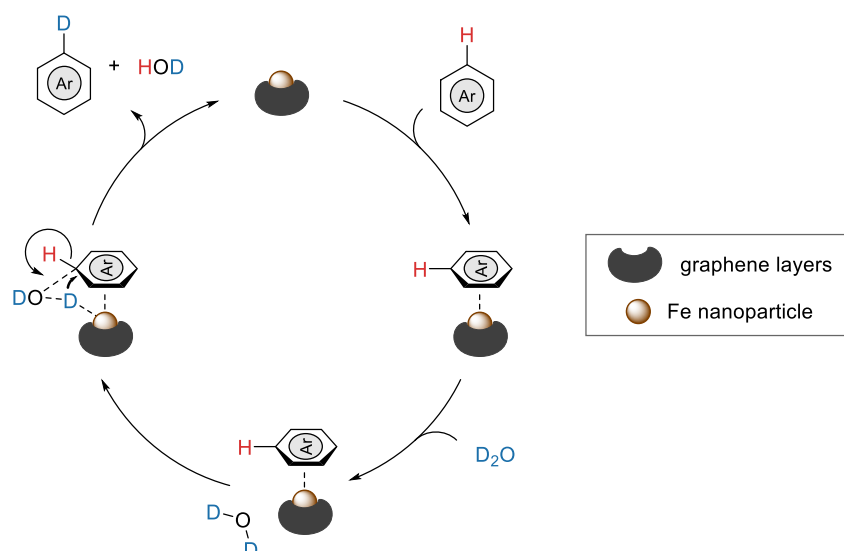


Figure 6. High resolution ABF-STEM (left) and HAADF-STEM (right) images of an Fe particle of Fe@Cellulose-1000.

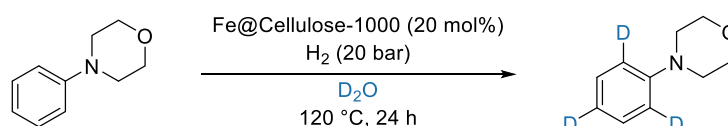
Following the characterisation of this catalyst, Electron Paramagnetic Resonance (EPR) studies were performed to gain insight into the mechanism. After heating the catalyst in D₂O and quenching this mixture with 5,5-dimethyl-1-pyrroline-*N*-oxide (DMPO) as radical trap, the EPR spectrum showed a characteristic signal corresponding to a DMPO–OD spin adduct which is formed by trapping •OD radicals with DMPO. When adding our model substrate 4-phenylmorpholine, an additional organic radical signal was detected. However, this signal is not present when the reaction is performed in the absence of D₂O, which suggests that the •OD radical abstracts a hydrogen from the substrate, leading to HDO and an organic radical. Thus, we suggested the concerted mechanism represented in Scheme 25, in which Fe@Cellulose-1000 permits homolytic cleavage of D₂O, yet the resulting radicals are not liberated into the solution but remain adsorbed on the catalyst surface as activated •D and •OD radicals. The •OD radical abstracts a hydrogen atom from the phenyl ring, forming HDO and the corresponding phenyl radical which is subsequently deuterated. The high deuterium enrichment at the *ortho* and *para* positions follows the selectivity of classical electrophilic aromatic substitution reactions.



Scheme 25. Proposed catalytic cycle for the Fe@Cellulose-1000 methodology.

A key parameter in terms of heterogeneous catalysis is the reproducibility of a process, and it is well-known that heterogeneous materials, even though synthesised in the same fashion or marketed under the same designation, can have different activities. Accordingly, we performed quality control experiments, where the model reaction was performed multiple times. These results showcased the high repeatability of this process, both using different batches of catalysts (average total D=98.47%, standard deviation SD=1.37, Table 5 entries 1 – 6) or using

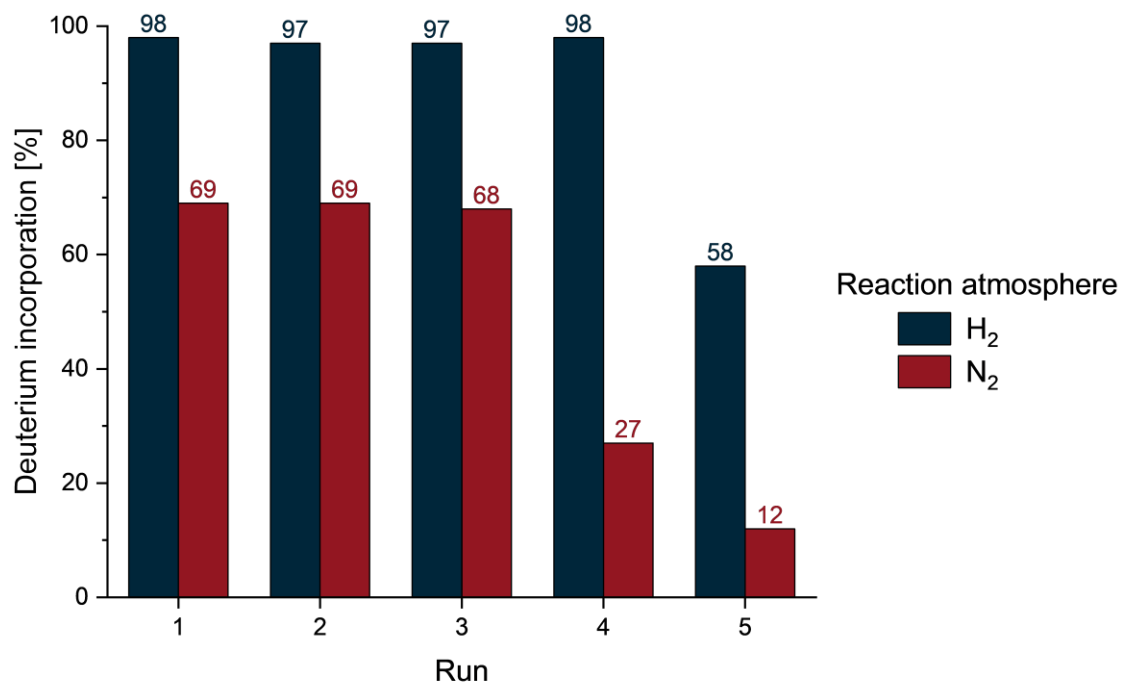
Table 5. Design of quality experiments for the labelling of 4-phenylmorpholine.



Entry	Batch	<i>ortho</i> -D [%]	<i>para</i> -D [%]	Total D [%]
1	1	98.83	99.85	99.17
2	2	93.95	99.14	95.68
3	3	99.08	99.79	99.32
4	4	99.16	99.42	99.25
5	5	97.87	97.76	97.83
6	6	99.35	99.98	99.56
7	7	99.11	99.60	99.27
8	7	97.87	97.76	97.83
9	7	98.93	99.54	99.13
10	7	98.74	99.67	99.05

Reaction conditions: 4-phenylmorpholine (41 mg, 0.25 mmol), Fe-Cellulose-1000 (61 mg, 20 mol% Fe), D₂O (3.0 mL), H₂ (20 bar), 24 h.

the same batch of catalyst (average total D=98.82%, SD=0.58, Table 5, entries 7 – 10). In order to be as accurate as possible, the deuterium content was measured using quantitative ^1H NMR.

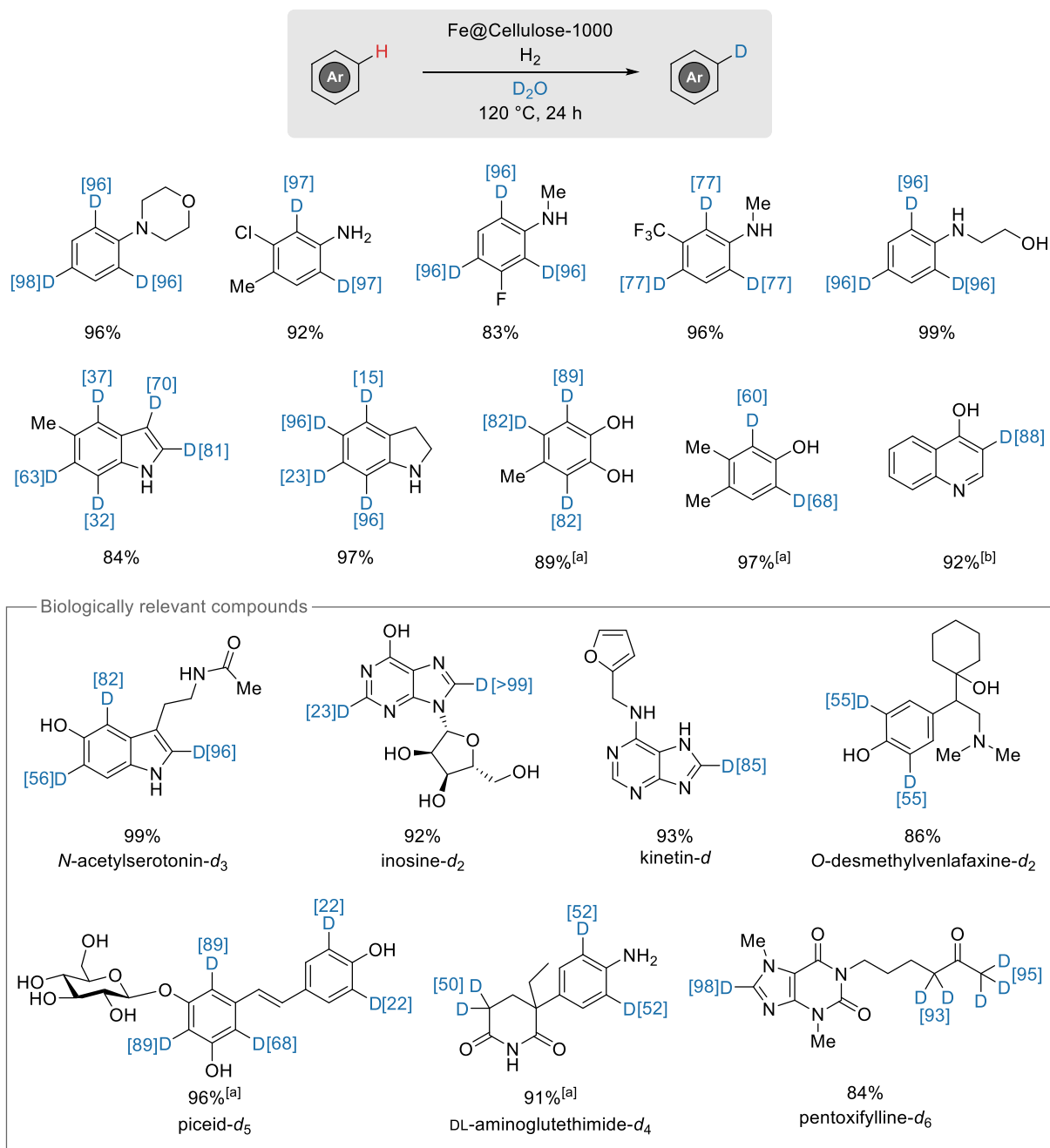


Reaction conditions: 4-phenylmorpholine (0.25 mmol, 40.8 mg), Fe@Cellulose-1000 (60 mg, 20 mol% Fe), D₂O (1.5 mL), H₂ or N₂ (20 bar), 120 °C, 24 h.

Figure 7. Recycling experiments of Fe@Cellulose-1000 under hydrogen and nitrogen atmospheres.

The used iron particles were covered by a layer of iron oxide (see above), which on the one hand might be formed by exposure of the nanoparticles to air, but their generation could also take place during the course of the reaction (in hydrogen or nitrogen). However, performing the reaction under a hydrogen atmosphere could reduce the formed iron oxide to metallic iron, thus improving the catalytic system. In fact, this effect is clearly observed during recycling experiments. While Fe@Cellulose-1000 was highly reusable (4 runs under our standard reaction conditions are possible without activity loss) under H₂, the reactivity was lowered when not using a reductive atmosphere (by around 30% D incorporation), and the activity dropped after the third run (Figure 7).

The applicability of this methodology was demonstrated by an extensive substrate scope of more than 80 compounds, including natural products and commercial drugs (Scheme 26). Moreover, taking advantage of the high recyclability of Fe@Cellulose-1000, the reaction could be scaled-up to >1 kg of combined product with the same catalyst batch.



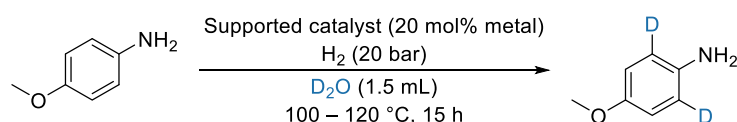
Reaction conditions: substrate (0.25 mmol), Fe@Cellulose-1000 (60 mg, 20 mol% Fe), D₂O (1.5 mL), H₂ (20 bar), 120 °C. ^[a] 72 h. ^[b] 140 °C.

Scheme 26. Selected scope entries for the Fe@Cellulose-1000 methodology.

3.4. Manganese-catalysed deuterium labelling of anilines and electron-rich (hetero)arenes

To complement our investigations presented in part 3.3, we were interested in the development of novel heterogeneous materials for HIE using different metals and heterogeneous supports. An extensive library of new materials was synthesised in a similar fashion and applied to the labelling of *para*-anisidine as model substrate. In addition to iron, manganese is a non-noble metal of choice owing to its broad availability, reasonable price, and rich redox chemistry. We were pleased to identify that manganese-based systems permitted a similar reactivity to iron (Table 6). Under our reaction conditions, we determined starch to be the source of carbon which provided the best results. Of equal importance, a high pyrolysis temperature was necessary for the production of highly active catalysts for HIE and increasing the reaction time from 15 h to 24 h improved the deuterium content.

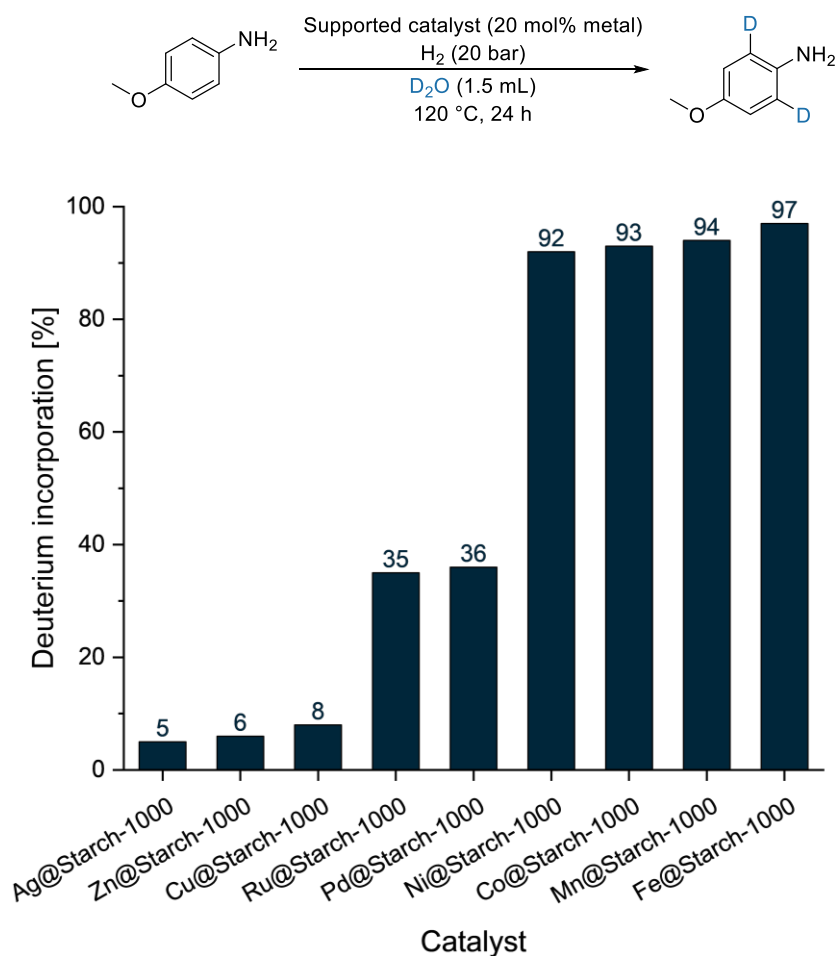
Table 6. Catalyst screening for the deuteration of *para*-anisidine as model substrate.



Entry	Catalyst Metal@Support-Pyrolysis temperature	Deuterium incorporation at 100 °C [%]	Deuterium incorporation at 120 °C [%]
1	Fe@Starch-800	35	76
2	Fe@Starch-1000	36	85 (97) ^[a]
3	Mn@Starch-800	<5	<5
4	Mn@Starch-1000	30	72 (94) ^[a]
5	Fe@Lignin-800	<5	8
6	Fe@Lignin-1000	<5	9
7	Mn@Lignin-800	<5	8
8	Mn@Lignin-1000	<5	9
9	Fe@Alginate-800	17	78
10	Fe@Alginate-1000	<5	27
11	Mn@Alginate-800	<5	8
12	Mn@Alginate-1000	21	67

Reaction conditions: *para*-anisidine (31 mg, 0.25 mmol), catalyst (20 mol% metal), D₂O (1.5 mL), H₂ (20 bar), 15 h.
^[a] 24 h.

Moreover, utilising starch as the source of carbon, we complemented our catalyst library with multiple supported metals (Figure 8). Next to iron and manganese, high deuterium contents (>90%) were induced by nickel and cobalt catalysts which outperformed noble metal-based systems relying on ruthenium or palladium (35% and 36%, respectively). Silver, zinc and copper systems were poorly active under these conditions. Amongst the most active metals and having previously disclosed the potency of iron nanoparticles for HIE, manganese was preferred for toxicity reasons.



Reaction conditions: *p*-anisidine (31 mg, 0.25 mmol), catalyst (20 mol% metal), D₂O (1.5 mL), H₂ (20 bar), 24 h.

Figure 8. Screening of metals using starch as carbon source for the labelling of *para*-anisidine.

Mn@Starch-1000 was characterised to investigate the structural variances in comparison with Fe@Cellulose-1000. Here, Mn/MnO_x core-shell particles are observed with a broad size distribution, the smallest being 10 nm, the majority between 40 and 70 nm and the largest ones up to 1.8 μm (Figure 9a and b), which is overall larger than the iron particles. The manganese concentration at the catalyst surface is also rather low, around 0.2 at.%, rendering XPS measurements challenging. Nevertheless, a peak distance of 5.6 eV in the Mn 3s region suggests Mn³⁺ as main oxidation state in the fresh catalyst (Figure 9e). Different from the iron particles,

the manganese-based material recycles poorly, with almost a 50% drop in the deuterium incorporation after one run under our recycling conditions. With only 0.013 ppm of manganese leaching measured by ICP-MS (Inductively Coupled Plasma Mass Spectrometry), we further investigated the used material to tentatively explain this drop in reactivity. A first observation is that the number of the core-shell particles is drastically reduced, with instead mostly pure Mn (Figure 9c) and MnO_x (Figure 9d) particles, but rarely some containing both. From an electronic point of view, two doublets with different peak separations (6.2 eV and 4.8 eV, Figure 9f) are discerned, which indicates the presence of at least two oxidation states such as Mn^{2+} and Mn^4 .

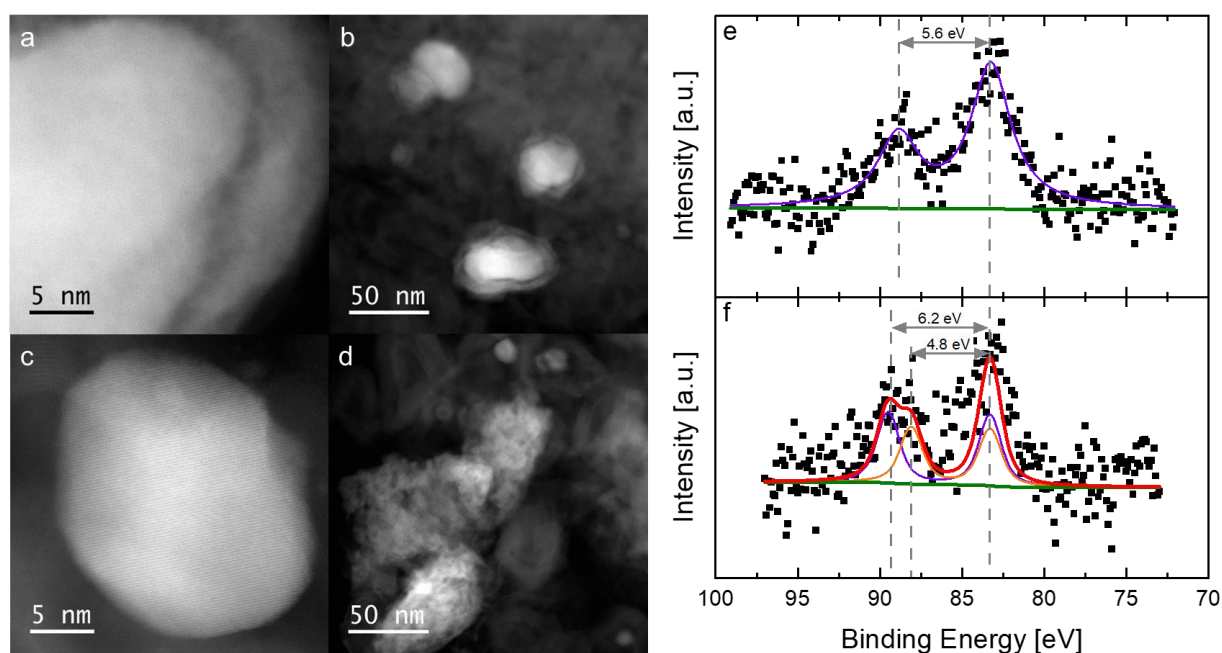
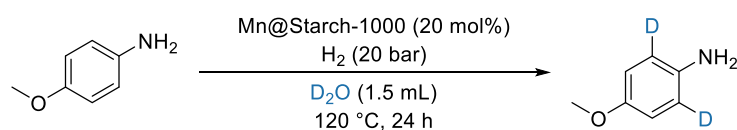


Figure 9. Left: HAADF-STEM images of freshly prepared Mn@Starch-1000 (a, b) and used Mn@Starch-1000 after one run of deuteration of *para*-anisidine (c, d). Right: XPS Mn 3s spectra of the fresh (e) and recycled catalyst (f).

We thus performed further optimisation of our model system. While the use of co-solvents, both protic and aprotic severely lowered the deuterium incorporation (Table 7, entry 2), the use of Lewis or Brønsted acids as additives had little to no effect on the reactivity (Table 7, entries 3–4). On the contrary, bases such as NEt_3 or NaOH proved to be detrimental to the reactivity (Table 7, entries 5–6). Then, we examined the reaction atmosphere and found that a reductive atmosphere was beneficial. Gratifyingly, the hydrogen pressure and the catalyst loading could be lowered (to 10 bar and 10 mol%, respectively), while maintaining an excellent 94% D (Table 7, entries 7–10). Absence of catalyst, manganese acetate or metal-free pyrolysed starch induced poor labelling (Table 7, entries 11–13).

Table 7. Optimisation of reaction conditions for the labelling of *para*-anisidine with Mn@Starch-1000

Entry	Deviation from the standard conditions	Deuterium incorporation [%]
1	-	94
2	<i>i</i> PrOH, THF or cyclohexane as co-solvents	5-8
3	Lewis acids as additives ^[a]	93–94
4	HCl as additive ^[a]	93
5	NEt ₃ as additive ^[a]	80
6	NaOH as additive ^[a]	34
7	N ₂ (20 bar)	94
8	N ₂ (5 bar)	81
9	10 mol% Mn, H ₂ (5 bar)	83
10	10 mol% Mn, H₂ (10 bar)	94
11	no catalyst	< 5
12	Mn(OAc) ₂ ·4H ₂ O as catalyst ^[a]	8
13	Starch-1000 as catalyst ^[b]	< 5

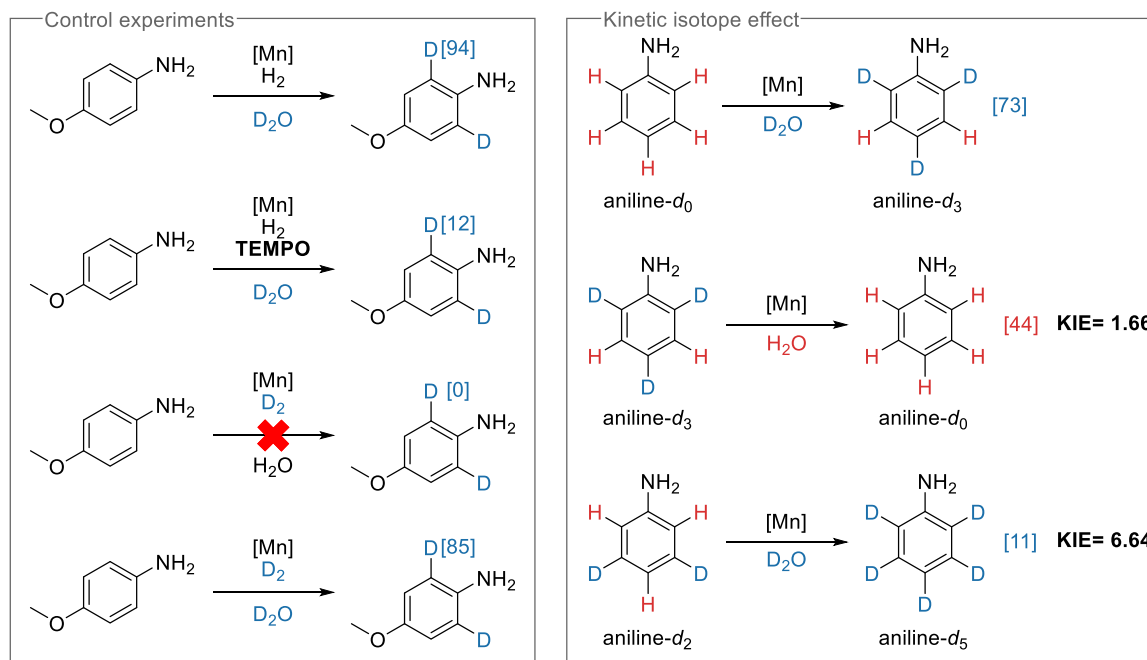
Reaction conditions: *para*-anisidine (0.25 mmol), Mn@Starch-1000 (58 mg, 20 mol% Mn), H₂ (20 bar), D₂O (1.5 mL), 24 h, 120 °C.

^[a] 20 mol%.

^[b] 60 mg.

Given the similarities between the Fe and the Mn catalysts structures and reactivities, we presumed the mechanisms would be analogous. To assess this, the model reaction was performed in the presence of TEMPO (2,2,6,6-tetramethylpiperidinyloxy) as a radical scavenger (Scheme 27) and the deuterium incorporation dropped to 12%. Coupled with the absence of labelling when the reaction is performed using D₂ in H₂O, we proposed a comparable mechanism involving D[•] radicals generated from D₂O (see Scheme 25 for the Fe@Cellulose-1000 mechanism). Besides, switching from H₂ as a reductant to D₂ lowered the labelling of *para*-anisidine from 94% to 85%, thus providing a secondary kinetic isotope effect of 1.1. Additionally, KIEs were monitored on aniline isotopologues with the de-deuteration of 2,4,6-trideuteroaniline and the deuteration of 3,5-dideuteroaniline. The former is predictable, whereas the

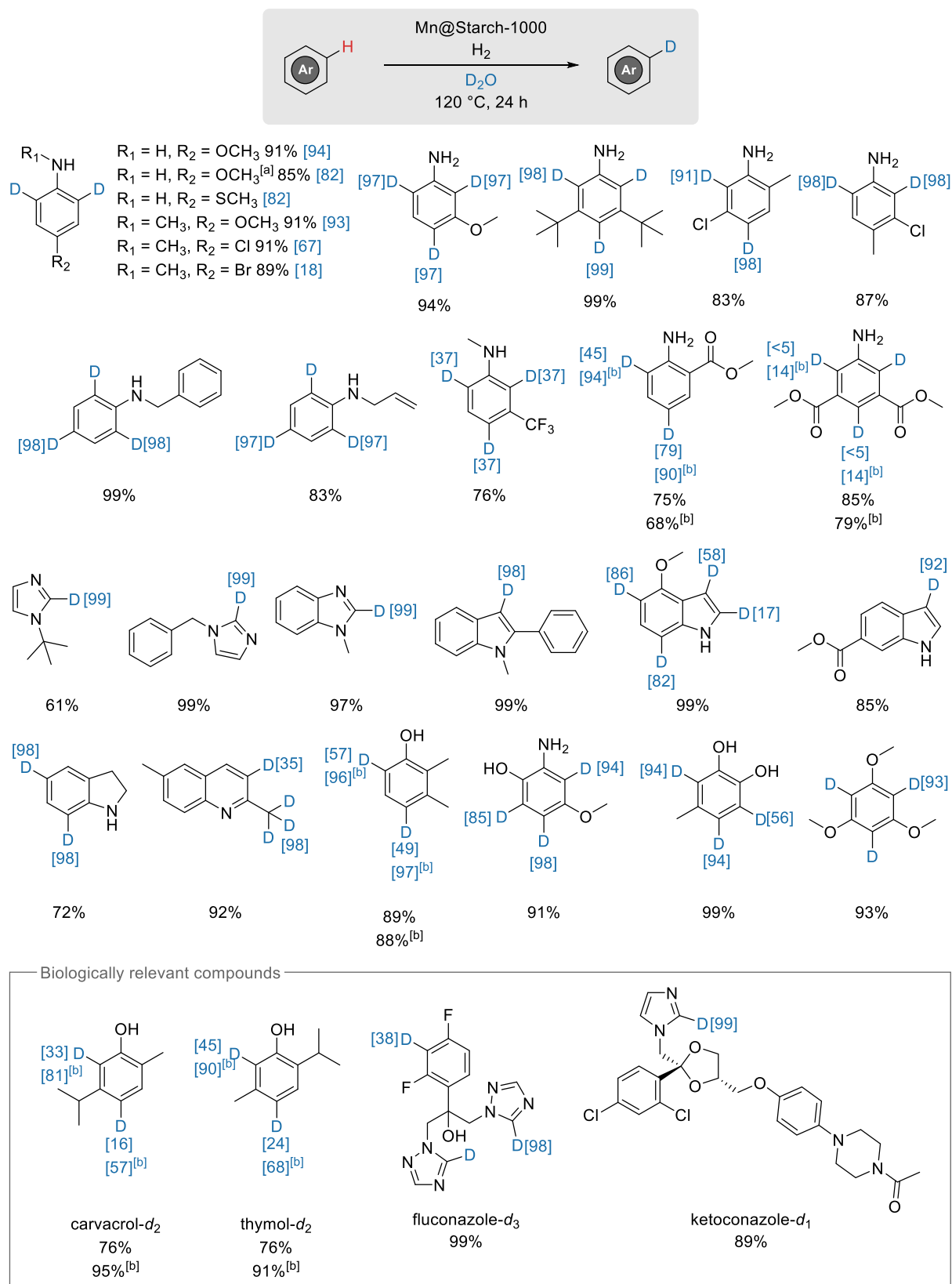
more surprising latter could result from a different coordination of the substrate on the catalyst surface.



Conditions for the control experiments: substrate (0.5 mmol), Mn@Starch-1000 (10 mol%), H_2O or D_2O (1.5 mL), H_2 or D_2 (10 bar), 120 °C, 24 h. Conditions for the KIE experiments: aniline isotopologue (0.5 mmol), Mn@Starch-1000 (5 mol% Mn), H_2 (10 bar), H_2O or D_2O (1.5 mL), 120 °C, 5 h.

Scheme 27. Control experiments – Kinetic isotope effect.

Then, Mn@Starch-1000 was employed for the labelling of numerous anilines, heterocycles and phenols with great functional group tolerance. Good to high deuterium incorporation was obtained in most cases, although for substrates bearing electron-withdrawing substituents or phenols an increase in temperature (from 120 °C to 140 °C) was necessary. Pleasingly, in addition to model compounds, marketed drugs such as ketoconazole and fluconazole were successfully labelled.



Reaction conditions: substrate (0.5 mmol), Mn@Starch-1000 (58 mg, 10 mol% Mn), H₂ (10 bar), D₂O (1.5 mL), 120 °C, 24 h.
 [a] 1 g scale. [b] 140 °C.

Scheme 28. Selected scope entries of the Mn@Starch-1000 methodology.

4. Conclusion and perspectives

The deuterium enrichment of organic molecules, initially purely an academic field of research, is undergoing an escalating interest in terms of industrial applications, as such a small variation can cause heavy changes in a final product. Whereas homogeneous iridium complexes with the use of deuterium gas dominated this field for many years, contemporary research exploits a diversity of techniques such as electro- and photochemistry. Clearly, molecularly defined complexes and other homogeneous systems still represent the majority of the novel methodologies, but the inclination is now to rely on non-noble metals and to make use of deuterium oxide as the most affordable isotope source. In this context, heterogeneous catalysts are much frequently less applied. In view of their numerous advantages, such as the easy separation from reaction mixtures and potential recycling, it is incontestable that heterogeneous catalysts are prime components of the deuterium labelling “toolkit”. Palladium, platinum and ruthenium catalysts unequivocally dominate this field of research, except for scarce examples of cobalt- or nickel-based systems. Therefore, supplemental methodologies relying on base-metals are highly desirable. This work presented two contributions to the field, with the preparation and application of original iron and manganese supported catalysts for the deuterium labelling of a broad range of electron-rich (hetero)arenes, using D₂O as isotope source. Such catalysts were prepared in a practical manner from broadly available biopolymers by a simple impregnation method and were fully characterised. In addition, a simple iron salt (Fe(OTf)₃) was showcased as a potent catalyst for the labelling of comparable compounds under mild reaction conditions.

Today, sustainability is an essential consideration in our daily life, and chemistry is an exceptional instrument to work towards this goal. While it is clear that resources have to be used with a more renewable attitude than in the previous decades, the development of innovative processes and materials is critical to success. In this regard, catalysis plays a fundamental role. Not only does it allow transformations in a more renewable manner than stoichiometric reactions, but the tools themselves, the catalysts, are becoming greener, and are more and more based on Earth-abundant metals. A lot has already been accomplished, but there is still a long way to go!

5. References

- [1] W. Grochala, *Nat. Chem.* **2015**, *7*, 264-264.
- [2] H. C. Urey, F. G. Brickwedde, G. M. Murphy, *Phys. Rev.* **1932**, *40*, 1-15.
- [3] "The Nobel Prize in Chemistry 1934" can be found under <https://www.nobelprize.org/prizes/chemistry/1934/summary>. Accessed on 04.09.2022.
- [4] It should be highlighted that the term "protium" refers specifically to the ^1H isotope when "hydrogen" includes both protium ^1H , deuterium ^2H and tritium ^3H .
- [5] J. Yang, in *Deuterium* (Ed.: J. Yang), Elsevier, **2016**, pp. 1-4.
- [6] M. Diem, in *Modern Vibrational Spectroscopy and Micro-Spectroscopy*, **2015**, pp. 397-398.
- [7] K. B. Wiberg, *Chem. Rev.* **1955**, *55*, 713-743.
- [8] S. L. Harbeson, R. D. Tung, in *Annual Reports in Medicinal Chemistry, Vol. 46*, Elsevier, **2011**, pp. 403-417.
- [9] J. Atzrodt, V. Derdau, W. J. Kerr, M. Reid, *Angew. Chem. Int. Ed.* **2018**, *57*, 1758-1784.
- [10] J. Atzrodt, V. Derdau, *J. Labelled Compd. Radiopharm.* **2010**, *53*, 674-685.
- [11] Y. Kostyukevich, T. Acter, A. Zherebker, A. Ahmed, S. Kim, E. Nikolaev, *Mass Spectrom. Rev.* **2018**, *37*, 811-853.
- [12] S.-N. Lin, T.-P. F. Wang, R. M. Caprioli, B. P. N. Mo, *J. Pharm. Sci.* **1981**, *70*, 1276-1279.
- [13] A. K. Pedersen, G. A. Fitzgerald, *J. Pharm. Sci.* **1985**, *74*, 188-192.
- [14] T. Berg, M. Karlsen, Å. M. L. Øiestad, J. E. Johansen, H. Liu, D. H. Strand, *J. Chromatogr. A* **2014**, *1344*, 83-90.
- [15] J. Jiang, X. Pang, L. Li, X. Dai, X. Diao, X. Chen, D. Zhong, Y. Wang, Y. Chen, *Drug Des. Dev. Ther.* **2016**, *10*, 2181-2191.
- [16] Z. Zhan, X. Peng, Y. Sun, J. Ai, W. Duan, *Chem. Res. Toxicol.* **2018**, *31*, 1213-1218.
- [17] E. Blum, J. Zhang, J. Zaluski, D. E. Einstein, E. E. Korshin, A. Kubas, A. Gruzman, G. P. Tochtrop, P. D. Kiser, K. Palczewski, *J. Med. Chem.* **2021**, *64*, 8287-8302.
- [18] T. M. Vail, P. R. Jones, O. D. Sparkman, *J. Anal. Toxicol.* **2007**, *31*, 304-312.
- [19] A. Matich, D. Rowan, *J. Agric. Food. Chem.* **2007**, *55*, 2727-2735.
- [20] M. Elsner, M. A. Jochmann, T. B. Hofstetter, D. Hunkeler, A. Bernstein, T. C. Schmidt, A. Schimmelmann, *Anal. Bioanal. Chem.* **2012**, *403*, 2471-2491.
- [21] Y. Gao, H. Zhang, L. Zou, P. Wu, Z. Yu, X. Lu, J. Chen, *Environ. Sci. Technol.* **2016**, *50*, 3746-3753.
- [22] X. Li, M. Wang, Y. Zhang, L. Lei, J. Hou, *Quat. Res.* **2017**, *87*, 455-467.
- [23] A. Nakanishi, Y. Fukushima, N. Miyazawa, K. Yoshikawa, T. Maeda, Y. Kurobayashi, *J. Agric. Food. Chem.* **2017**, *65*, 5026-5033.

- [24] K. Kadokami, D. Ueno, *Anal. Chem.* **2019**, *91*, 7749-7755.
- [25] X. Yan, C. S. Maier, in *Mass Spectrometry of Proteins and Peptides, Vol. 492* (Eds.: M. S. Lipton, L. Paša-Tolic), Humana Press, Totowa, NJ, **2009**, pp. 255-271.
- [26] L. Konermann, J. Pan, Y.-H. Liu, *Chem. Soc. Rev.* **2011**, *40*, 1224-1234.
- [27] D. Houde, S. A. Berkowitz, J. R. Engen, *J. Pharm. Sci.* **2011**, *100*, 2071-2086.
- [28] E. I. James, T. A. Murphree, C. Vorauer, J. R. Engen, M. Guttman, *Chem. Rev.* **2022**, *122*, 7562-7623.
- [29] M. Gómez-Gallego, M. A. Sierra, *Chem. Rev.* **2011**, *111*, 4857-4963.
- [30] E. M. Simmons, J. F. Hartwig, *Angew. Chem. Int. Ed.* **2012**, *51*, 3066-3072.
- [31] S. Kopf, F. Bourriquen, W. Li, H. Neumann, K. Junge, M. Beller, *Chem. Rev.* **2022**, *122*, 6634-6718.
- [32] E. D. Williams, K. A. Krieger, A. R. Day, *J. Am. Chem. Soc.* **1953**, *75*, 2404-2407.
- [33] K. G. Kosnik, S. W. Benson, *J. Phys. Chem.* **1983**, *87*, 2790-2795.
- [34] C. P. Casey, J. B. Johnson, *J. Am. Chem. Soc.* **2005**, *127*, 1883-1894.
- [35] M. Hassam, A. Taher, G. E. Arnott, I. R. Green, W. A. L. van Otterlo, *Chem. Rev.* **2015**, *115*, 5462-5569.
- [36] C. C. Tong, K. C. Hwang, *J. Phys. Chem. C* **2007**, *111*, 3490-3494.
- [37] T. D. Nguyen, G. Hukic-Markosian, F. Wang, L. Wojcik, X.-G. Li, E. Ehrenfreund, Z. V. Vardeny, *Nat. Mater.* **2010**, *9*, 345-352.
- [38] T. A. Darwish, A. R. G. Smith, I. R. Gentle, P. L. Burn, E. Luks, G. Moraes, M. Gillon, P. J. Holden, M. James, *Tetrahedron Lett.* **2012**, *53*, 931-935.
- [39] P. Wang, F.-F. Wang, Y. Chen, Q. Niu, L. Lu, H.-M. Wang, X.-C. Gao, B. Wei, H.-W. Wu, X. Cai, D.-C. Zou, *J. Mater. Chem. C* **2013**, *1*, 4821.
- [40] H. Tsuji, C. Mitsui, E. Nakamura, *Chem. Commun.* **2014**, *50*, 14870-14872.
- [41] H. J. Bae, J. S. Kim, A. Yakubovich, J. Jeong, S. Park, J. Chwae, S. Ishibe, Y. Jung, V. K. Rai, W. J. Son, S. Kim, H. Choi, M. H. Baik, *Adv. Opt. Mater.* **2021**, *9*, 2100630.
- [42] X. Liu, C.-Y. Chan, F. Mathevet, M. Mamada, Y. Tsuchiya, Y.-T. Lee, H. Nakanotani, S. Kobayashi, M. Shiochi, C. Adachi, *Small Sci.* **2021**, *1*, 2000057.
- [43] W. Li, A. Wu, T. Fu, X. Gao, Y. Wang, D. Xu, C. Zhang, Z. Sun, Y. Lu, D. J. Young, H. Li, X.-C. Hang, *J. Phys. Chem. Lett.* **2022**, *13*, 1494-1499.
- [44] J. B. Grimm, L. Xie, J. C. Casler, R. Patel, A. N. Tkachuk, N. Falco, H. Choi, J. Lippincott-Schwartz, T. A. Brown, B. S. Glick, Z. Liu, L. D. Lavis, *JACS Au* **2021**, *1*, 690-696.
- [45] K. Roßmann, K. C. Akkaya, P. Poc, C. Charbonnier, J. Eichhorst, H. Gonschior, A. Valavalkar, N. Wendler, T. Cordes, B. Dietzek-Ivanšić, B. Jones, M. Lehmann, J. Broichhagen, *Chem. Sci.* **2022**, *13*, 8605-8617.

- [46] J.-F. Cheng, F.-C. Kong, K. Zhang, J.-H. Cai, Y. Zhao, C.-K. Wang, J. Fan, L.-S. Liao, *Chem. Eng. J.* **2022**, *430*, 132822.
- [47] M. Shao, J. Keum, J. Chen, Y. He, W. Chen, J. F. Browning, J. Jakowski, B. G. Sumpter, I. N. Ivanov, Y.-Z. Ma, C. M. Rouleau, S. C. Smith, D. B. Geohegan, K. Hong, K. Xiao, *Nat. Commun.* **2014**, *5*, 3180.
- [48] J. Jakowski, J. Huang, S. Garashchuk, Y. Luo, K. Hong, J. Keum, B. G. Sumpter, *J. Phys. Chem. Lett.* **2017**, *8*, 4333-4340.
- [49] T. N. K. Raju, *The Lancet* **2000**, *355*, 1022.
- [50] T. Pirali, M. Serafini, S. Cargnin, A. A. Genazzani, *J. Med. Chem.* **2019**, *62*, 5276-5297.
- [51] E. M. Russak, E. M. Bednarczyk, *Ann. Pharmacother.* **2019**, *53*, 211-216.
- [52] C.-H. Chen, *Deuterium Oxide and Deuteration in Biosciences*, Springer International Publishing, Cham, **2022**.
- [53] C. Schmidt, *Nat. Biotechnol.* **2017**, *35*, 493-494.
- [54] S. Qin, F. Bi, S. Gu, Y. Bai, Z. Chen, Z. Wang, J. Ying, Y. Lu, Z. Meng, H. Pan, P. Yang, H. Zhang, X. Chen, A. Xu, C. Cui, B. Zhu, J. Wu, X. Xin, J. Wang, J. Shan, J. Chen, Z. Zheng, L. Xu, X. Wen, Z. You, Z. Ren, X. Liu, M. Qiu, L. Wu, F. Chen, *J. Clin. Oncol.* **2021**, *39*, 3002-3011.
- [55] S. J. Keam, S. Duggan, *Drugs* **2021**, *81*, 1915-1920.
- [56] H. Bethany, *C&EN Global Enterp* **2016**, *94*, 32-36.
- [57] M. Dean, V. Sung, *Drug Des. Dev. Ther.* **2018**, *12*, 313-319.
- [58] S. H. DeWitt, B. E. Maryanoff, *Biochemistry* **2018**, *57*, 472-473.
- [59] T. Junk, W. J. Catallo, *Chem. Soc. Rev.* **1997**, *26*, 401-406.
- [60] J. Atzrodt, V. Derdau, T. Fey, J. Zimmermann, *Angew. Chem. Int. Ed.* **2007**, *46*, 7744-7765.
- [61] W. J. S. Lockley, J. R. Heys, *J. Labelled Compd. Radiopharm.* **2010**, *53*, 635-644.
- [62] A. Michelotti, F. Rodrigues, M. Roche, *Org. Process Res. Dev.* **2017**, *21*, 1741-1744.
- [63] J. Atzrodt, V. Derdau, W. J. Kerr, M. Reid, *Angew. Chem. Int. Ed.* **2018**, *57*, 3022-3047.
- [64] A. Sattler, *ACS Catal.* **2018**, *8*, 2296-2312.
- [65] W. J. Kerr, G. J. Knox, L. C. Paterson, *J. Labelled Compd. Radiopharm.* **2020**, *63*, 281-295.
- [66] H. Yang, D. Hesk, *J. Labelled Compd. Radiopharm.* **2020**, *63*, 296-307.
- [67] M. Valero, V. Derdau, *J. Labelled Compd. Radiopharm.* **2020**, *63*, 266-280.
- [68] D. Hesk, *J. Labelled Compd. Radiopharm.* **2020**, *63*, 247-265.
- [69] M. Lepron, M. Daniel-Bertrand, G. Mencia, B. Chaudret, S. Feuillastre, G. Pieters, *Acc. Chem. Res.* **2021**, *54*, 1465-1480.
- [70] J. Steverlynck, R. Sitdikov, M. Rueping, *Chem. Eur. J.* **2021**, *27*, 11751-11772.
- [71] Q. Sun, J.-F. Soulé, *Chem. Soc. Rev.* **2021**, *50*, 10806-10835.

- [72] Z. P. Vang, S. J. Hintzsche, J. R. Clark, *Chem. Eur. J.* **2021**, *27*, 9988-10000.
- [73] R. Zhou, L. Ma, X. Yang, J. Cao, *Org. Chem. Front.* **2021**, *8*, 426-444.
- [74] Q.-K. Kang, H. Shi, *Synlett* **2022**, *33*, 329-338.
- [75] A. Behr, P. Neubert, *Applied homogeneous catalysis*, Wiley-VCH, Weinheim, **2012**.
- [76] S. Mosafari, R. E. Jelley, B. Fedrizzi, D. Barker, *Tetrahedron Lett.* **2020**, *61*, 152642.
- [77] B.-C. Chen, M. S. Bednarz, H. Zhang, P. Guo, M. Jemal, J. A. Robl, S. A. Biller, J. E. Sundeen, B. Balasubramanian, J. C. Barrish, *J. Labelled Compd. Radiopharm.* **2006**, *49*, 311-319.
- [78] A. Ueda, M. Oba, Y. Izumi, Y. Sueyoshi, M. Doi, Y. Demizu, M. Kurihara, M. Tanaka, *Tetrahedron* **2016**, *72*, 5864-5871.
- [79] M. Makarova, R. C. Barrientos, O. B. Torres, G. R. Matyas, A. E. Jacobson, A. Sulima, K. C. Rice, *J. Labelled Compd. Radiopharm.* **2020**, *63*, 564-571.
- [80] M. G. Yang, M. Beaudoin-Bertrand, Z. Xiao, D. Marcoux, C. A. Weigelt, S. Yip, D.-R. Wu, M. Ruzanov, J. S. Sack, J. Wang, M. Yarde, S. Li, D. J. Shuster, J. H. Xie, T. Sherry, M. T. Obermeier, A. Fura, K. Stefanski, G. Cornelius, P. Khandelwal, A. Karmakar, M. Basha, V. Babu, A. K. Gupta, A. Mathur, L. Salter-Cid, R. Denton, Q. Zhao, T. G. M. Dhar, *J. Med. Chem.* **2021**, *64*, 2714-2724.
- [81] R. Sigüeiro, J. Loureiro, P. González-Berdullas, A. Mouriño, M. A. Maestro, *J. Steroid Biochem. Mol. Biol.* **2019**, *185*, 248-250.
- [82] C. Chapuis, C. Cantatore, P. Fankhauser, R. Challand, J.-J. Riedhauser, *Helv. Chim. Acta* **2009**, *92*, 1782-1799.
- [83] E. D. Styduhar, A. D. Hutters, N. A. Weires, N. K. Garg, *Angew. Chem. Int. Ed.* **2013**, *52*, 12422-12425.
- [84] E. J. Velthuisen, T. M. Baughman, B. A. Johns, D. P. Temelkoff, J. G. Weatherhead, *Eur. J. Med. Chem.* **2013**, *63*, 202-212.
- [85] C. Porcelli, J. Kreissl, M. Steinhaus, *J. Labelled Compd. Radiopharm.* **2020**, *63*, 476-481.
- [86] A. A. B. Robertson, N. P. Botting, *J. Labelled Compd. Radiopharm.* **2006**, *49*, 1201-1211.
- [87] J. Rouleau, C. Guillou, *J. Labelled Compd. Radiopharm.* **2008**, *51*, 236-238.
- [88] Y. Wang, J. Ai, J. Yue, X. Peng, Y. Ji, A. Zhao, X. Gao, Y. Wang, Y. Chen, G. Liu, Z. Gao, M. Geng, A. Zhang, *MedChemComm* **2012**, *3*, 1423-1427.
- [89] X. Dai, C. Lv, J. Sun, S. Li, *J. Labelled Compd. Radiopharm.* **2021**, *64*, 217-224.
- [90] Y. Zhu, J. Zhou, B. Jiao, *ACS Med. Chem. Lett.* **2013**, *4*, 349-352.
- [91] M. A. Fomich, A. V. Bekish, D. Vidovic, C. R. Lamberson, I. L. Lysenko, P. Lawrence, J. T. Brenna, O. L. Sharko, V. V. Shmanai, M. S. Shchepinov, *ChemistrySelect* **2016**, *1*, 4758-4764.

- [92] J. Raap, S. Nieuwenhuis, A. Creemers, S. Hexspoor, U. Kragl, J. Lugtenburg, *Eur. J. Org. Chem.* **1999**, 1999, 2609-2621.
- [93] M. Regner, A. Bartuce, D. Padmakshan, J. Ralph, S. D. Karlen, *ChemSusChem* **2018**, *11*, 1600-1605.
- [94] X. Gan, M. W. Wilson, T. S. Beyett, B. Wen, D. Sun, S. D. Larsen, J. J. G. Tesmer, A. R. Saltiel, H. D. Showalter, *J. Labelled Compd. Radiopharm.* **2019**, *62*, 202-208.
- [95] Z.-Z. Zhou, J.-H. Zhao, X.-Y. Gou, X.-M. Chen, Y.-M. Liang, *Org. Chem. Front.* **2019**, *6*, 1649-1654.
- [96] B. Higginson, J. Sanjosé-Orduna, Y. Gu, R. Martin, *Synlett* **2021**, *32*, 1633-1636.
- [97] R. Iakovenko, J. Hlaváč, *Green Chem.* **2021**, *23*, 440-446.
- [98] L. Yang, C. P. Zhang, *Asian Journal of Organic Chemistry* **2021**, *10*, 2157-2160.
- [99] H. I. M. Amin, C. Raviola, A. A. Amin, B. Mannucci, S. Protti, M. Fagnoni, *Molecules* **2019**, *24*, 2164.
- [100] Y. Lang, X. Peng, C.-J. Li, H. Zeng, *Green Chem.* **2020**, *22*, 6323-6327.
- [101] T. Shao, Y. Li, N. Ma, C. Li, G. Chai, X. Zhao, B. Qiao, Z. Jiang, *iScience* **2019**, *16*, 410-419.
- [102] G. Zhao, W. Yao, J. N. Mauro, M.-Y. Ngai, *J. Am. Chem. Soc.* **2021**, *143*, 1728-1734.
- [103] J. R. Cockrell, R. W. Murray, *J. Electrochem. Soc.* **1972**, *119*, 849.
- [104] R. N. Renaud, *Can. J. Chem.* **1974**, *52*, 376-380.
- [105] J. Grimshaw, J. Trocha-Grimshaw, *J. Chem. Soc., Perkin Trans. 2* **1975**, 215-218.
- [106] M. Kimura, H. Miyahara, N. Moritani, Y. Sawaki, *J. Org. Chem.* **1990**, *55*, 3897-3902.
- [107] K. Mitsudo, T. Okada, S. Shimohara, H. Mandai, S. Suga, *Electrochemistry* **2013**, *81*, 362-364.
- [108] B. Zhang, C. Qiu, S. Wang, H. Gao, K. Yu, Z. Zhang, X. Ling, W. Ou, C. Su, *Science Bulletin* **2021**, *66*, 562-569.
- [109] C. Liu, S. Han, M. Li, X. Chong, B. Zhang, *Angew. Chem. Int. Ed.* **2020**, *59*, 18527-18531.
- [110] P. Li, C. Guo, S. Wang, D. Ma, T. Feng, Y. Wang, Y. Qiu, *Nat. Commun.* **2022**, *13*, 3774.
- [111] H. Kameo, J. Yamamoto, A. Asada, H. Nakazawa, H. Matsuzaka, D. Bourissou, *Angew. Chem. Int. Ed.* **2019**, *58*, 18783-18787.
- [112] F. Pape, L. T. Brechmann, J. F. Teichert, *Chem. Eur. J.* **2019**, *25*, 985-988.
- [113] J. J. Gair, R. L. Grey, S. Giroux, M. A. Brodney, *Org. Lett.* **2019**, *21*, 2482-2487.
- [114] M. Kuriyama, S. Kujirada, K. Tsukuda, O. Onomura, *Adv. Synth. Catal.* **2017**, *359*, 1043-1048.
- [115] Z. Kuang, S. Mai, K. Yang, Q. Song, *Science Bulletin* **2019**, *64*, 1685-1690.
- [116] N. Li, F. Xiong, K. Gao, *J. Org. Chem.* **2021**, *86*, 1972-1979.

- [117] A. Xia, X. Xie, X. Hu, W. Xu, Y. Liu, *J. Org. Chem.* **2019**, *84*, 13841-13857.
- [118] X. Wang, M.-H. Zhu, D. P. Schuman, D. Zhong, W.-Y. Wang, L.-Y. Wu, W. Liu, B. M. Stoltz, W.-B. Liu, *J. Am. Chem. Soc.* **2018**, *140*, 10970-10974.
- [119] B. Singh, J. Ahmed, A. Biswas, R. Paira, S. K. Mandal, *J. Org. Chem.* **2021**, *86*, 7242-7255.
- [120] M. Han, X. Ma, S. Yao, Y. Ding, Z. Yan, A. Adijiang, Y. Wu, H. Li, Y. Zhang, P. Lei, Y. Ling, *J. An, J. Org. Chem.* **2017**, *82*, 1285-1290.
- [121] H. Li, Y. Hou, C. Liu, Z. Lai, L. Ning, R. Szostak, M. Szostak, *J. An, Org. Lett.* **2020**, *22*, 1249-1253.
- [122] S. Luo, C. Weng, Y. Ding, C. Ling, M. Szostak, X. Ma, *J. An, Synlett* **2021**, *32*, 51-56.
- [123] B. Zhang, H. Li, Y. Ding, Y. Yan, *J. An, J. Org. Chem.* **2018**, *83*, 6006-6014.
- [124] Y. Ding, S. Luo, A. Adijiang, H. Zhao, *J. An, J. Org. Chem.* **2018**, *83*, 12269-12274.
- [125] Y. Ding, S. Luo, C. Weng, *J. An, J. Org. Chem.* **2019**, *84*, 15098-15105.
- [126] L. Ning, H. Li, Z. Lai, M. Szostak, X. Chen, Y. Dong, S. Jin, *J. An, J. Org. Chem.* **2021**, *86*, 2907-2916.
- [127] Z. Yang, X. Zhu, S. Yang, W. Cheng, X. Zhang, Z. Yang, *Adv. Synth. Catal.* **2020**, *362*, 5496-5505.
- [128] W. Ou, X. Xiang, R. Zou, Q. Xu, K. P. Loh, C. Su, *Angew. Chem. Int. Ed.* **2021**, *60*, 6357-6361.
- [129] Y. Gao, X. Zhang, R. D. Laishram, J. Chen, K. Li, K. Zhang, G. Zeng, B. Fan, *Adv. Synth. Catal.* **2019**, *361*, 3991-3997.
- [130] M. C. Carrión, M. Ruiz-Castañeda, G. Espino, C. Aliende, L. Santos, A. M. Rodríguez, B. R. Manzano, F. A. Jalón, A. Lledós, *ACS Catal.* **2014**, *4*, 1040-1053.
- [131] M. Ruiz-Castañeda, M. C. Carrión, L. Santos, B. R. Manzano, G. Espino, F. A. Jalón, *ChemCatChem* **2018**, *10*, 5541-5550.
- [132] P. Yang, L. Zhang, K. Fu, Y. Sun, X. Wang, J. Yue, Y. Ma, B. Tang, *Org. Lett.* **2020**, *22*, 8278-8284.
- [133] Z. P. Vang, A. Reyes, R. E. Sonstrom, M. S. Holdren, S. E. Sloane, I. Y. Alansari, J. L. Neill, B. H. Pate, J. R. Clark, *J. Am. Chem. Soc.* **2021**, *143*, 7707-7718.
- [134] S. Guo, X. Wang, J. S. Zhou, *Org. Lett.* **2020**, *22*, 1204-1207.
- [135] M. Espinal-Viguri, S. E. Neale, N. T. Coles, S. A. Macgregor, R. L. Webster, *J. Am. Chem. Soc.* **2019**, *141*, 572-582.
- [136] J. C. L. Walker, M. Oestreich, *Org. Lett.* **2018**, *20*, 6411-6414.
- [137] L. Li, G. Hilt, *Org. Lett.* **2020**, *22*, 1628-1632.
- [138] J. S. Rowbotham, M. A. Ramirez, O. Lenz, H. A. Reeve, K. A. Vincent, *Nat. Commun.* **2020**, *11*, 1454.
- [139] S. Vaidyanathan, B. W. Surber, *Tetrahedron Lett.* **2005**, *46*, 5195-5197.

- [140] A. Martins, M. Lautens, *Org. Lett.* **2008**, *10*, 4351-4353.
- [141] K. Müller, A. Seubert, *Isot. Environ. Health Stud.* **2014**, *50*, 88-93.
- [142] Y. Huang, J. Chen, B. Liu, H. Wang, L. Zhang, Z. Chen, Y. Zhang, *J. Labelled Compd. Radiopharm.* **2018**, *61*, 355-361.
- [143] O. Fischer, A. Hubert, M. R. Heinrich, *J. Org. Chem.* **2020**, *85*, 11856-11866.
- [144] M. Zhan, R. Xu, Y. Tian, H. Jiang, L. Zhao, Y. Xie, Y. Chen, *Eur. J. Org. Chem.* **2015**, *2015*, 3370-3373.
- [145] A. K. Greene, L. T. Scott, *J. Org. Chem.* **2013**, *78*, 2139-2143.
- [146] A. Tortajada, E. Hevia, *J. Am. Chem. Soc.* **2022**, *144*, 20237-20242.
- [147] T. He, H. F. T. Klare, M. Oestreich, *J. Am. Chem. Soc.* **2022**, *144*, 4734-4738.
- [148] J. L. Garnett, M. A. Long, R. F. W. Vining, T. Mole, *J. Am. Chem. Soc.* **1972**, *94*, 5913-5914.
- [149] M. A. Long, J. L. Garnett, R. F. W. Vining, *J. Chem. Soc., Perkin Trans. 2* **1975**, 1298.
- [150] J. C. Seibles, D. M. Bollinger, M. Orchin, *Angew. Chem. Int. Ed.* **1977**, *16*, 656-657.
- [151] G. Qiao-Xia, S. Bao-Jian, G. Hai-Qing, T. Tamotsu, *Chin. J. Chem.* **2005**, *23*, 341-344.
- [152] M. J. Bezdek, S. Guo, P. J. Chirik, *Science* **2016**, *354*, 730-733.
- [153] W. Li, M.-M. Wang, Y. Hu, T. Werner, *Org. Lett.* **2017**, *19*, 5768-5771.
- [154] B. Dong, X. Cong, N. Hao, *RSC Adv.* **2020**, *10*, 25475-25479.
- [155] Y. Chang, A. Yesilcimen, M. Cao, Y. Zhang, B. Zhang, J. Z. Chan, M. Wasa, *J. Am. Chem. Soc.* **2019**, *141*, 14570-14575.
- [156] J. Garnett, W. Sollich, *Aust. J. Chem.* **1961**, *14*, 441.
- [157] J. Garnett, *J. Catal.* **1963**, *2*, 339-347.
- [158] J. L. Garnett, R. J. Hodges, *J. Am. Chem. Soc.* **1967**, *89*, 4546-4547.
- [159] J. L. Garnett, M. A. Long, A. B. McLaren, K. B. Peterson, *J. Chem. Soc., Chem. Commun.* **1973**, 749.
- [160] D. Hesk, P. R. Das, B. Evans, *J. Labelled Compd. Radiopharm.* **1995**, *36*, 497-502.
- [161] G. J. Ellames, J. S. Gibson, J. M. Herbert, A. H. McNeill, *Tetrahedron* **2001**, *57*, 9487-9497.
- [162] J. M. Herbert, *J. Labelled Compd. Radiopharm.* **2010**, *53*, 658-661.
- [163] J. A. Brown, S. Irvine, A. R. Kennedy, W. J. Kerr, S. Andersson, G. N. Nilsson, *Chem. Commun.* **2008**, 1115.
- [164] J. A. Brown, A. R. Cochrane, S. Irvine, W. J. Kerr, B. Mondal, J. A. Parkinson, L. C. Paterson, M. Reid, T. Tuttle, S. Andersson, G. N. Nilsson, *Adv. Synth. Catal.* **2014**, *356*, 3551-3562.
- [165] A. R. Cochrane, C. Idziak, W. J. Kerr, B. Mondal, L. C. Paterson, T. Tuttle, S. Andersson, G. N. Nilsson, *Org. Biomol. Chem.* **2014**, *12*, 3598-3603.

- [166] J. Atzrodt, V. Derdau, W. J. Kerr, M. Reid, P. Rojahn, R. Weck, *Tetrahedron* **2015**, *71*, 1924-1929.
- [167] W. J. Kerr, M. Reid, T. Tuttle, *ACS Catal.* **2015**, *5*, 402-410.
- [168] W. J. Kerr, D. M. Lindsay, P. K. Owens, M. Reid, T. Tuttle, S. Campos, *ACS Catal.* **2017**, *7*, 7182-7186.
- [169] A. R. Cochrane, S. Irvine, W. J. Kerr, M. Reid, S. Andersson, G. N. Nilsson, *J. Labelled Compd. Radiopharm.* **2013**, *56*, 451-454.
- [170] K. Jess, V. Derdau, R. Weck, J. Atzrodt, M. Freytag, P. G. Jones, M. Tamm, *Adv. Synth. Catal.* **2017**, *359*, 629-638.
- [171] A. Burhop, R. Weck, J. Atzrodt, V. Derdau, *Eur. J. Org. Chem.* **2017**, *2017*, 1418-1424.
- [172] A. Burhop, R. Prohaska, R. Weck, J. Atzrodt, V. Derdau, *J. Labelled Compd. Radiopharm.* **2017**, *60*, 343-348.
- [173] W. Liu, L. Cao, Z. Zhang, G. Zhang, S. Huang, L. Huang, P. Zhao, X. Yan, *Org. Lett.* **2020**, *22*, 2210-2214.
- [174] C. P. Lenges, P. S. White, M. Brookhart, *J. Am. Chem. Soc.* **1999**, *121*, 4385-4396.
- [175] S. Ma, G. Villa, P. S. Thuy-Boun, A. Homs, J.-Q. Yu, *Angew. Chem. Int. Ed.* **2014**, *53*, 734-737.
- [176] V. Müller, R. Weck, V. Derdau, L. Ackermann, *ChemCatChem* **2020**, *12*, 100-104.
- [177] J. Zhang, S. Zhang, T. Gogula, H. Zou, *ACS Catal.* **2020**, *10*, 7486-7494.
- [178] S. Kopf, H. Neumann, M. Beller, *Chem. Commun.* **2021**, *57*, 1137-1140.
- [179] S. Bag, M. Petzold, A. Sur, S. Bhowmick, D. B. Werz, D. Maiti, *Chem. Eur. J.* **2019**, *25*, 9433-9437.
- [180] A. Gholap, S. Bag, S. Pradhan, A. R. Kapdi, D. Maiti, *ACS Catal.* **2020**, *10*, 5347-5352.
- [181] H. Xu, M. Liu, L.-J. Li, Y.-F. Cao, J.-Q. Yu, H.-X. Dai, *Org. Lett.* **2019**, *21*, 4887-4891.
- [182] R. Pony Yu, D. Hesk, N. Rivera, I. Pelczer, P. J. Chirik, *Nature* **2016**, *529*, 195-199.
- [183] J. Corpas, P. Viereck, P. J. Chirik, *ACS Catal.* **2020**, *10*, 8640-8647.
- [184] S. Garhwal, A. Kaushansky, N. Fridman, L. J. W. Shimon, G. d. Ruiter, *J. Am. Chem. Soc.* **2020**, *142*, 17131-17139.
- [185] H. Yang, C. Zarate, W. N. Palmer, N. Rivera, D. Hesk, P. J. Chirik, *ACS Catal.* **2018**, *8*, 10210-10218.
- [186] C. Zarate, H. Yang, M. J. Bezdek, D. Hesk, P. J. Chirik, *J. Am. Chem. Soc.* **2019**, *141*, 5034-5044.
- [187] W. N. Palmer, P. J. Chirik, *ACS Catal.* **2017**, *7*, 5674-5678.
- [188] J. B. Roque, T. P. Pabst, P. J. Chirik, *ACS Catal.* **2022**, 8877-8885.
- [189] M. H. G. Prechtel, M. Hölscher, Y. Ben-David, N. Theyssen, R. Loschen, D. Milstein, W. Leitner, *Angew. Chem. Int. Ed.* **2007**, *46*, 2269-2272.

- [190] B. G. Hashiguchi, K. J. H. Young, M. Yousufuddin, W. A. Goddard, R. A. Periana, *J. Am. Chem. Soc.* **2010**, *132*, 12542-12545.
- [191] M. Farizyan, A. Mondal, S. Mal, F. Deufel, M. van Gemmeren, *J. Am. Chem. Soc.* **2021**, *143*, 16370-16376.
- [192] P. Wedi, M. Farizyan, K. Bergander, C. Mück-Lichtenfeld, M. Gemmeren, *Angew. Chem. Int. Ed.* **2021**, *60*, 15641-15649.
- [193] L. Neubert, D. Michalik, S. Bähn, S. Imm, H. Neumann, J. Atzrodt, V. Derdau, W. Holla, M. Beller, *J. Am. Chem. Soc.* **2012**, *134*, 12239-12244.
- [194] B. Chatterjee, V. Krishnakumar, C. Gunanathan, *Org. Lett.* **2016**, *18*, 5892-5895.
- [195] L. V. A. Hale, N. K. Szymczak, *J. Am. Chem. Soc.* **2016**, *138*, 13489-13492.
- [196] E. Khaskin, D. Milstein, *ACS Catal.* **2013**, *3*, 448-452.
- [197] B. Chatterjee, C. Gunanathan, *Org. Lett.* **2015**, *17*, 4794-4797.
- [198] S. Kar, A. Goeppert, R. Sen, J. Kothandaraman, G. K. Surya Prakash, *Green Chem.* **2018**, *20*, 2706-2710.
- [199] Y. Y. Loh, K. Nagao, A. J. Hoover, D. Hesk, N. R. Rivera, S. L. Colletti, I. W. Davies, D. W. C. MacMillan, *Science* **2017**, *358*, 1182-1187.
- [200] H. Yang, Z. Huang, D. Lehnher, Y.-h. Lam, S. Ren, N. A. Strotman, *J. Am. Chem. Soc.* **2022**, *144*, 5010-5022.
- [201] W. J. Kerr, R. J. Mudd, M. Reid, J. Atzrodt, V. Derdau, *ACS Catal.* **2018**, *8*, 10895-10900.
- [202] K. L. Tuck, P. J. Hayball, *J. Labelled Compd. Radiopharm.* **2001**, *44*, 1005-1011.
- [203] K. L. Tuck, H.-W. Tan, P. J. Hayball, *J. Labelled Compd. Radiopharm.* **2000**, *43*, 817-823.
- [204] C. Boix, M. Poliakoff, *Tetrahedron Lett.* **1999**, *40*, 4433-4436.
- [205] A. L. Waterhouse, H. Rapoport, *J. Labelled Compd. Radiopharm.* **1985**, *22*, 201-216.
- [206] J. Helfenbein, C. Lartigue, E. Noirault, E. Azim, J. Legailiard, M. J. Galmier, J. C. Madelmont, *J. Med. Chem.* **2002**, *45*, 5806-5808.
- [207] A. Damont, S. Garcia-Argote, D.-A. Buisson, B. Rousseau, F. Dollé, *J. Labelled Compd. Radiopharm.* **2015**, *58*, 1-6.
- [208] M. Artelsmair, P. Miranda-Azpiazu, L. Kingston, J. Bergare, M. Schou, A. Varrone, C. S. Elmore, *J. Labelled Compd. Radiopharm.* **2019**, *62*, 265-279.
- [209] H. Sajiki, T. Kurita, H. Esaki, F. Aoki, T. Maegawa, K. Hirota, *Org. Lett.* **2004**, *6*, 3521-3523.
- [210] J. B. Kristensen, S. K. Johansen, J. S. Valsborg, L. Martiny, C. Foged, *J. Labelled Compd. Radiopharm.* **2003**, *46*, 475-488.
- [211] J. Soponpong, K. Dolsophon, C. Thongpanchang, A. Linden, T. Thongpanchang, *Tetrahedron Lett.* **2019**, *60*, 497-500.

- [212] P. L. Norcott, *Chem. Commun.* **2022**, 58, 2944-2953.
- [213] P. Ranjan, S. Pillitteri, E. V. Van der Eycken, U. K. Sharma, *Green Chem.* **2020**, 22, 7725-7736.
- [214] C. Liu, Z. Chen, C. Su, X. Zhao, Q. Gao, G.-H. Ning, H. Zhu, W. Tang, K. Leng, W. Fu, B. Tian, X. Peng, J. Li, Q.-H. Xu, W. Zhou, K. P. Loh, *Nat. Commun.* **2018**, 9, 80.
- [215] M. Maeda, O. Ogawa, Y. Kawazoe, *Chem. Pharm. Bull.* **1977**, 25, 3329-3333.
- [216] M. Maeda, Y. Kawazoe, *Tetrahedron Lett.* **1975**, 16, 1643-1646.
- [217] M. Yamamoto, Y. Yokota, K. Oshima, S. Matsubara, *Chem. Commun.* **2004**, 1714-1715.
- [218] J. G. Atkinson, M. O. Luke, R. S. Stuart, *Can. J. Chem.* **1967**, 45, 1511-1518.
- [219] H. Sajiki, F. Aoki, H. Esaki, T. Maegawa, K. Hirota, *Org. Lett.* **2004**, 6, 1485-1487.
- [220] T. Maegawa, A. Akashi, H. Esaki, F. Aoki, H. Sajiki, K. Hirota, *Synlett* **2005**, 0845-0847.
- [221] H. Sajiki, H. Esaki, F. Aoki, T. Maegawa, K. Hirota, *Synlett* **2005**, 1385-1388.
- [222] H. Esaki, N. Ito, S. Sakai, T. Maegawa, Y. Monguchi, H. Sajiki, *Tetrahedron* **2006**, 62, 10954-10961.
- [223] T. Kurita, F. Aoki, T. Mizumoto, T. Maejima, H. Esaki, T. Maegawa, Y. Monguchi, H. Sajiki, *Chem. Eur. J.* **2008**, 14, 3371-3379.
- [224] T. Kurita, K. Hattori, S. Seki, T. Mizumoto, F. Aoki, Y. Yamada, K. Ikawa, T. Maegawa, Y. Monguchi, H. Sajiki, *Chem. Eur. J.* **2008**, 14, 664-673.
- [225] N. Modutlwa, T. Maegawa, Y. Monguchi, H. Sajiki, *J. Labelled Compd. Radiopharm.* **2010**, 53, 686-692.
- [226] Y. Sawama, Y. Monguchi, H. Sajiki, *Synlett* **2012**, 23, 959-972.
- [227] T. Yamada, Y. Sawama, K. Shibata, K. Morita, Y. Monguchi, H. Sajiki, *RSC Adv.* **2015**, 5, 13727-13732.
- [228] T. Yamada, K. Park, N. Yasukawa, K. Morita, Y. Monguchi, Y. Sawama, H. Sajiki, *Adv. Synth. Catal.* **2016**, 358, 3277-3282.
- [229] K. Park, T. Matsuda, T. Yamada, Y. Monguchi, Y. Sawama, N. Doi, Y. Sasai, S.-i. Kondo, Y. Sawama, H. Sajiki, *Adv. Synth. Catal.* **2018**, 360, 2303-2307.
- [230] H. Sajiki, N. Ito, H. Esaki, T. Maesawa, T. Maegawa, K. Hirota, *Tetrahedron Lett.* **2005**, 46, 6995-6998.
- [231] N. Ito, T. Watahiki, T. Maesawa, T. Maegawa, H. Sajiki, *Adv. Synth. Catal.* **2006**, 348, 1025-1028.
- [232] Y. Sawama, T. Yamada, Y. Yabe, K. Morita, K. Shibata, M. Shigetsura, Y. Monguchi, H. Sajiki, *Adv. Synth. Catal.* **2013**, 355, 1529-1534.
- [233] Y. Sawama, A. Nakano, T. Matsuda, T. Kawajiri, T. Yamada, H. Sajiki, *Org. Process Res. Dev.* **2019**, 23, 648-653.

- [234] V. Derdau, J. Atzrodt, J. Zimmermann, C. Kroll, F. Brückner, *Chem. Eur. J.* **2009**, *15*, 10397-10404.
- [235] K. Park, N. Oka, Y. Sawama, T. Ikawa, T. Yamada, H. Sajiki, *Org. Chem. Front.* **2022**, *9*, 1986-1991.
- [236] V. Pfeifer, T. Zeltner, C. Fackler, A. Kraemer, J. Thoma, A. Zeller, R. Kiesling, *Angew. Chem. Int. Ed.* **2021**, *60*, 26671-26676.
- [237] T. Maegawa, Y. Fujiwara, Y. Inagaki, Y. Monguchi, H. Sajiki, *Adv. Synth. Catal.* **2008**, *350*, 2215-2218.
- [238] L. Gao, S. Perato, S. Garcia-Argote, C. Taglang, L. M. Martínez-Prieto, C. Chollet, D.-A. Buisson, V. Dauvois, P. Lesot, B. Chaudret, B. Rousseau, S. Feuillastre, G. Pieters, *Chem. Commun.* **2018**, *54*, 2986-2989.
- [239] A. Palazzolo, T. Naret, M. Daniel-Bertrand, D. A. Buisson, S. Tricard, P. Lesot, Y. Coppel, B. Chaudret, S. Feuillastre, G. Pieters, *Angew. Chem. Int. Ed.* **2020**, *59*, 20879-20884.
- [240] G. Pieters, C. Taglang, E. Bonnefille, T. Gutmann, C. Puente, J.-C. Berthet, C. Dugave, B. Chaudret, B. Rousseau, *Angew. Chem. Int. Ed.* **2014**, *53*, 230-234.
- [241] C. Taglang, L. M. Martínez-Prieto, I. del Rosal, L. Maron, R. Poteau, K. Philippot, B. Chaudret, S. Perato, A. Sam Lone, C. Puente, C. Dugave, B. Rousseau, G. Pieters, *Angew. Chem. Int. Ed.* **2015**, *54*, 10474-10477.
- [242] A. Palazzolo, S. Feuillastre, V. Pfeifer, S. Garcia-Argote, D. Bouzouita, S. Tricard, C. Chollet, E. Marcon, D. A. Buisson, S. Cholet, F. Fenaille, G. Lippens, B. Chaudret, G. Pieters, *Angew. Chem. Int. Ed.* **2019**, *58*, 4891-4895.
- [243] M. Valero, D. Bouzouita, A. Palazzolo, J. Atzrodt, C. Dugave, S. Tricard, S. Feuillastre, G. Pieters, B. Chaudret, V. Derdau, *Angew. Chem. Int. Ed.* **2020**, *59*, 3517-3522.
- [244] M. Daniel-Bertrand, S. Garcia-Argote, A. Palazzolo, I. Mustieles Marin, P. F. Fazzini, S. Tricard, B. Chaudret, V. Derdau, S. Feuillastre, G. Pieters, *Angew. Chem. Int. Ed.* **2020**, *59*, 21114-21120.
- [245] T. Maegawa, Y. Fujiwara, Y. Inagaki, H. Esaki, Y. Monguchi, H. Sajiki, *Angew. Chem. Int. Ed.* **2008**, *47*, 5394-5397.
- [246] E. Alexakis, J. R. Jones, W. J. S. Lockley, *Tetrahedron Lett.* **2006**, *47*, 5025-5028.
- [247] A. Zuluaga-Villamil, G. Mencia, J. M. Asensio, P.-F. Fazzini, E. A. Baquero, B. Chaudret, *Organometallics* **2022**.
- [248] L. M. Martínez-Prieto, P. W. N. M. van Leeuwen, in *Recent Advances in Nanoparticle Catalysis* (Eds.: P. W. N. M. van Leeuwen, C. Claver), Springer International Publishing, Cham, **2020**, pp. 407-448.
- [249] W. M. Lauer, L. A. Errede, *J. Am. Chem. Soc.* **1954**, *76*, 5162-5163.
- [250] C. G. Macdonald, J. S. Shannon, *Tetrahedron Lett.* **1964**, *5*, 3351-3354.

- [251] J. R. Heys, *J. Labelled Compd. Radiopharm.* **2010**, *53*, 716-721.
- [252] D. Bouzouita, J. M. Asensio, V. Pfeifer, A. Palazzolo, P. Lecante, G. Pieters, S. Feuillastre, S. Tricard, B. Chaudret, *Nanoscale* **2020**, *12*, 15736-15742.
- [253] M. Mamoru, T. Hirohisa, M. Shuntaro, T. Masashi, T. Takehito, N. Yoshiaki, *Chem. Lett.* **1996**, *25*, 165-166.
- [254] G. R. Clemo, G. A. Swan, *J. Chem. Soc.* **1942**, 395-397.
- [255] B. Belleau, J. Burba, M. Pindell, J. Reiffenstein, *Science* **1961**, *133*, 102-104.
- [256] See publication for details.
- [257] M. Hadzic, B. Braïda, F. Volatron, *Org. Lett.* **2011**, *13*, 1960-1963.
- [258] This description denotes Metal@Support-Pyrolysis temperature.

6. Selected publications

The following chapter contains the original publications wherein the previously presented research was reported. My contribution to each publication is outlined in the corresponding subchapter.

Homogenous iron-catalysed deuteration of electron-rich arenes and heteroarenes

Florian Bourriquen, Kathrin Junge,* and Matthias Beller*

Synlett, **2023**, *34*, 332–336.

DOI: 10.1055/a-1992-6596

© Thieme. *Synlett* published by Georg Thieme Verlag KG.

Electronic supporting information is available online.

Contribution

In this paper, I designed the model reaction, optimised the reaction conditions, performed the substrate scope, isolated the products and analysed the data. In addition, I wrote the initial draft of the paper and the supporting information. My contribution accounts for 80%.

Signature of the student

Florian Bourriquen

Signature of the supervisor

Prof. Matthias Beller

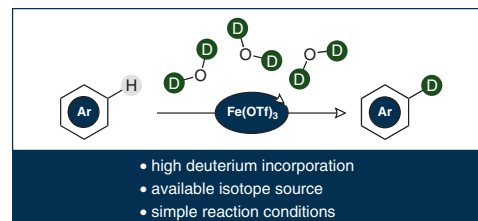
Homogenous Iron-Catalysed Deuteration of Electron-Rich Arenes and Heteroarenes

Florian Bourriquen¹

Kathrin Junge*

Matthias Beller*¹

Leibniz-Institut für Katalyse e.V., Albert-Einstein-Straße 29a,
18059 Rostock, Germany
kathrin.junge@catalysis.de
matthias.beller@catalysis.de



Received: 04.11.2022

Accepted after revision: 27.11.2022

Published online: 04.12.2022 (Accepted Manuscript),

03.01.2023 (Version of Record)

DOI: 10.1055/a-1992-6596; Art ID: ST-2022-11-0473-L



Abstract Deuterated organic molecules are of interest for many applications ranging from mechanistic investigations in basic organic and physical chemistry to the development of new pharmaceuticals. Thus, methodologies for isotope-labelling reactions continue to be important. Here, a convenient methodology for hydrogen/deuterium exchange reactions in electron-rich arenes is reported using simple iron salts and deuterium oxide as isotope source.

Key words catalysis, deuterium, heavy water, isotopic labelling, Lewis acid

Procedures for deuterium incorporation in organic molecules continue to attract the interest of many chemists. Indeed, deuterium-labelled compounds are well-known as standards in mass spectrometry¹ and are of interest in materials sciences to improve properties of polymers,² organic light-emitting diodes (OLEDs),³ and fluorophores.⁴ Regarding life science applications,⁵ in medicinal chemistry the exchange of hydrogen atoms by its stable isotope deuterium not only permits improved absorption, distribution, metabolism, and excretion (ADME) properties of potential drug candidates, but it is also a useful technique to follow metabolic pathways during the drug discovery process.⁶ Attesting the importance given to labelled compounds, three of them were recently authorised as medications for human use. Deutetrabenazine has first been approved in 2017 by the American Food and Drug Administration (FDA) for the treatment of chorea associated with Huntington's disease,⁷ followed by donafenib in China for the treatment of unresectable hepatocellular carcinoma (Figure 1).⁸ Earlier this year, the third one was deucravacitinib, approved by the FDA for the treatment of plaque psoriasis.⁹

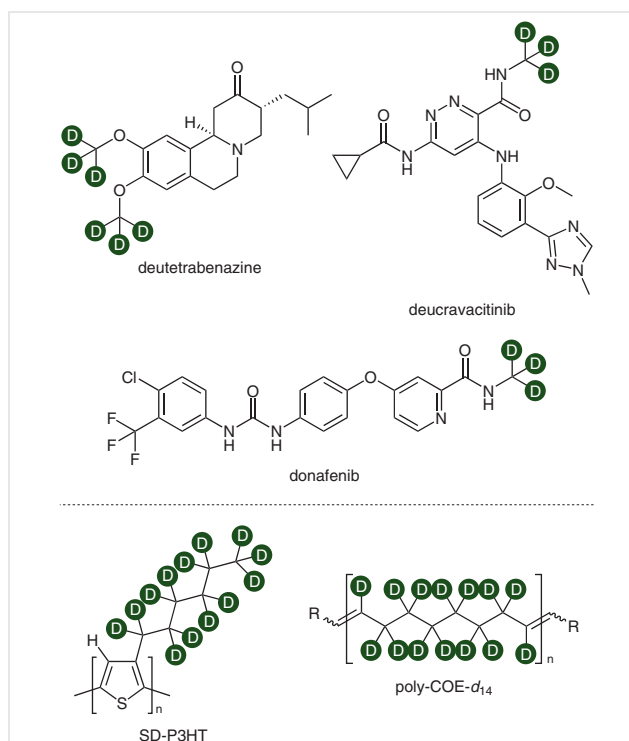


Figure 1 Selected applications of deuterated compounds: structures of marketed deuterated pharmaceuticals; SD-P3HT and polycyclooctene- d_{14} (poly-COE- d_{14}) as deuterated materials

In order to introduce deuterium atoms in organic molecules, numerous approaches are feasible.¹⁰ Simple by conception yet challenging by implementation, hydrogen-isotope exchange (HIE) reactions are among the most desirable techniques for the labelling of organic molecules. Prevalent for numerous years, iridium-catalysed HIE procedures are now supplemented by base-metal catalysis,¹¹ no-

tably with the use of iron¹² and nickel¹³ molecularly defined complexes. Similarly, photocatalytic¹⁴ and electrocatalytic¹⁵ labelling reactions are on the rise. In addition, the use of supported catalysts becomes important in the field of HIE, with reports utilising ruthenium,¹⁶ iridium,¹⁷ palladium,¹⁸ rhodium,¹⁹ iron,²⁰ and manganese²¹ nanoparticles. Another trend in HIE reactions is the use of frustrated Lewis pairs (FLP) and Lewis acids (LA) for the incorporation of deuterium atoms in electron-rich arenes and heteroarenes. In this respect, Werner and co-workers showed the efficacy of tris(pentafluorophenyl)borane (B(C₆F₅)₃) for the labelling of electron-rich arenes and heteroarenes in 2017.²² More recently, Cong and Hao described a similar reactivity of Ag(OTf)₂.²³ Interestingly, both systems use CDCl₃ and D₂O as practical and – relatively – inexpensive solvent mixture and isotope source. Interested in the development of new methodologies for deuterium labelling, we envisioned the use of other Lewis acids as practical and accessible catalysts to complement the already reported investigations.²⁴

We initiated our investigations with the testing of several metal triflate salts for the labelling of 1,2,3,4-tetrahydroquinoline as model substrate. Surprisingly, except for Mg(OTf)₂, all the tested catalysts showed activity and allowed a deuterium content >70% at both the *ortho* and *para* position relative to the nitrogen (Figure 2). In addition, in the presence of D₂O the labile N–H is exchanged to a N–D bond. However, by aqueous workup after the reaction the N–H bond is regenerated. Under the applied reaction conditions, Fe(OTf)₃ was identified as the most active LA, which was also applied in different solvents and at various temperatures (see the Supporting Information for details). In general, a reaction temperature of 90 °C was crucial for the success of this methodology. Then, we examined the effect of the variation of the catalyst loading and quantity of D₂O for our model reaction. Using 2.5 mol% catalyst, the deuterium content is increased to >95% at both the *ortho* and *para* position with 50 equiv of deuterium oxide, highlighting the possibility to reach high deuterium incorporation using this methodology. On the opposite, using only 10 equiv of heavy water lowered the deuterium incorporation (Table 1, entries 1–3). Comparable results were obtained using half of this catalyst loading (Table 1, entries 4–6). The limit of our catalytic system was reached using 0.5 mol% Fe(OTf)₃ (Table 1, entries 7–10). Applying this low catalyst loading, 92% and 93% deuterium incorporation are detected at the *ortho* and *para* positions, respectively (Table 1, entry 8), which are not increased by performing the reaction in CD₃CN. Interestingly, the labelling is not increased with 50 equiv of D₂O. Using 0.1 mol% of Fe(OTf)₃ or D₂O as solvent showed poor deuterium incorporation, possibly due to solubility issues. Considering the higher deuterium enrichment at the *para* position compared to the *ortho* in Table 1, we subsequently monitored a kinetic profile for our model reaction. As can be seen in Figure 3, the deuterium incorporation at the *para* position takes place more rapidly than at the *ortho* position.

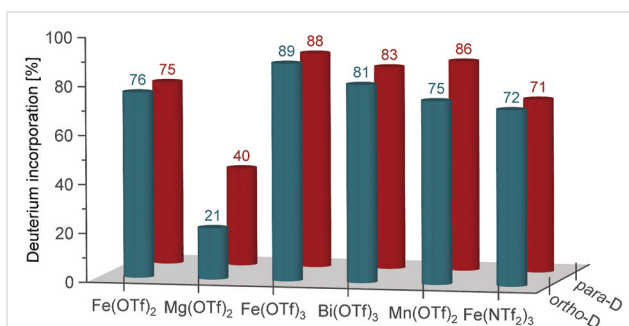
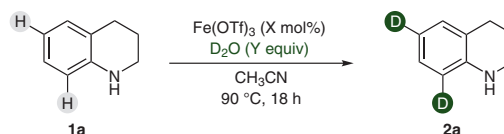


Figure 2 Evaluation of various Lewis acids for the deuterium labelling of 1,2,3,4-tetrahydroquinoline. Reagents and conditions: 1,2,3,4-tetrahydroquinoline (0.5 mmol), Lewis acid (2.5 mol%), D₂O (20 equiv., 180 μL), CH₃CN (1 mL), 90 °C, 18 h.

Table 1 Variation of the Catalyst Loading and Amount of D₂O^a



Entry	Fe(OTf) ₃ (X mol%)	D ₂ O (Y equiv)	<i>ortho</i> -D (%)	<i>para</i> -D (%)
1	2.5	20	90	90
2	2.5	50	95	96
3	2.5	10	83	84
4	1.25	10	81	81
5	1.25	20	90	90
6	1.25	50	95	96
7	0.5	10	83	84
8	0.5	20	92	93
9	0.5	50	65	90
10 ^b	0.5	Solvent	27	41
11	0.1	20	33	57
12	0.1	50	25	45
13	0.1	100	30	54
14 ^b	0.1	Solvent	5	16

^a Reaction conditions: 1,2,3,4-tetrahydroquinoline (0.5 mmol), Fe(OTf)₃ (2.5–0.1 mol%), CH₃CN (1 mL), 90 °C, 18 h.

^b D₂O (1 mL) instead of CH₃CN.

This phenomenon can be explained by the higher stability of Wheland intermediates at the *para* position of amines compared to the *ortho* position.²⁵ Furthermore, a reaction time of 18 h proved to be necessary to achieve high deuterium contents. Besides deuterium incorporation, tritium enrichment is a complementary subject of interest in isotopic labelling.^{5,12a,13,14,26} Inherent to the radioactive nature of tritium, high reaction rates, short reaction times, and the use of small quantities of the isotope source are highly desired.

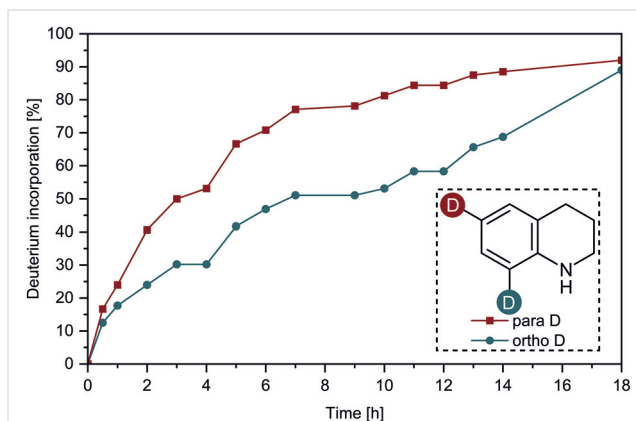
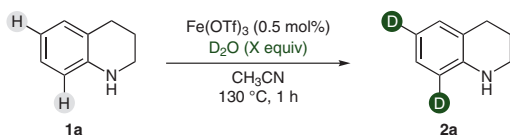


Figure 3 Kinetic profile for the deuterium labelling of 1,2,3,4-tetrahydroquinoline

able. Thus, we explored this methodology at higher temperature (130 °C) for 1 h and observed a deuterium content superior to 80% using 20 equiv of deuterium oxide (Table 2). Pleasingly, only 2 equivalents of D₂O are sufficient to induce a labelling >50%.

Table 2 Deuterium Labelling at High Temperature^a

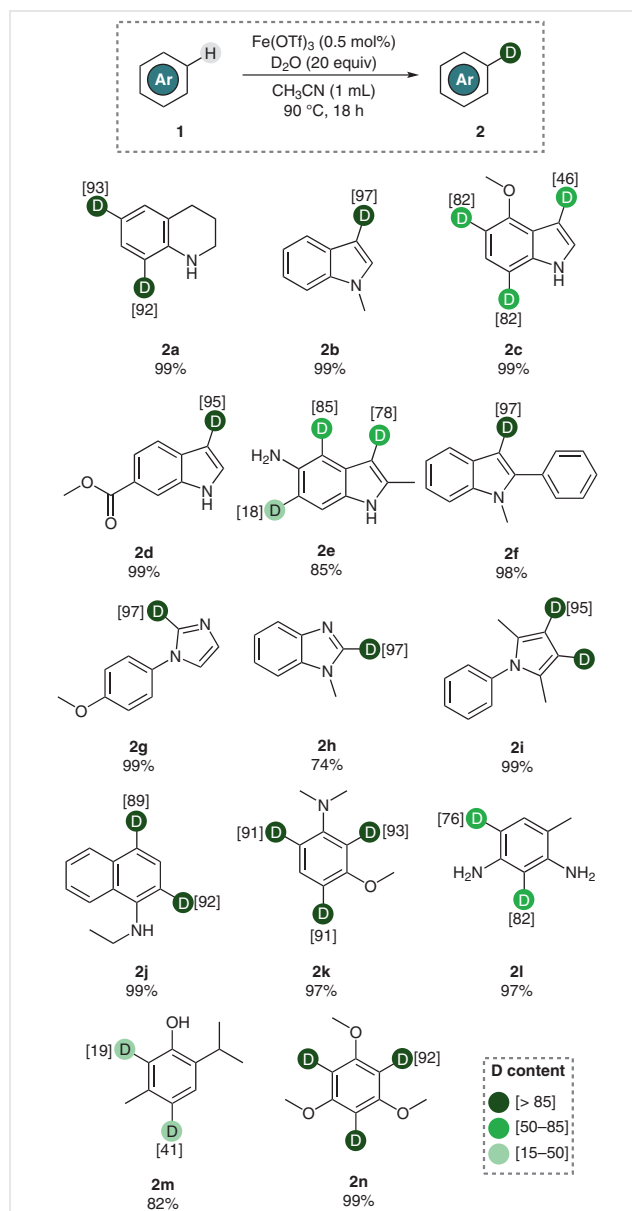


Entry	D ₂ O (X equiv)	ortho-D (%)	para-D (%)
1	20	80	89
2	10	75	85
3	5	71	74
4	2	53	54
5	1	33	36

^a Reaction conditions: 1,2,3,4-tetrahydroquinoline (0.5 mmol), Fe(OTf)₃ (0.5 mol%), CH₃CN (1 mL), 130 °C, 1 h.

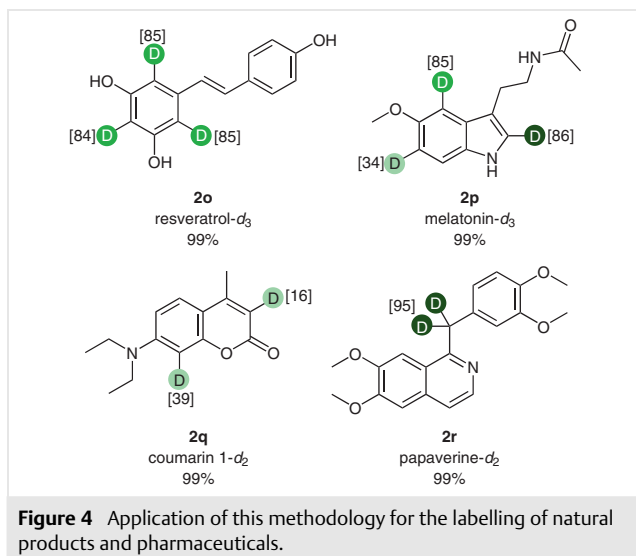
The scope of this methodology was investigated under our optimal reaction conditions (Table 1, entry 8) and is represented in Scheme 1. Gratifyingly, high deuterium incorporation is achievable in a number of indole substrates, preferentially but not limited to the C3 position. Electron-donating substituents such as methoxy (**2c**) or amine (**2e**) increase the overall labelling by permitting isotope incorporation on the benzene ring, when withdrawing ones such as the methyl ester in **2d** allow high deuterium content specifically at C3. Under these conditions, other common *N*-containing heterocycles imidazole (**2g**) and benzimidazole (**2h**) provided a high deuterium content (97%) at the C2 position. Similarly, pyrrole **2i** showed a D enrichment of 95%. When anilines were subjected to our methodology, good to

high deuterium incorporation was observed (**2j–l**). Deuterium content in natural terpenoid **2m** is lower (19% in *ortho*, 41% in *para*), possibly due to the reduced electron-donating properties of phenols in comparison with anilines. Finally, 1,3,5-trimethoxybenzene **1n** provided the corresponding deuterated product with 92% D. Besides model substrates, the applicability of this methodology is showcased with the labelling of natural products and pharmaceuticals (Figure 4). Pleasingly, under our standard reaction conditions, high deuterium incorporation was detected in resveratrol **2o**. Moreover, human hormone melatonin (**2p**) is efficiently la-



Scheme 1 Scope of arenes labelled by the iron triflate methodology. Reagents and conditions: 1,2,3,4-tetrahydroquinoline (0.5 mmol), Fe(OTf)₃ (0.5 mol%), CH₃CN (1 mL), 90 °C, 18 h.

belled at the 2-, 4- and 6-positions. Other relevant substrates labelled by this methodology are the dye coumarin 1 (**2q**), even though with a limited deuterium incorporation for this electron-deficient compound, and alkaloid papaverine (**2r**). In this latter case, the activated methylene group α to the nitrogen is the sole deuterated position as already reported in previous Lewis acid based methodologies.²³



In conclusion, we demonstrate that relatively simple, commercially available Lewis acids can be used for deuterium incorporation in electron-rich positions of arenes and heteroarenes.²⁷ In particular, $\text{Fe}(\text{OTf})_3$ shows good activity and allows for the labelling of a variety of model substrates as well as natural products, dyes, and commercial medications. All these labelling reactions are possible using D_2O as the most available deuterium source.

Conflict of Interest

The authors declare no conflict of interest.

Funding Information

This project has received funding from the European Union's Horizon 2020 research and innovation programme (Grant No 862179).

Acknowledgment

We thank the LIKAT analytical department for excellent service. We thank Sara Kopf (LIKAT) for constructive discussions.

Supporting Information

Supporting information for this article is available online at <https://doi.org/10.1055/a-1992-6596>.

References and Notes

- (a) Atzrodt, J.; Derdau, V. *J. Labelled Compd. Radiopharm.* **2010**, *53*, 674. (b) Lorjaroenphon, Y.; Cadwallader, K. R. *J. Agric. Food Chem.* **2015**, *63*, 776. (c) Engen, J. R.; Botzanowski, T.; Peterle, D.; Georgescauld, F.; Wales, T. E. *Anal. Chem.* **2021**, *93*, 567. (d) James, E. I.; Murphree, T. A.; Vorauer, C.; Engen, J. R.; Guttman, M. *Chem. Rev.* **2022**, *122*, 7562.
- (a) Shao, M.; Keum, J.; Chen, J.; He, Y.; Chen, W.; Browning, J. F.; Jakowski, J.; Sumpster, B. G.; Ivanov, I. N.; Ma, Y.-Z.; Rouleau, C. M.; Smith, S. C.; Geohegan, D. B.; Hong, K.; Xiao, K. *Nat. Commun.* **2014**, *5*, 3180. (b) Li, L.; Jakowski, J.; Do, C.; Hong, K. *Macromolecules* **2021**, *54*, 3555. (c) Tan, X.; Du, J.; Liu, Y.; Ba, J.; Yang, X.; Yang, X.; Liu, M.; Luo, W. *Polymer* **2022**, *251*, 124891.
- Bae, H. J.; Kim, J. S.; Yakubovich, A.; Jeong, J.; Park, S.; Chwae, J.; Ishibe, S.; Jung, Y.; Rai, V. K.; Son, W. J.; Kim, S.; Choi, H.; Baik, M. H. *Adv. Opt. Mater.* **2021**, *9*, 2100630.
- Grimm, J. B.; Xie, L.; Casler, J. C.; Patel, R.; Tkachuk, A. N.; Falco, N.; Choi, H.; Lippincott-Schwartz, J.; Brown, T. A.; Glick, B. S.; Liu, Z.; Lavis, L. D. *JACS Au* **2021**, *1*, 690.
- Atzrodt, J.; Derdau, V.; Kerr, W. J.; Reid, M. *Angew. Chem. Int. Ed.* **2018**, *57*, 1758.
- Pirali, T.; Serafini, M.; Cargini, S.; Genazzani, A. A. *J. Med. Chem.* **2019**, *62*, 5276.
- Schmidt, C. *Nat. Biotechnol.* **2017**, *35*, 493.
- Keam, S. J.; Duggan, S. *Drugs* **2021**, *81*, 1915.
- Treitler, D. S.; Soumeillant, M. C.; Simmons, E. M.; Lin, D.; Inankur, B.; Rogers, A. J.; Dummeldinger, M.; Kolotuchin, S.; Chan, C.; Li, J.; Freitag, A.; Lora Gonzalez, F.; Smith, M. J.; Sfougataki, C.; Wang, J.; Benkovics, T.; Deerberg, J.; Simpson, J. H.; Chen, K.; Tymonko, S. *Org. Process Res. Dev.* **2022**, *26*, 1202.
- (a) Atzrodt, J.; Derdau, V.; Kerr, W. J.; Reid, M. *Angew. Chem. Int. Ed.* **2018**, *57*, 3022. (b) Kopf, S.; Bourriquen, F.; Li, W.; Neumann, H.; Junge, K.; Beller, M. *Chem. Rev.* **2022**, *122*, 6634. (c) Prakash, G.; Paul, N.; Oliver, G. A.; Werz, D. B.; Maiti, D. *Chem. Soc. Rev.* **2022**, *51*, 3123.
- Yang, H.; Hesk, D. *J. Labelled Compd. Radiopharm.* **2020**, *63*, 296.
- (a) Yu, R. P.; Hesk, D.; Rivera, N.; Pelczar, I.; Chirik, P. J. *Nature* **2016**, *529*, 195. (b) Corpas, J.; Viereck, P.; Chirik, P. J. *ACS Catal.* **2020**, *10*, 8640.
- (a) Yang, H.; Zarate, C.; Palmer, W. N.; Rivera, N.; Hesk, D.; Chirik, P. J. *ACS Catal.* **2018**, *8*, 10210. (b) Zarate, C.; Yang, H.; Bezdek, M. J.; Hesk, D.; Chirik, P. J. *J. Am. Chem. Soc.* **2019**, *141*, 5034.
- Yang, H.; Huang, Z.; Lehnerr, D.; Lam, Y.-h.; Ren, S.; Strotman, N. A. *J. Am. Chem. Soc.* **2022**, *144*, 5010.
- (a) Lu, L.; Li, H.; Zheng, Y.; Bu, F.; Lei, A. *CCS Chem.* **2021**, *3*, 2669. (b) Norcott, P. L. *Chem. Commun.* **2022**, *58*, 2944. (c) Li, P.; Guo, C.; Wang, S.; Ma, D.; Feng, T.; Wang, Y.; Qiu, Y. *Nat. Commun.* **2022**, *13*, 3774.
- (a) Pieters, G.; Taglang, C.; Bonnefille, E.; Gutmann, T.; Puente, C.; Berthet, J.-C.; Dugave, C.; Chaudret, B.; Rousseau, B. *Angew. Chem. Int. Ed.* **2014**, *53*, 230. (b) Zuluaga-Villamil, A.; Mencia, G.; Asensio, J. M.; Fazzini, P.-F.; Baquero, E. A.; Chaudret, B. *Organometallics* **2022**, *41*, 3313.
- Valero, M.; Bouzouita, D.; Palazzolo, A.; Atzrodt, J.; Dugave, C.; Tricard, S.; Feuillastre, S.; Pieters, G.; Chaudret, B.; Derdau, V. *Angew. Chem. Int. Ed.* **2020**, *59*, 3517.
- Pfeifer, V.; Zeltner, T.; Fackler, C.; Kraemer, A.; Thoma, J.; Zeller, A.; Kiesling, R. *Angew. Chem. Int. Ed.* **2021**, *60*, 26671.
- Levernier, E.; Tatoueix, K.; Garcia-Argote, S.; Pfeifer, V.; Kiesling, R.; Gravel, E.; Feuillastre, S.; Pieters, G. *JACS Au* **2022**, *2*, 801.

- (20) Li, W.; Rabeah, J.; Bourriquen, F.; Yang, D.; Kreyenschulte, C.; Rockstroh, N.; Lund, H.; Bartling, S.; Surkus, A.-E.; Junge, K.; Brückner, A.; Lei, A.; Beller, M. *Nat. Chem.* **2022**, *14*, 334.
- (21) Bourriquen, F.; Rockstroh, N.; Bartling, S.; Junge, K.; Beller, M. *Angew. Chem. Int. Ed.* **2022**, *61*, e202202423.
- (22) Li, W.; Wang, M.-M.; Hu, Y.; Werner, T. *Org. Lett.* **2017**, *19*, 5768.
- (23) Dong, B.; Cong, X.; Hao, N. *RSC Adv.* **2020**, *10*, 25475.
- (24) Munz, D.; Webster-Gardiner, M.; Fu, R.; Strassner, T.; Goddard, W. A.; Gunnoe, T. B. *ACS Catal.* **2015**, *5*, 769.
- (25) Hadzic, M.; Braïda, B.; Volatron, F. *Org. Lett.* **2011**, *13*, 1960.
- (26) (a) Voges, R.; Heys, J. R.; Moenius, T. *Preparation of Compounds Labeled with Tritium and Carbon-14*; John Wiley & Sons: Chichester, **2009**. (b) Loh, Y. Y.; Nagao, K.; Hoover, A. J.; Hesk, D.; Rivera, N. R.; Colletti, S. L.; Davies, I. W.; MacMillan, D. W. C. *Science* **2017**, *358*, 1182. (c) Koniarczyk, J. L.; Hesk, D.; Overgard, A.; Davies, I. W.; McNally, A. J. *Am. Chem. Soc.* **2018**, *140*, 1990.
- (27) **General Procedure for the Labelling of Electron-Rich (Hetero)arenes**
A 4 mL vial was charged under argon with the substrate (0.5

mmol), Fe(OTf)₃ (1 mL from a stock solution of 14 mg in 10 mL CH₃CN) and D₂O (180 μL, 20 equiv). The reaction mixture was stirred overnight at 90 °C in an aluminium bloc. After return to room temperature, the media was diluted with EtOAc (2 mL) and a saturated aqueous NaHCO₃ solution (1 mL). The aqueous phase was further extracted with EtOAc (3 × 2 mL). The combined organic phases were dried over MgSO₄, filtered, and concentrated under reduced pressure. Obtained products were submitted for NMR analyses to determine the deuterium content. Typical reaction with 1,2,3,4-tetrahydroquinoline (**1a**, 65.5 mg) as substrate provided 1,2,3,4-tetrahydroquinoline-6,8-d₂ (**2a**, brown oil, quantitative). ¹H NMR (300 MHz, CDCl₃): δ = 7.07–6.96 (m, 2 H), 6.66 (t, *J* = 7.4 Hz, 7% ¹H, 1 H), 6.58–6.44 (m, 8% ¹H, 1 H), 3.81 (s, 1 H), 3.38–3.29 (m, 2 H), 2.82 (t, *J* = 6.4 Hz, 2 H), 2.06–1.91 (m, 2 H). ¹³C NMR (75 MHz, CDCl₃): δ = 144.8, 129.4 (m), 126.5 (m), 121.5, 116.7 (m), 113.9 (m), 42.0, 27.0, 22.2. ESI-MS: *m/z* calcd for C₉H₉D₂N: 135; found: 135 (81), 134 (100), 133 (29), 132 (18), 131 (7), 120 (27), 106 (11), 93 (7), 79 (10), 66 (6).

Scalable and selective deuteration of (hetero)arenes

Wu Li, Jabor Rabeah, Florian Bourriquen, Dali Yang, Carsten Kreyenschulte, Nils Rockstroh, Henrik Lund, Stephan Bartling, Annette-Enrica Surkus, Kathrin Junge, Angelika Brückner,* Aiwun Lei,* and Matthias Beller*

Nat. Chem. **2022**, *14*, 334–341

DOI:10.1038/s41557-021-00846-4

This document is available under the CC BY 4.0 license. © The Authors 2022. Nature Chemistry published by Springer Nature.

Electronic supporting information is available online.

Contribution

For this project, I participated in the discussions, synthesised the catalyst and applied it for substrate scope and mechanistic investigations. My contribution to this paper accounts for 20%.

Signature of the student

Florian Bourriquen

Signature of the supervisor

Prof. Matthias Beller



OPEN

Scalable and selective deuteration of (hetero)arenes

Wu Li¹, Jabor Rabeah¹, Florian Bourriquen¹, Dali Yang², Carsten Kreyenschulte¹, Nils Rockstroh¹, Henrik Lund¹, Stephan Bartling¹, Annette-Enrica Surkus¹, Kathrin Junge¹, Angelika Brückner¹✉, Aiwen Lei²✉ and Matthias Beller¹✉

Isotope labelling, particularly deuteration, is an important tool for the development of new drugs, specifically for identification and quantification of metabolites. For this purpose, many efficient methodologies have been developed that allow for the small-scale synthesis of selectively deuterated compounds. Due to the development of deuterated compounds as active drug ingredients, there is a growing interest in scalable methods for deuteration. The development of methodologies for large-scale deuterium labelling in industrial settings requires technologies that are reliable, robust and scalable. Here we show that a nanostructured iron catalyst, prepared by combining cellulose with abundant iron salts, permits the selective deuteration of (hetero)arenes including anilines, phenols, indoles and other heterocycles, using inexpensive D₂O under hydrogen pressure. This methodology represents an easily scalable deuteration (demonstrated by the synthesis of deuterium-containing products on the kilogram scale) and the air- and water-stable catalyst enables efficient labelling in a straightforward manner with high quality control.

Isotope labelling methodologies play an essential part in the development of new pharmaceuticals and agrochemicals¹ (Fig. 1a). For example, in the pharmaceutical industry, isotopes of active drugs are commonly prepared to understand their metabolism and to identify specific metabolites (Fig. 1b). The most common isotopic labels are deuterium atoms, which are also well suited to determine kinetic isotope effects (KIEs) in fundamental mechanistic investigations that result from differences in the rate of C–H versus C–D bond cleavage^{2,3} (Fig. 1c). Deuterium-labelled compounds show virtually identical physical behaviour to that of their hydrogen analogues, whilst differing in molecular mass, and thus are the primary source for the preparation of internal standards for liquid chromatography–mass spectrometry (LC–MS) analysis in the investigation of environmental, animal and human samples^{4,5} (Fig. 1d). Accordingly, deuteration facilitates advancements in metabolomics including metabolite identification and quantification, in toxicogenomic studies for the related reactive metabolites and in proteomics studies.

Due to the potentially improved pharmacokinetic and pharmacological properties of deuterium-labelled compounds, while retaining almost the same chemical structure and physical properties as the unlabelled counterparts, in recent years this class of compounds has gained increasing interest as actual medications^{6,7}. Notably, in 2017 the Food and Drug Administration (FDA) cleared the first deuterated drug, Austedo, for the treatment of Huntington's-disease-related disorders⁸. Meanwhile, several deuterated compounds are in clinical trials for various applications. Based on these developments, there is growing potential and interest in accessing selectively deuterated building blocks on a larger scale. In this context, specific and practical labelling methodologies for arenes/heteroarenes as well as amines, which are found in most small-molecule-based drugs, are of increasing importance. Critical parameters for such applications are the availability and price of the

labelling reagent, catalysts and so on, and the feasibility of the process in an industrial setting. Notably, precise control of impurities, degree of deuteration and consistency are also prerequisites for any real-life implementation⁹.

Acid-mediated hydrogen–deuterium exchange reactions (H/D exchange) are among the oldest methods known for labelling of arenes. Nevertheless, they allow selective incorporation of deuterium only for simple substrates following an electrophilic aromatic substitution mechanism (Fig. 1e)¹⁰. In most of the known protocols, the necessity to use high temperatures and stoichiometric amounts of concentrated strong acids leads to poor functional group tolerances and safety risks, especially on a larger scale¹¹.

Based on advances in homogeneous metal-catalysed C–H activation, a variety of organometallic complexes have evolved for catalytic H/D exchange reactions of arenes, as well as aliphatic amines in the α or β positions (Fig. 1f)^{12–15}. For example, homogeneous iridium-based Crabtree and Kerr catalysts have been used for C(*sp*²)–H hydrogen isotope exchange reactions using D₂ gas^{16,17}. Chirik and co-workers first reported the use of a molecularly defined iron catalyst for the tritiation/deuteration of pharmaceutical drugs at aromatic C–H moieties using D₂ and T₂ gas¹⁸. More recently, the MacMillan group developed a photochemical-catalysed hydrogen-isotope-exchange (HIE) method for the selective labelling of *N*-alkylamine-based drugs¹⁹.

Apart from photocatalysts and defined organometallic complexes, heterogeneous materials have also been studied in labelling reactions. So far, Pd/C and Pt/C are known to catalyse multi H/D exchange of arenes and heterocyclic amines²⁰. In addition, ruthenium- and iridium-based catalysts in the presence of D₂ have been developed with promising activity^{21,22}. Unfortunately, in all these cases the selectivity and the tolerance of easily reducible functional groups and halogens is challenging. Furthermore, besides those based on nickel²³, all heterogeneous catalysts known

¹Leibniz-Institut für Katalyse e.V., Rostock, Germany. ²Institute for Advanced Studies (IAS), Wuhan University, Wuhan, P. R. China.

✉e-mail: angelika.brueckner@catalysis.de; aiwenlei@whu.edu.cn; matthias.beller@catalysis.de

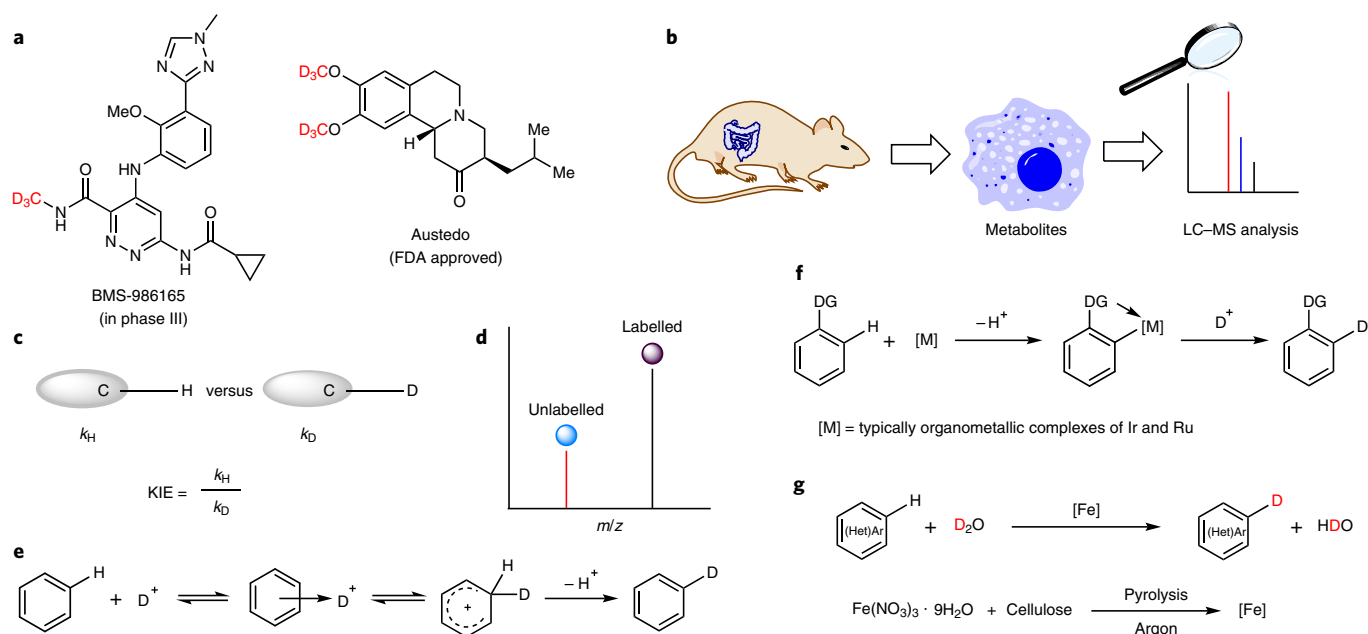


Fig. 1 | Applications of deuteration and methods for H/D exchange. **a**, Deuterated drug molecules: Austedo has been approved by the FDA and BMS-986165 is under trial. **b**, Identification of specific metabolites using LC-MS: accurate analysis of metabolites based on stable isotope labelling coupled with LC-MS analysis. **c**, KIE investigations based on C-H versus C-D bond cleavage. **d**, Preparation of internal standards for LC-MS analysis. The isotopically labelled internal standards can be used for quantitative determination. **e**, Acid-mediated H/D exchange. **f**, Transition-metal-catalysed H/D exchange. DG, directing group. **g**, This work: nanostructured iron catalyst for H/D exchange of (hetero)arenes using D_2O .

for deuteration rely on expensive precious metals, which hamper their use in the agrochemical, pharmaceutical or food industries as those metals must be removed completely from the final products according to regulations. Apart from the catalyst and the reaction conditions, the source of deuterium is critical for the application of such methodologies. This is especially true for the preparation of labelled building blocks on the multi-gram or even kilogram scale. In this respect, cheap, safe and operationally convenient D_2O is the ideal source for such transformations because it is basically the parent compound for all other deuteration reagents, including D_2 .

In this article we report a unique heterogeneous iron catalyst for general and practical deuteration of arenes and heteroarenes. Using D_2O in the presence of a biomass-derived iron catalyst under hydrogen pressure allows for the preparation of >90 selectively deuterated building blocks, representative drugs and natural products with high and reliable deuterium incorporation (Fig. 1g).

Results and discussion

Reaction development. Initially, we tested standard, commercially available heterogeneous catalysts and tailor-made supported nanoparticles (NPs) for selective deuteration of 4-phenylmorpholine in D_2O (Supplementary Table 1). This benchmark substrate was chosen because it permits labelling both at the nitrogen-containing heterocycle and the phenyl ring. In all cases, the extent of isotopic exchange was determined using 1H NMR spectroscopy. In agreement with previous works²⁴, Pd/C led to deuterium incorporation at the α position of the nitrogen atom on the morpholine ring (Supplementary Table 1, entry 1). Recently, we introduced a variety of supported 3d-metal NPs for selective hydrogenation and oxidation reactions^{25,26}. In this context, iron-based NPs are particularly attractive to us due to the abundance, low cost and negligible safety concerns of iron salts. Much to our surprise, pyrolysis of $Fe(NO_3)_3 \cdot 9H_2O$ with cellulose resulted in highly active and selective catalytic systems for deuteration of the phenyl ring in the *ortho* and *para* positions, which even outperformed commercial

catalysts such as Pt/C, Au/C and Ru/C (Supplementary Table 1, entry 10 versus entries 2 and 4). The deuterium incorporation could be further improved under hydrogen pressure (Supplementary Table 1, entry 12). Furthermore, the stability and recyclability of the catalyst under H_2 are better (Supplementary Information, section 5). Pseudo in situ X-ray photoelectron spectroscopy (XPS) studies show that the iron oxides formed on the surface of the catalyst during the catalysis could be partially reduced to Fe(0) when heating the sample under H_2 (Supplementary Fig. 6). Finally, the benchmark reaction performed with D_2O in the presence of hydrogen at 120 °C gave nearly quantitative deuteration (see Supplementary Table 1 for more details).

Catalyst characterization. To understand the structure of the most active material (Fe-Cellulose-1000), powder X-ray diffraction, XPS, scanning transmission electron microscopy (STEM) and X-ray absorption spectroscopy (XAS) investigations were performed. These results show that the freshly pyrolysed catalyst consists of Fe/ Fe_3C particles 20–50 nm in size, covered by a shell of up to 30 graphene layers with an overall thickness of 6–10 nm. Embedding the particles in the carbon matrix prevents them from undesired aggregation. During the early stages of the catalytic reaction, the graphene cover is partly removed, thus enabling the contact of the iron surface with reactants. Then, during the reaction, Fe_3C is partly converted to metallic iron which is considered as active phase in the reaction (for details see Supplementary Information, section 6).

Mechanistic studies. Next, investigations of KIE and electron paramagnetic resonance (EPR) studies were performed to obtain a better mechanistic understanding (Supplementary Information, section 7). According to comparison experiments of the model substrate, the reaction is roughly four times faster in H_2O than in D_2O . Apparently, the cleavage of the D-OD bond is the rate-limiting step in this process (Fig. 2a and Supplementary Fig. 13). Interestingly, by comparing the deuteration of aniline and 3,5-dideuterioaniline, a

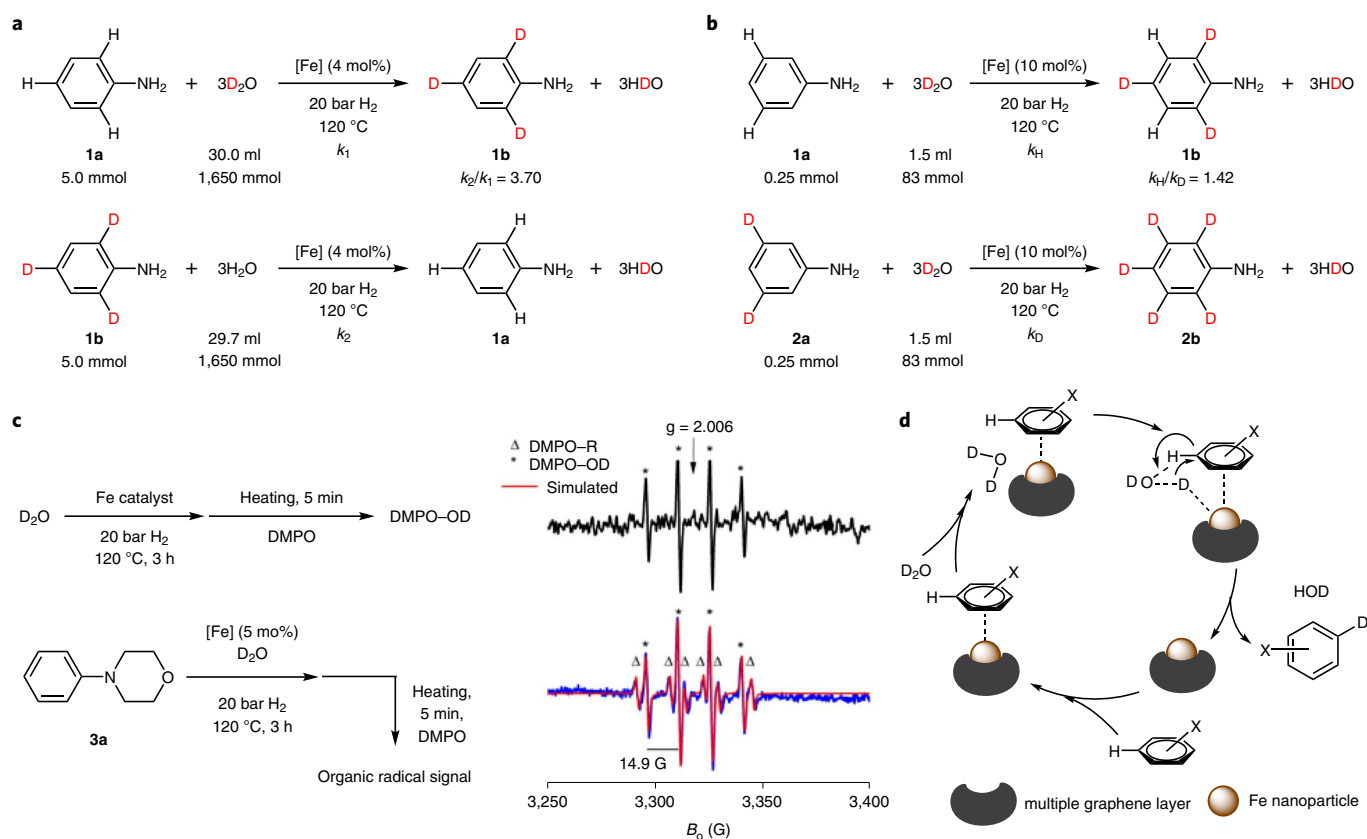


Fig. 2 | Mechanistic studies and proposed mechanism. **a**, Aniline in D_2O and aniline-2,4,6- d_3 in H_2O were used for the KIE studies. The reaction in H_2O is roughly four times faster than the reaction in D_2O . **b**, Deuteration of aniline and 3,5-dideuterioaniline in D_2O were performed for KIE studies, and a minor secondary KIE was observed. **c**, EPR studies: $\ast\text{OD}$ radical trapping using DMPO and detection of the DMPO-R spin adduct. This indicates that formation of radical intermediates is a consequence of homolytic D-OD scission initiated by the iron catalyst. **d**, Proposed mechanism: the multiple graphene layer is removed during the early stages of the catalytic reaction, thus enabling contact of the iron surface with D_2O and reactants. The key step of the reaction is D_2O splitting by the iron catalyst. The resulting radicals are not liberated into the solution but remain adsorbed on the catalyst surface.

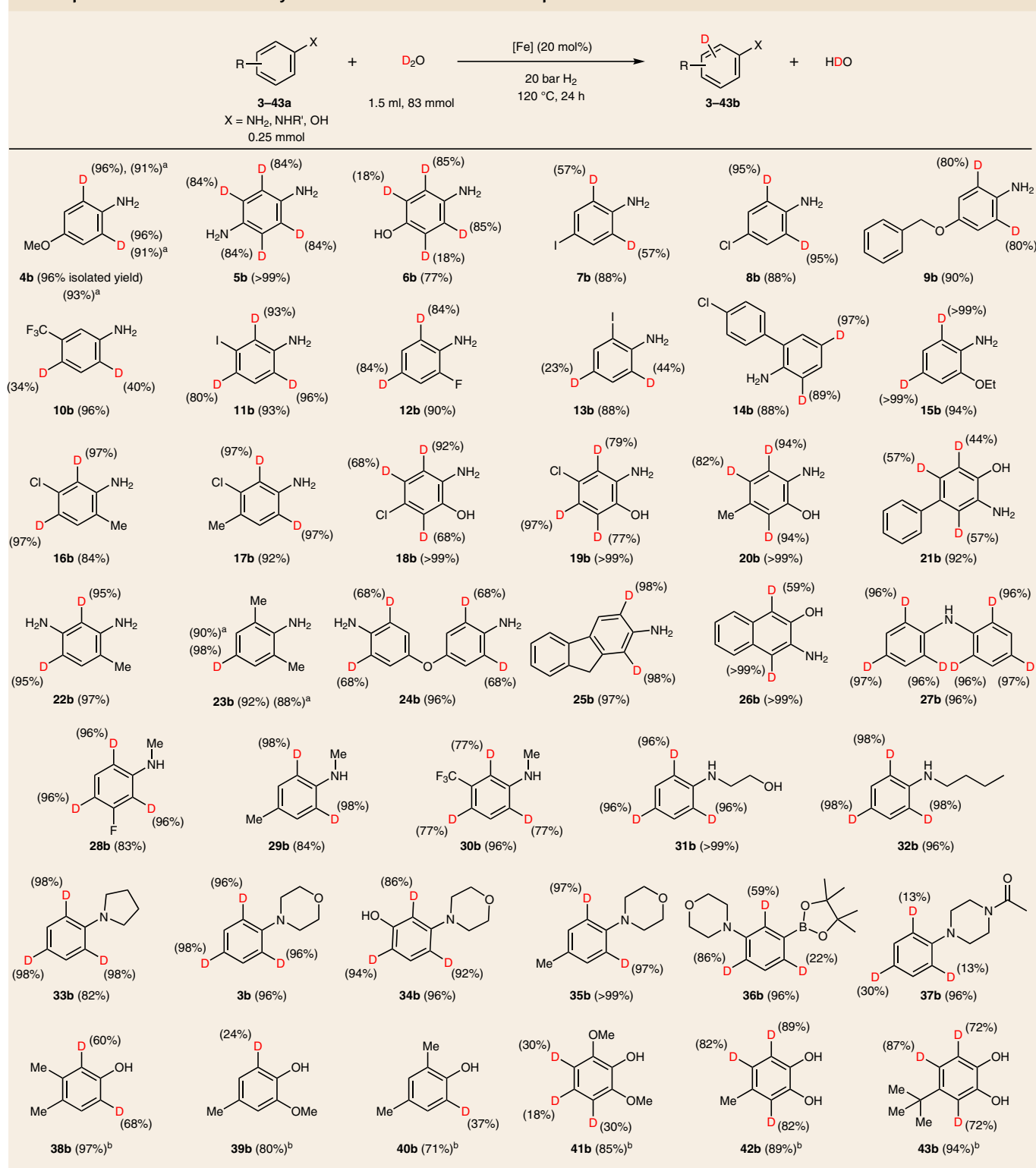
minor secondary KIE is also observed (Fig. 2b and Supplementary Fig. 14). This kinetically relevant result may be explained by the slightly different coordination of the deuterated and non-deuterated substrate to active catalyst centres on the surface. To check whether radicals are formed upon cleavage of the D-OD bond, EPR measurements with the spin trap 5,5-dimethyl-1-pyrroline-*N*-oxide (DMPO) have been performed (Supplementary Information, section 7.2). In a blind experiment, the catalyst was heated in D_2O before DMPO was added, and an EPR spectrum was recorded immediately after quenching the reaction to room temperature. This spectrum showed only a weak but characteristic hyperfine structure quartet signal of DMPO-OD spin adducts²⁷ which results from trapping $\ast\text{OD}$ radicals by DMPO (Fig. 2c black line). This shows that the iron catalyst can promote to a small extent homolytic splitting of D_2O . However, in the presence of 4-phenylmorpholine, an additional hyperfine structure sextet characteristic of a DMPO-R spin adduct²⁸ was detected (Fig. 2c, blue line), suggesting that $\ast\text{OD}$ subtract hydrogen atoms from the substrate, forming HOD, leaving behind $\ast\text{R}$ radicals. Interestingly, no $\ast\text{R}$ radicals were detected when the iron catalyst and the 4-phenylmorpholine substrate were heated in toluene, which indicates that formation of radical intermediates is a consequence of homolytic D-OD scission initiated by the iron catalyst. Considering the well-known fact that $\ast\text{OD}$ radicals are very reactive and unselective, the observed high selectivity is surprising.

Proposed mechanism. We propose a concerted mechanism in which D_2O is split homogeneously by the iron catalyst, yet the

resulting radicals are not liberated into the solution but remain adsorbed on the catalyst surface as activated D^\ast and $\ast\text{OD}$ species. $\ast\text{OD}$ abstracts a hydrogen atom from the phenyl ring, forming HOD and the corresponding phenyl \ast species^{29,30}, which subsequently produces D-R (Fig. 2c,d). The observed high *ortho/para* selectivity may be a result of electron density transfer from the electron-rich metallic iron particle to the adsorbed aromatic ring because this is well known to promote electrophilic *ortho/para* substitutions.

Synthetic scope. Building blocks. Having established the optimized conditions, we then evaluated the substrate scope of the system and its tolerance towards functional groups. Because anilines are used for the synthesis of diverse building blocks for agrochemicals and pharmaceuticals, we started to explore the deuteration of functionalized anilines. Indeed, Fe-Cellulose-1000 permitted smooth deuteration of 35 different anilines with excellent chemo- and regioselectivity (Table 1, 3–37b).

In general, the transformations can be easily run on the gram-scale (4b and 23b). Diverse halogen-containing (for example, chlorine and iodine) anilines afforded the deuterated products (7b, 8b, 11–14b and 16–19b) without notable dehalogenation side-reactions, which is a common problem of precious-metal-based catalysts. We demonstrated the isotopic purity of chloro-, bromo- and iodo-containing compounds by LC-MS (Supplementary Information, section 8.3). Furthermore, deuteration of some phenols in the presence of the iron catalyst showed deuterium incorporation after an extended time (Table 1,

Table 1 | Nanostructured iron catalyst for deuteration of anilines and phenols

Deuterium content determined by quantitative ¹H NMR. ^aThe reaction was performed on the gram scale. ^bThe reaction time was 72 h.

38–43b). Like the model system, negligible or no deuterium incorporation is observed for several representative substrates (**3a**, **4a**, **38a**, **44a**, **52a** and **67a**) in the absence of the iron catalyst (Supplementary Fig. 16).

Next, deuteration of different nitrogen-containing heteroarenes such as pyridines, tetrahydroquinolines, phenothiazines, phenoxazines, indoles, indolines and quinolines, and even those

bearing two nitrogen atoms, were investigated. Such heterocycles are representative structural components of modern pharmaceuticals: 59% of FDA-approved drugs contain a nitrogen heterocyclic motif³¹. As shown in Table 2, catalytic labelling provided the corresponding products (**44–66b**). Notably, for anilines and phenols the regioselectivity of the labelling reaction is in accordance with an electrophilic aromatic substitution mechanism. However,

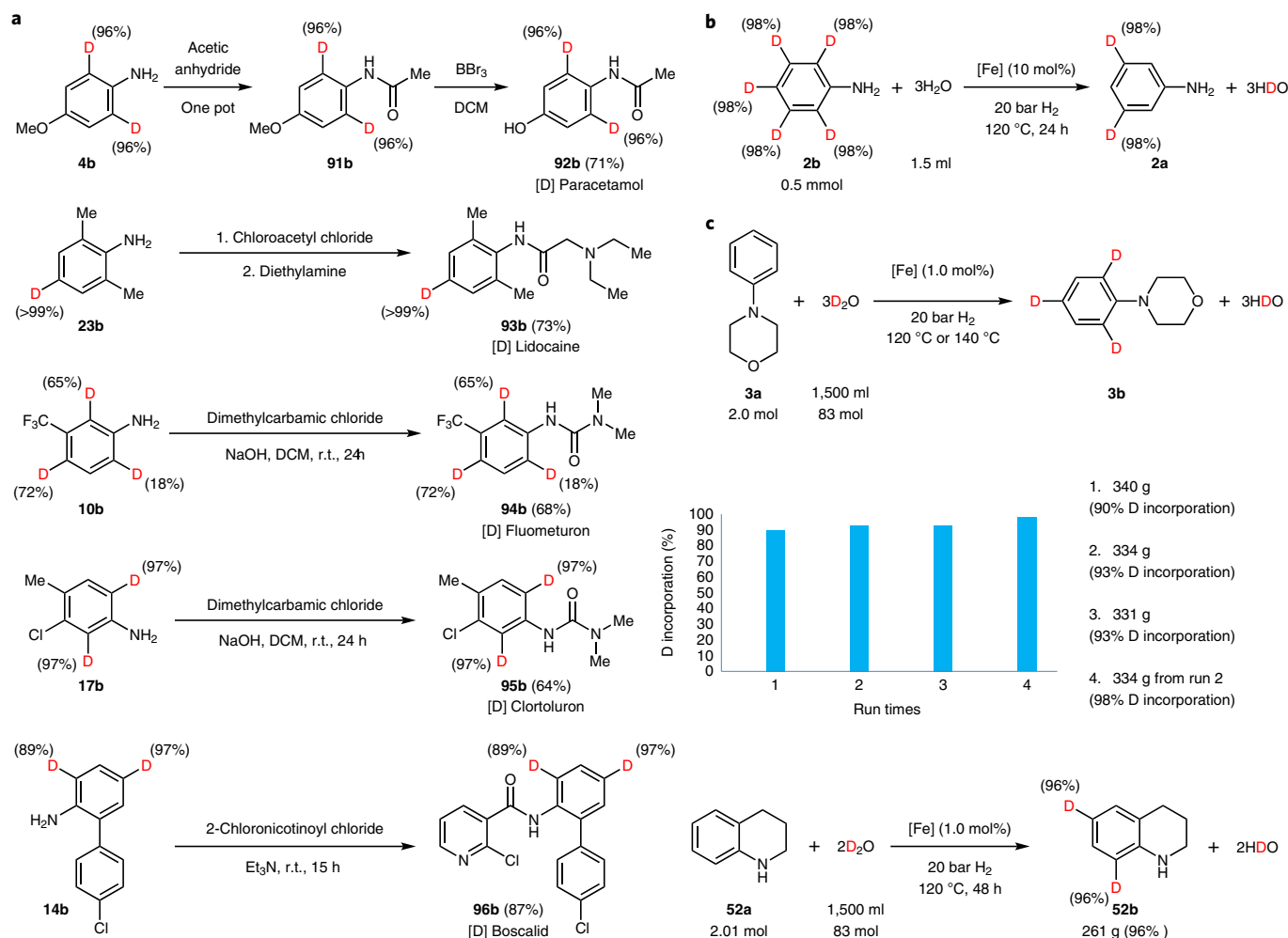


Fig. 3 | Synthetic applications and large-scale synthesis. **a**, Preparation of deuterated *N*-acylated anilines. Deuterated drugs, herbicides and fungicide were prepared from the corresponding deuterated anilines. **b**, Dedeuteration of perdeuterated aniline using H₂O to 3,5-dideuterioaniline. **c**, Scale-up reactions: reuse of the iron catalyst on the 2.0 mol scale. Overall, 1.005 kg 4-phenylmorpholine (6.17 mol) was deuterated using the same catalyst batch; >95% deuterium-labelled 4-phenylmorpholine and 1,2,3,4-tetrahydroquinoline were produced.

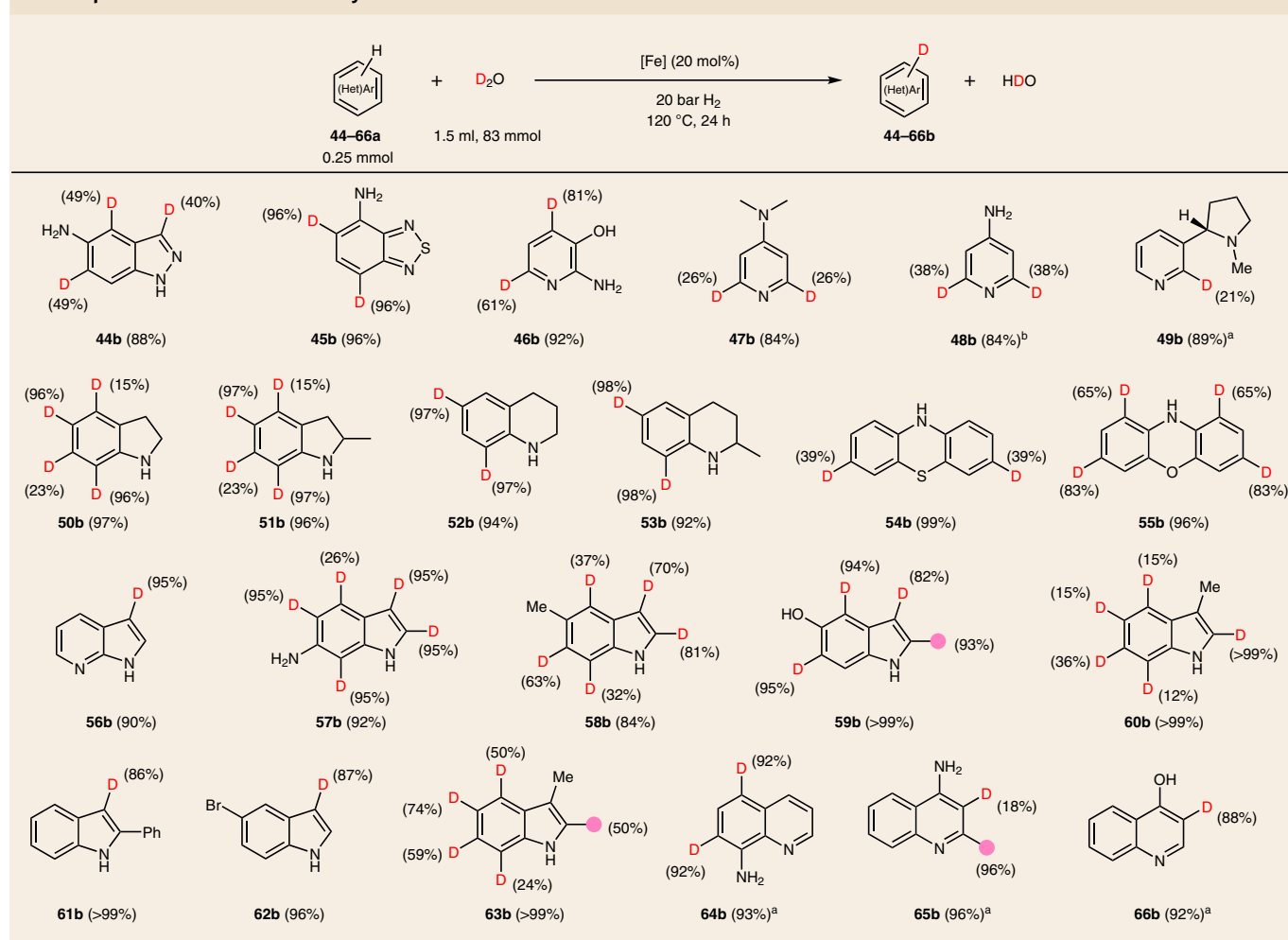
using pyridines, indoles or indolines, different reactivity patterns are observed, which hints towards a different process.

Natural products and pharmaceuticals. To further showcase the utility of iron-catalysed H/D exchange reactions, late-stage deuteration of representative drugs and natural products was investigated (Table 3). For example, melatonin is converted into the deuterated **67b** with high levels of deuterium incorporation. Similarly, *N*-acetylserotonin is deuterated to give **68b**. Purine-containing compounds, such as nucleoside analogues kinetin, inosine, pentoxifylline and the nucleobase adenine, are labelled to the products **69–71b** and **73b**. Alkaloids, for example, brucine and strychnine, are deuterated at both aromatic rings and in the heterocyclic ring in the α position to the nitrogen (**74b** and **75b**). In the case of nicotinic acid, labelling occurred with relatively lower deuterium incorporation selectively to give **76b**. Furthermore, natural phenol derivatives, for example, tyrosol, resveratrol, thymol, arbutin and piceid, were evaluated (**77–81b**). Tetrahydroquinoline alkaloids, for example, augustureine and galipinine, also proceeded with deuterium labelling (**82b** and **83b**). Aniline derivatives such as dropropizine, DL-aminogluthethimide and nimodipine-NH₂ were deuterated with good selectivity (**84–86b**). Notably, medications such as carvedol, estradiol and

O-desmethylvenlafaxine gave the deuterium analogues **87–89b**. As an example, for selective deuteration of an aromatic amino acid, L-tryptophan was employed to directly give **90b**. In all cases shown above the standard catalytic protocol was used and no further optimization was performed. However, it should be noted that the deuterium incorporation can be substantially improved at higher temperature (**84b** and **90b**).

Following standard conditions, deuteration of *N*-acylated anilines is more difficult; however, such labelled products can be conveniently prepared from the corresponding deuterated anilines (Fig. 3a). For instance, 2,6-D-labelled paracetamol **92b** was readily synthesized with excellent deuterium incorporation. Deuterated lidocaine **93b**, herbicides fluometuron **94b** and chlortoluron **95b** as well as fungicide boscalid **96b** were obtained from the corresponding deuterated anilines.

All these cases demonstrate that the presented methodology works well with amino- and/or hydroxyl-substituted arenes as well as heteroarenes; however, less electron-rich benzenes, for example, 1-bromo-, 1-chloro- and 1-fluoro-4-methoxybenzene and 1-methyl-4-(trifluoromethyl)benzene, showed no notable deuterium incorporation under standard conditions. In case of successful labelling as described above deuteration occurred at the most

Table 2 | Nanostructured iron catalyst for deuteration of heteroarenes

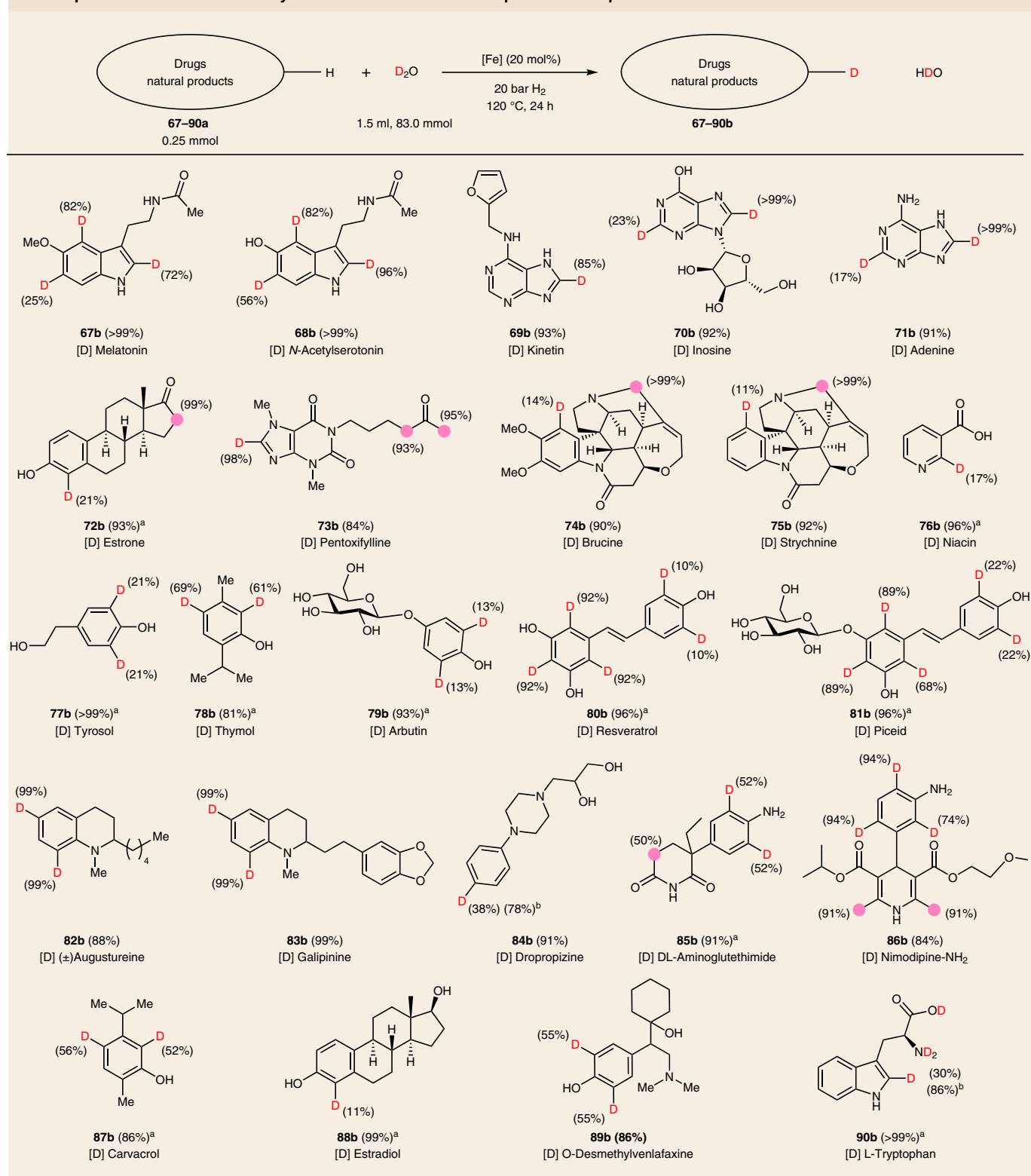
Deuterium content determined by quantitative ¹H NMR. ^aThe reaction was performed at 140 °C for 24 h. The pink circles and numbers denote the positions of the C–H bonds that are labelled and the percentage incorporation of the hydrogen isotope, respectively.

electron-rich positions. Obviously, this limits the possibilities to obtain deuterated compounds at other positions. For example, 2,4,6-trideuterated anilines are conveniently available, while selective deuteration at the 3- and 5-positions are apparently not possible. However, we envisioned a convenient strategy to overcome this limitation: non-selective deuteration of anilines is known in the presence of Pt/C (ref. ³²). Subsequent selective D/H exchange using our Fe-Cellulose-1000 catalyst in water makes it possible to selectively obtain deuterium isomers at positions that are not prone to electrophilic substitution reactions. Thus, 3,5-dideuterioaniline **2a** is obtained from aniline via the perdeuterated derivative (Fig. 3b).

Having established complementary approaches for selective deuteration of a variety of substrates, we then evaluated some practical aspects of our catalyst system. It should be noted that most of the reactions shown above have been performed on a scale typically used in drug discovery. However, as shown in Fig. 3c it is possible to conveniently run such labelling reactions on the 20 to >300 g scale (Supplementary Information, section 9), with the only limitation being the size of the commercial autoclave. In general, stability, reusability and avoidance of metal contamination are intrinsic advantages to the use of any heterogeneous catalyst. To demonstrate these benefits, the iron catalyst was recycled up to five times for the benchmark reaction. As depicted in Supplementary Fig. 18, no substantial loss of activity was observed. During deuteration reactions, an oxidic structure composed of Fe²⁺ and Fe³⁺ was formed as proven by XPS (Supplementary Fig. 5). With respect to metal contamination of the

product, inductively coupled plasma optical emission spectrometry measurements of the D₂O solution detected no iron leaching in any of these runs (Supplementary Table 8). Notably, the recycled catalyst system can also be used for different substrates, which is important in the context of multipurpose batch reactors, which dominate in the pharmaceutical industry. Thus, labelled products with high deuterium incorporation were produced on >1 kg scale from the same catalyst batch (Fig. 3c and Supplementary Information, section 9).

In summary, we have developed a general methodology for heterogeneous iron-catalysed deuteration reactions. We believe this protocol paves the way for practical labelling processes and the large-scale synthesis of specific deuterated building blocks. Although the quality of different deuteration reactions was performed as accurately as possible (Supplementary Tables 5 and 6), all presented developments took place under conditions that did not conform to good manufacturing practice. The optimal biomass-derived catalyst allows for an activation and utilization of low-cost D₂O. The performance of this catalyst system is improved in the presence of hydrogen, which leads to in situ reduction of iron oxides on the surface as indicated by pseudo in situ XPS measurements (Supplementary Fig. 6). The presented system is effective for the selective deuteration of anilines, indoles, phenols and other heterocyclic compounds, including late-stage labelling of natural products and bioactive molecules, and can be readily used for the preparation of deuterated compounds on the kilogram scale. By using complementary approaches, different positional deuterated products can also be obtained in a practical manner.

Table 3 | Nanostructured iron catalyst for deuteration of natural products and pharmaceuticals

Representative drugs, hormones, nucleobases, steroids, alkaloids, amino acids, upscale and applications. Deuterium content determined by quantitative ¹H NMR. ^aThe reaction time was 72 h. ^bThe reaction was performed at 140 °C for 24 h. The pink circles and numbers denote the positions of the C-H bonds that are labelled and the percentage incorporation of the hydrogen isotope, respectively.

Online content

Any methods, additional references, Nature Research reporting summaries, source data, extended data, supplementary information, acknowledgements, peer review information; details of author contributions and competing interests; and statements of

data and code availability are available at <https://doi.org/10.1038/s41557-021-00846-4>.

Received: 27 October 2020; Accepted: 25 October 2021;
Published online: 13 January 2022

References

1. Prechtl, M. H., Teltewskoi, M., Dimitrov, A., Kemnitz, E. & Braun, T. Catalytic C–H bond activation at nanoscale Lewis acidic aluminium fluorides: H/D exchange reactions at aromatic and aliphatic hydrocarbons. *Chem. Eur. J.* **17**, 14385–14388 (2011).
2. Simmons, E. M. & Hartwig, J. F. On the interpretation of deuterium kinetic isotope effects in C–H bond functionalizations by transition-metal complexes. *Angew. Chem. Int. Ed.* **51**, 3066–3072 (2012).
3. Zhan, M. et al. A simple and cost-effective method for the regioselective deuteration of phenols. *Eur. J. Org. Chem.* **2015**, 3370–3373 (2015).
4. Smith, J. A. et al. Preparation of cyclohexene isotopologues and stereoisotopomers from benzene. *Nature* **581**, 288–293 (2020).
5. Atzrodt, J., Deraud, V., Fey, T. & Zimmermann, J. The renaissance of H/D exchange. *Angew. Chem. Int. Ed.* **46**, 7744–7765 (2007).
6. Sanderson, K. Big interest in heavy drugs. *Nature* **458**, 269 (2009).
7. Katsnelson, A. Heavy drugs draw heavy interest from pharma backers. *Nat. Med.* **19**, 656 (2013).
8. Schmidt, C. First deuterated drug approved. *Nat. Biotechnol.* **35**, 493–494 (2017).
9. Czeskis, B. et al. Deuterated active pharmaceutical ingredients: a science-based proposal for synthesis, analysis, and control. Part 1: Framing the problem. *J. Labelled Comp. Radiopharm.* **62**, 690–694 (2019).
10. Martins, A. & Lautens, M. A simple, cost-effective method for the regioselective deuteration of anilines. *Org. Lett.* **10**, 4351–4353 (2008).
11. Magano, J. & Dunetz, J. R. Large-scale applications of transition metal-catalyzed couplings for the synthesis of pharmaceuticals. *Chem. Rev.* **111**, 2177–2250 (2011).
12. Atzrodt, J., Deraud, V., Kerr, W. J. & Reid, M. C–H functionalisation for hydrogen isotope exchange. *Angew. Chem. Int. Ed.* **57**, 3022–3047 (2018).
13. Hesk, D. Highlights of C(sp²)–H hydrogen isotope exchange reactions. *J. Labelled Comp. Radiopharm.* **63**, 247–265 (2020).
14. Qiao-Xia, G., Bao-Jian, S., Hai-Qing, G. & Tamotsu, T. Aromatic H/D exchange reaction catalyzed by groups 5 and 6 metal chlorides. *Chin. J. Chem.* **23**, 341–344 (2005).
15. Müller, V., Weck, R., Deraud, V. & Ackermann, L. Ruthenium(II)-catalyzed hydrogen isotope exchange of pharmaceutical drugs by C–H deuteration and C–H tritiation. *ChemCatChem* **12**, 100–104 (2019).
16. Crabtree, R. H., Felkin, H. & Morris, G. E. Cationic iridium diolefin complexes as alkene hydrogenation catalysts and the isolation of some related hydrido complexes. *J. Organomet. Chem.* **141**, 205–215 (1977).
17. Nilsson, G. N. & Kerr, W. J. The development and use of novel iridium complexes as catalysts for *ortho*-directed hydrogen isotope exchange reactions. *J. Labelled Comp. Radiopharm.* **53**, 662–667 (2010).
18. Yu, R. P., Hesk, D., Rivera, N., Pelczar, I. & Chirik, P. J. Iron-catalysed tritiation of pharmaceuticals. *Nature* **529**, 195–199 (2016).
19. Loh, Y. Y. et al. Photoredox-catalyzed deuteration and tritiation of pharmaceutical compounds. *Science* **358**, 1182–1187 (2017).
20. Sajiki, H., Sawama, Y. & Monguchi, Y. Efficient H–D exchange reactions using heterogeneous platinum-group metal on carbon–H₂–D₂O System. *Synlett* **23**, 959–972 (2012).
21. Pieters, G. et al. Regioselective and stereospecific deuteration of bioactive aza compounds by the use of ruthenium nanoparticles. *Angew. Chem. Int. Ed.* **53**, 230–234 (2014).
22. Valero, M. et al. NHC-stabilized iridium nanoparticles as catalysts in hydrogen isotope exchange reactions of anilines. *Angew. Chem. Int. Ed.* **59**, 3517–3522 (2020).
23. Heys, J. R. Nickel-catalyzed hydrogen isotope exchange. *J. Labelled Comp. Radiopharm.* **53**, 716–721 (2010).
24. Sajiki, H. et al. Efficient and selective deuteration of phenylalanine derivatives catalyzed by Pd/C. *Synlett* **2005**, 0845–0847 (2005).
25. Jagadeesh, R. V. et al. Nanoscale Fe₂O₃-based catalysts for selective hydrogenation of nitroarenes to anilines. *Science* **342**, 1073–1076 (2013).
26. Cui, X. et al. Synthesis and characterization of iron-nitrogen-doped graphene/core-shell catalysts: efficient oxidative dehydrogenation of N-heterocycles. *J. Am. Chem. Soc.* **137**, 10652–10658 (2015).
27. Belhadj, H., Melchers, S., Robertson, P. K. J. & Bahnemann, D. W. Pathways of the photocatalytic reaction of acetate in H₂O and D₂O: a combined EPR and ATR-FTIR study. *J. Catal.* **344**, 831–840 (2016).
28. Dai, X. et al. Sustainable co-synthesis of glycolic acid, formamides and formates from 1,3-dihydroxyacetone by a Cu/Al₂O₃ catalyst with a single active sites. *Angew. Chem. Int. Ed.* **58**, 5251–5255 (2019).
29. Mader, E. A., Davidson, E. R. & Mayer, J. M. Large ground-state entropy changes for hydrogen atom transfer reactions of iron complexes. *J. Am. Chem. Soc.* **129**, 5153–5166 (2007).
30. Barckholtz, C., Barckholtz, T. A. & Hadad, C. M. A mechanistic study of the reactions of H, O (3P), and OH with monocyclic aromatic hydrocarbons by density functional theory. *J. Phys. Chem. A* **105**, 140–152 (2001).
31. Vitaku, E., Smith, D. T. & Njardarson, J. T. Analysis of the structural diversity, substitution patterns, and frequency of nitrogen heterocycles among US FDA approved pharmaceuticals. *J. Med. Chem.* **57**, 10257–10274 (2014).
32. Ito, N. et al. Efficient and selective Pt/C-catalyzed H–D exchange reaction of aromatic rings. *Bull. Chem. Soc. Jpn.* **81**, 278–286 (2008).

Publisher's note Springer Nature remains neutral with regard to jurisdictional claims in published maps and institutional affiliations.



Open Access This article is licensed under a Creative Commons Attribution 4.0 International License, which permits use, sharing, adaptation, distribution and reproduction in any medium or format, as long as you give appropriate credit to the original author(s) and the source, provide a link to the Creative Commons license, and indicate if changes were made. The images or other third party material in this article are included in the article's Creative Commons license, unless indicated otherwise in a credit line to the material. If material is not included in the article's Creative Commons license and your intended use is not permitted by statutory regulation or exceeds the permitted use, you will need to obtain permission directly from the copyright holder. To view a copy of this license, visit <http://creativecommons.org/licenses/by/4.0/>.

© The Author(s) 2022

Methods

Determination of deuterium incorporation. The positions and percentage of deuterium incorporation were determined by ^1H NMR. The equation below was used to determine the degree of deuterium incorporation; peaks were calibrated against a signal corresponding to an unlabelled position. The labelling position was determined by ^1H NMR according to the chemical shifts and peak multiplicity. In addition, deuterium incorporations were confirmed using high-resolution MS by comparison of all the labelled and unlabelled compounds (note that high-resolution MS serves here to substantiate the results of quantitative NMR analysis).

$$\% \text{ deuteration} = 100 - \left[\left(\frac{\text{residual integral}}{\text{number of labelling sites}} \times 100 \right) \right]$$

Procedure for the preparation of the catalyst. A 250 ml oven-dried single-necked round-bottomed flask equipped with a reflux condenser and a Teflon-coated, egg-shaped magnetic stir bar (40 mm \times 18 mm) was charged with $\text{Fe}(\text{NO}_3)_3 \cdot 9\text{H}_2\text{O}$ (404 mg, 1.0 mmol) dissolved in ethanol (150 ml). Then, this solution was heated to 80 °C (r.t. to 80 °C) in an oil bath and stirred for 1 h. To the reaction solution, 6.0 g cellulose was added via a glass funnel, and the resulting heterogeneous mixture was stirred at 450 r.p.m. for 15 h at 80 °C. The flask was taken out from the bath and cooled to ambient temperature. The solvent was removed in vacuum and then dried under an oil pump vacuum for 4 h to give a yellow solid. The sample was transferred to a ceramic crucible and placed in an oven. The latter was evacuated to ~ 5 mbar and then flushed with argon three times. The furnace was heated to 1,000 °C at a rate of 25 °C min^{-1} and held at 1,000 °C for 2 h under argon atmosphere. After the heating was switched off, the oven was allowed to reach r.t., giving the Fe-Cellulose-1000 catalyst as a black powder (note that throughout the process, argon was constantly passed through the oven).

General procedure for the deuteration reactions. In a 4 ml vial fitted with a magnetic stir bar and septum cap, iron catalyst (60 mg, 20 mol%) and substrate (0.25 mmol) were added. Then, a needle was inserted in the septum, allowing gaseous reagents to enter. After adding the solvent deuterium oxide (1.5 ml), the vials (up to eight) were set in an alloy plate and then placed into a 300 ml steel Parr autoclave. The autoclave was flushed with hydrogen six times at 10 bar and finally pressurized to the desired value (20 bar). Then, it was placed into an aluminium block and heated to the desired temperature. At the end of the reaction, the autoclave was quickly cooled down to r.t. with an ice bath and vented. Finally, the samples were removed from the autoclave, and ethyl acetate was added to the crude mixture. This mixture was centrifuged, and the organic layer was removed from the vials (three times). After removal of all volatiles in vacuo, the desired products were obtained. In case of anilines with deuterium labelling on the nitrogen, 1 ml H_2O was added during work up and N-D was replaced by N-H.

General procedure for the >300 g scale reactions. To a 21 steel Parr autoclave containing 28.0 g Fe-Cellulose-1000 catalyst (1 mol%), 340 g 4-phenylmorpholine

(2.09 mol) and deuterium oxide (1,500 ml, 83 mol) were added. The autoclave was flushed with hydrogen six times at 10 bar and finally pressurized to the desired value (20 bar). Then, it was placed into an equipment (see Supplementary Section 9 for more details) for the autoclave and heated to 120 °C, and then held at 120 °C for 120 h. At the end of the reaction, the autoclave was quickly cooled down to r.t. with an ice bath and vented. Finally, the crude reaction was added to ethyl acetate (1.5 l). The reaction mixture was filtered with filter paper. The D_2O layer was removed from the mixture and washed with ethyl acetate (1.5 l, three times). After removal of all volatiles in vacuo, 341 g of deuterium product was obtained. It is important to note that during the cool down, trace amounts of gas can stay in the solid phase (product and catalyst). Thus, the solid phase should be dissolved slowly in ethyl acetate.

Data availability

All data generated or analysed in this study are available in this article and its Supplementary Information.

Acknowledgements

We thank the analytical staff of the Leibniz-Institute for Catalysis, Rostock, for their excellent service, specifically W. Baumann for his accurate quantitative ^1H NMR analysis, R Jackstell for offering the 21 autoclave and D.K. Leonard for assistance in the preparation of the manuscript. We gratefully acknowledge support from the Federal Ministry of Education and Research (BMBF), the State of Mecklenburg-Vorpommern, EU (FLIX project) and the European Research Council (ERC; project NoNaCat 670986).

Author contributions

M.B. and W.L. conceived and designed the project. W.L. and F.B. developed and prepared the catalysts and performed all catalytic experiments and analysed the data. A.B. and J.R. were responsible for the EPR experiments. D.Y. and A.L. were responsible for the XAFS experiments. C.K. and N.R. were responsible for the TEM experiments. H.L. was responsible for the X-ray diffraction experiments. S.B. was responsible for the XPS experiments. K.J., A.-E.S. and A.B. participated in the discussions and supported the project. W.L., J.R., A.B. and M.B. co-wrote the paper.

Competing interests

The authors declare no competing interests.

Additional information

Supplementary information The online version contains supplementary material available at <https://doi.org/10.1038/s41557-021-00846-4>.

Correspondence and requests for materials should be addressed to Angelika Brückner, Aiwen Lei or Matthias Beller.

Peer review information *Nature Chemistry* thanks Marc Reid and the other, anonymous, reviewer(s) for their contribution to the peer review of this work.

Reprints and permissions information is available at www.nature.com/reprints.

Manganese-catalysed deuterium labelling of anilines and electron-rich (hetero)arenes

Florian Bourriquen, Nils Rockstroh, Stephan Bartling, Kathrin Junge,* and Matthias Beller*

Angew. Chem. Int. Ed. **2022**, *61*, e202202423

DOI: 10.1002/anie.202202423

This document is available under the CC BY-NC 4.0 license. © 2022 The Authors. *Angewandte Chemie International Edition* published by Wiley-VCH GmbH.

Angew. Chem. **2022**, *134*, e202202423

DOI: 10.1002/ange.202202423

This document is available under the CC BY-NC 4.0 license. © 2022 The Authors. *Angewandte Chemie* published by Wiley-VCH GmbH.

Electronic supporting information is available online.

Contribution

Here, I synthesised and tested the heterogeneous catalysts used in this work. Furthermore, I optimised the reaction conditions, investigated the substrate scope, and performed the mechanistic investigations. In addition, I wrote the initial draft of this paper and supplementary information.* My contribution to this paper accounts for 70%.

*Please note that the parts dealing with catalyst characterisations were written by the people who performed said investigation: Dr. Nils Rockstroh for STEM analyses and Dr. Stephan Bartling for XPS measurements.

Signature of the student

Florian Bourriquen

Signature of the supervisor

Prof. Matthias Beller



Deuterium Labelling Hot Paper

 How to cite: *Angew. Chem. Int. Ed.* **2022**, *61*, e202202423

International Edition: doi.org/10.1002/anie.202202423

German Edition: doi.org/10.1002/ange.202202423

Manganese-Catalysed Deuterium Labelling of Anilines and Electron-Rich (Hetero)Arenes

Florian Bourriquen, Nils Rockstroh, Stephan Bartling, Kathrin Junge,* and Matthias Beller*

Abstract: There is a constant need for deuterium-labelled products for multiple applications in life sciences and beyond. Here, a new class of heterogeneous catalysts is reported for practical deuterium incorporation in anilines, phenols, and heterocyclic substrates. The optimal material can be conveniently synthesised and allows for high deuterium incorporation using deuterium oxide as isotope source. This new catalyst has been fully characterised and successfully applied to the labelling of natural products as well as marketed drugs.

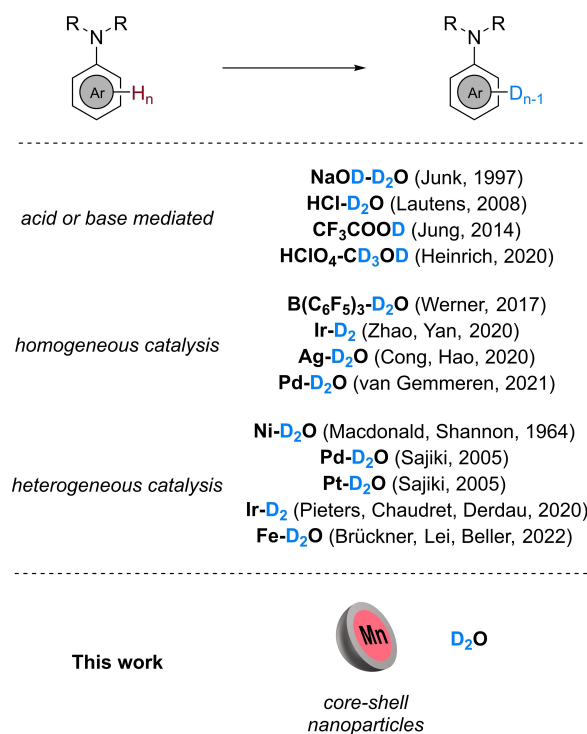
Introduction

Constant growth in the use of deuterium-labelled compounds is observed in various scientific fields. Such compounds are of interest for instance as standards for mass spectrometry,^[1] to prove reaction mechanisms,^[2] to tune the properties of materials,^[3,4] or to elucidate protein conformations.^[5] However, they are mainly applied for the development of drugs in the pharmaceutical industry,^[6–8] where labelling compounds is a prime technique for the investigation of metabolic pathways of a respective drug candidate. Interestingly, deuterium incorporation allows fine tuning of the pharmacokinetic properties of drug molecules, as the deuteration of specific positions might modify a drug's absorption, distribution, metabolism, and excretion properties. Furthermore, as C–D bond cleavage requires additional energy compared to C–H bonds, drugs containing labelled moieties can be more resistant towards metabolic degradation. As a result, a similar therapeutic effect might be achieved with a lower dosage. Consequently, in 2017, Austedo, the first deuterated drug on the market, was approved by the U.S. Food and Drug Administration for the treatment of chorea associated with Huntington's disease.^[9]

[*] F. Bourriquen, Dr. N. Rockstroh, Dr. S. Bartling, Dr. K. Junge, Prof. Dr. M. Beller
 Leibniz-Institut für Katalyse e.V.
 Albert-Einstein-Straße 29a, 18059 Rostock (Germany)
 E-mail: kathrin.junge@catalysis.de
 matthias.beller@catalysis.de

© 2022 The Authors. *Angewandte Chemie International Edition* published by Wiley-VCH GmbH. This is an open access article under the terms of the Creative Commons Attribution Non-Commercial License, which permits use, distribution and reproduction in any medium, provided the original work is properly cited and is not used for commercial purposes.

Owing to the demand for labelled compounds, the development of novel, diverse methodologies for deuterium labelling has attracted considerable research interest.^[10–12] Amongst the available methods, the most elegant is Hydrogen Isotope Exchange (HIE), where catalysts allow deuterium incorporation at specific positions. Consequently, HIE is of great importance for late-stage functionalisation of bioactive compounds.^[13–19] In this respect, anilines are key building blocks in molecular chemistry, as reflected by their occurrence in 3 of the top 10 selling medications of 2019.^[20] Owing to the significance of such compounds, a number of methodologies has been reported for the deuterium labelling of anilines (Scheme 1). For instance, deuterium incorporation is achieved at elevated temperatures by the use of strong bases^[21] or acids, in particular hydrochloric and trifluoroacetic acids.^[22,23] Recent studies showed such reactivity is equally feasible with perchloric acid at reduced temperatures.^[24] Inherently, such approaches can be challenging in presence of acid-sensitive functional groups. Exploiting the concept of frustrated Lewis pairs, Werner and co-workers demonstrated the efficiency of the relatively



Scheme 1. Selected approaches for the deuteration of aniline substrates (for respective references see text).

expensive tris(pentafluorophenyl)-borane as catalyst for H/D exchange at the *ortho*- and *para*-positions relative to the nitrogen using D₂O as isotope source.^[25] Additionally, molecularly defined complexes can efficiently promote H/D exchange in anilines such as the mesoionic carbene-iridium complex presented by Zhao, Yan and co-workers in 2020 for selective *ortho*-labelling.^[26] However, despite the high deuterium content achieved, this methodology suffers by requiring a quantitative amount of base. The same year, a silver-catalysed methodology for HIE in electron-rich arenes was presented by Cong, Hao, and co-workers. Notably, this methodology is not limited to anilines, as nitrogen-containing heterocycles such as indoles and imidazoles could similarly undergo this transformation.^[27] Recently, the van Gemmeren group introduced novel N,N-bidentate ligands embodying an *N*-acylsulfonamide moiety for the nondirected labelling of a broad scope of (hetero)arenes.^[28] Here, one aniline substrate is presented with high deuterium incorporation at the *ortho*- and *para*-positions although concomitant labelling of the *meta*-position takes place to a lesser extent.

Due to the advantages regarding catalyst separation from reaction mixtures as well as potentially uncomplicated purification of the desired products, the use of heterogeneous catalysts became a topic of interest in HIE. In particular, in the presence of D₂O and hydrogen, commercially available Pt/C and Pd/C are valuable tools for HIE at the aromatic and aliphatic positions, respectively,^[29] and were successfully applied for the perdeuteration of anilines.^[30,31] Besides, in line with work based on ruthenium nanoparticles,^[32] Pieters, Chaudret, Derdau and co-workers presented air-stable NHC-stabilised iridium nanoparticles for HIE in anilines.^[33] Employing deuterium gas as isotope source, *ortho*-deuteration is achieved with remarkable selectivity. Examples of the use of supported non-noble metals for aniline labelling are scarce. One of the rare instances applies Raney Nickel as described by Macdonald and Shannon already in 1964.^[34]

Considering the increasing importance of labelled compounds, we envisioned the need for easy-to-operate and affordable methodologies for deuterium incorporation on multi-gram scale. In this respect, we recently disclosed the use of a simple pyrolysed iron catalyst for HIE.^[35] Based on this work, we were interested in the development of new base-metal catalysed hydrogen/deuterium exchange reactions. Apart from iron, manganese appeared as an ideal candidate due to its availability, affordable price, and rich redox chemistry. While homogeneous manganese catalysts have been considerably investigated in recent years,^[36,37] heterogeneous catalysts based solely on manganese were rarely studied, apart from electrocatalysis,^[38–40] and there remain many opportunities in this area. In fact, to the best of our knowledge, no heterogeneous catalytic system for deuterium incorporation relying on manganese has been reported before. Noteworthy, here we present a practical methodology at comparably low catalyst loading and hydrogen pressure using D₂O as the most affordable deuterium source available.

Results and Discussion

At the start of this work, several iron and manganese salts were mixed with widely available biopolymers and subsequently pyrolysed at different temperatures. In this straightforward way it is possible to prepare a variety of the corresponding nanoparticles supported on carbon. All the materials were applied to the labelling of 4-methoxyaniline **1a** with D₂O as model reaction. As depicted in Table S1, the pyrolysis process and support are crucial for the formation of active materials for isotopic labelling. More specifically, a temperature of 1000 °C and starch as carbon source gave the best results. Thus, nine starch-based materials consisting of different metals were synthesised and tested (Table S2). Remarkably, iron and manganese catalysts outperformed even noble metals such as ruthenium and palladium under our reaction conditions. Pleasingly, using Mn@Starch-1000 and employing deuterium oxide as isotope source, a deuterium incorporation of 94 % at the *ortho*-positions of **2a** is obtained using 20 mol % of metal under hydrogen pressure (Table 1, entry 1).^[41] In the presence of organic co-solvents the deuterium incorporation decreased (Table 1, entries 2 and 3). On the contrary, water stable Lewis acids such as zinc, indium, or lanthanum triflates had no effect on the efficiency of this manganese-catalysed reaction. Surprisingly, an acidic media did not impede the catalyst activity while the labelling was lowered to 80 % in the presence of triethylamine and dropped to 34 % in the presence of a stronger base such as sodium hydroxide (Table 1, entries 5–7). Investigations of the gaseous atmosphere showed a similar deuterium incorporation under 20 bar of nitrogen instead of hydrogen. Lowering the catalyst loading to

Table 1: Optimisation of reaction conditions.

Entry ^[a]	Deviation from the standard conditions	Deuterium incorporation [%]
1	–	94
2	100 °C instead of 120 °C	30
3	¹ PrOH, THF or cyclohexane as co-solvents	5–8
4	Lewis acids as additives ^[b]	93–94
5	HCl as additive ^[b]	93
6	NEt ₃ as additive ^[b]	80
7	NaOH as additive ^[b]	34
8	N ₂ (20 bar)	94
9	N ₂ (5 bar)	81
10	10 mol % Mn, H ₂ (5 bar)	83
11	10 mol % Mn, H₂ (10 bar)	94
12	no catalyst	< 5
13	Mn(OAc) ₂ ·4 H ₂ O as catalyst ^[b]	8
14	Starch-1000 as catalyst ^[c]	< 5

[a] Reaction conditions: *p*-anisidine (0.25 mmol), Mn@Starch-1000 (58 mg, 20 mol % Mn), H₂ (20 bar), D₂O (1.5 mL), 24 h, 120 °C. [b] 20 mol %. [c] 60 mg.

10 mol % still gave a deuteration yield of >80 % (Table 1, entries 10 and 11). Finally, control reactions showed poor labelling of the model substrate without the use of catalyst, or when manganese acetate or pyrolysed starch were used as catalysts (Table 1, entries 12–14).

Owing to the heterogeneous nature of the catalyst, its simple removal from the reaction mixture is achieved either by centrifugation or filtration, yielding deuterated *p*-anisidine **2a** without further purification. Recycling experiments of the recovered material were performed (see Supporting Information for details), revealing a reduced catalytic activity of the recycled material. To characterise the surface of our novel catalyst material and to understand the partial deactivation processes, initially X-ray Photoelectron Spectroscopy (XPS) measurements were applied.

Accordingly, the surface of the fresh catalyst consists mainly of C (96.2 at. %), O, and Mn as well as small amounts of Si, K, and P, probably residuals from the preparation process and/or support material, see Table S5 for quantification data and Figure S1 for survey spectra. The Mn concentration at the surface is rather low with about 0.2 at. %. The Mn 2p region with the Mn 2p_{3/2} peak at 641.5 eV is shown in Figure S2a. While the Mn 2p spectra of some oxidation states of Mn are rather similar,^[42,43] the Mn 3s region has been mainly used to identify the present oxidation states and is shown in Figure S2c. Here, a peak distance of about 5.6 eV can be found, which indicates Mn³⁺ as main oxidation state^[43] for the fresh catalyst. Comparing the Mn 2p spectra of the fresh and recycled catalyst (Figure S2a and b), small structural changes can be noted. The satellite feature at 646 eV (an indication for MnO) is more pronounced in the recycled catalyst. Furthermore, the first fitting component at 639 eV is less intense in the recycled sample. Looking at the Mn 3s region (Figure S2c and d), the two peaks for the fresh catalyst change in the recycled sample. Here, two broad features are observed indicating the coexistence of at least two different oxidation states like Mn²⁺ and Mn⁴⁺. It is important to mention that the surface concentration of Mn is very low, which makes the characterization challenging (especially for Mn 3s) even after long integration times. Next, Scanning Transmission Electron Microscopy (STEM) was applied to study the structural features of the fresh and recycled catalyst and to elucidate potential changes in the two samples. As can be seen in Figure 1, numerous Mn/MnO_x core-shell particles are observed in fresh Mn@Starch-1000. The number of these particles is drastically reduced in the recycled Mn@Starch-1000 material, which in turn exhibits either Mn or MnO_x particles, but in most cases no particles containing both Mn and MnO_x (see Supporting Information). Generally, the Mn-containing particles are irregularly distributed over the support. The particle sizes of the Mn-containing particles cover a broad range in fresh Mn@Starch-1000, with the smallest being around 10 nm, the majority having sizes between 40 and 70 nm and the largest ones forming entities of up to 1.8 μm. These sizes remain relatively constant even after one reaction (see Supporting Information). In light of these two results, we presume that the decreased activity of

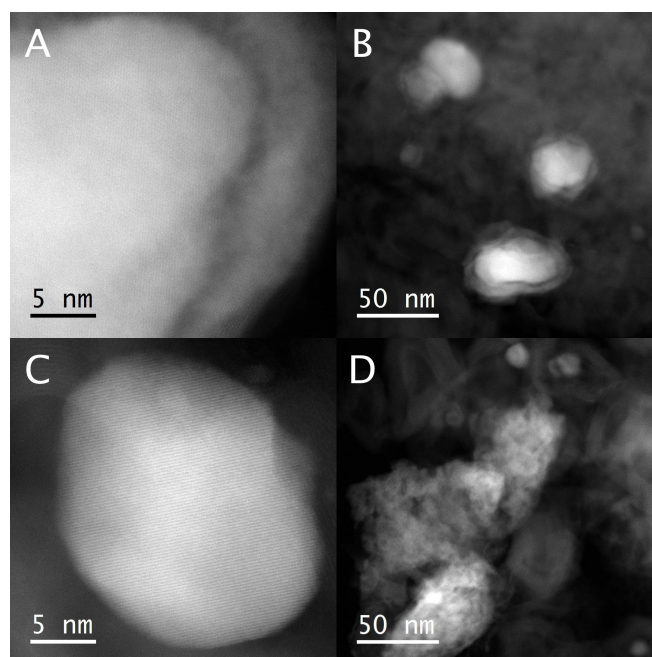
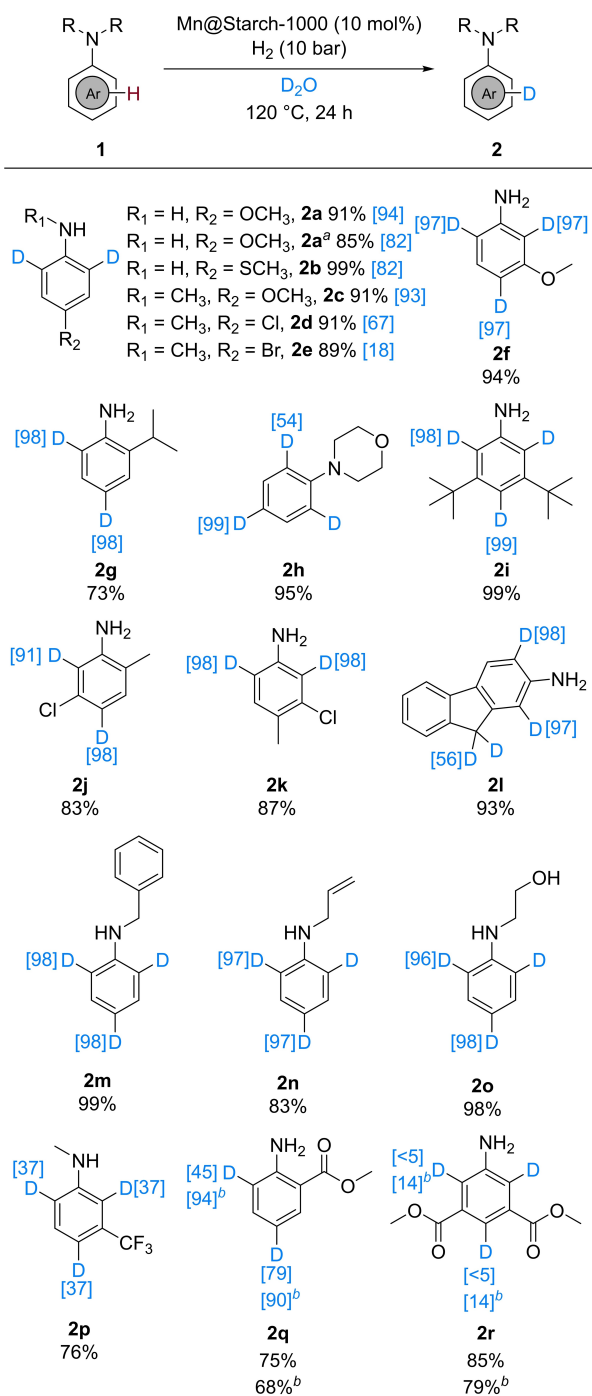


Figure 1. HAADF-STEM images of A), B) Freshly prepared Mn@Starch-1000. C), D) Mn@Starch-1000 recovered after deuteration of *p*-anisidine at 120 °C, 10 bar H₂, 24 h in D₂O. While the fresh catalyst exhibits a considerable share of Mn/MnO_x core-shell particles, there are predominantly either pure Mn (C) or pure MnO_x particles present in the recycled catalyst.

the catalyst is related to these structural changes occurring during the course of the reaction.

With the optimised reaction conditions in hand (10 mol % Mn, 10 bar H₂, 120 °C, 24 h), we examined the scope of this novel catalyst system. The *ortho*- and *para*-positions of a variety of anilines were readily labelled with deuterium contents up to 98 % and high selectivity (Scheme 2). In particular, our model substrate *para*-anisidine **1a** can easily be converted in two steps to the common medication paracetamol.^[44] Pleasingly, this catalyst material tolerates halogens (**2d**, **2e**, **2j**, **2k**) and the thioether functionality, as illustrated by the 82 % deuterium incorporation in 4-(methylthio)aniline **2b**. In addition, our procedure is not limited to primary amines, as secondary and tertiary amines such as 4-phenylmorpholine **1h** were smoothly deuterated. Moreover, the 4-position of 3,5-di-*tert*-butylaniline **2i** was successfully deuterated, highlighting the possibility of labelling sterically demanding substrates. The high specificity of this process towards labelling electron-rich aromatic rings is emphasised when *N*-benzylaniline **1m** was tested as substrate. Indeed, the benzyl ring was unaffected, and exclusively the aniline ring of **2m** was labelled with excellent deuterium incorporation (98 %). A comparable result is observed with 9*H*-fluoren-2-amine **1l**. Interestingly, in this case labelling of the activated C9 position concomitantly takes place. Anilines containing allyl as well as hydroethyl moieties are also efficiently converted to their deuterated counterparts (**2n**, **2o**). Finally, anilines containing electron-withdrawing substituents were subjected

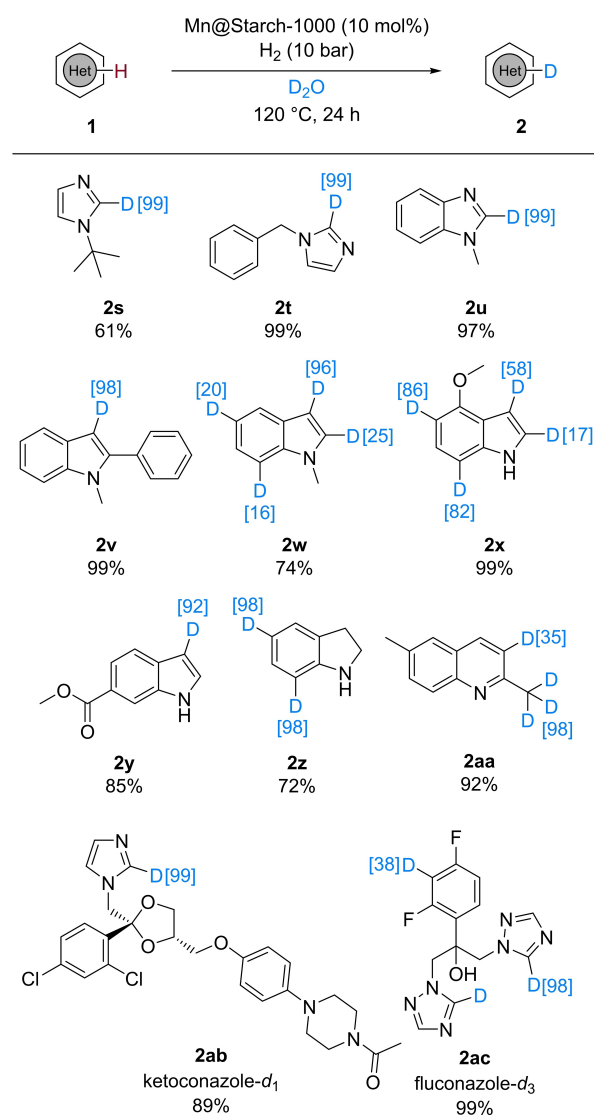


Scheme 2. Scope of anilines. Substrate (0.5 mmol), Mn@Starch-1000 (58 mg, 10 mol% Mn), H₂ (10 bar), D₂O (1.5 mL), 120 °C, 24 h. Isolated yields. The blue numbers between brackets represent the deuterium incorporation. [a] 1 g scale. [b] 140 °C.

to our labelling procedure. Unsurprisingly, the deuterium content is reduced, as it was already observed in chloro- and bromo-containing substituents (**2d**, **2e**). Nevertheless, even in the presence of a trifluoromethyl group (**2p**) deuterium incorporation of 37% is detected. Moderate to high deuterium contents (45% and 79% at the *ortho*- and *para*-positions, relative to the amine, respectively) are obtained

with methyl 2-aminobenzoate (**2q**). In this case, an increased reaction temperature provides a 90% deuterium incorporation at both positions. However, for electron-poor arenes such as **1r**, bearing two methyl ester substituents, a 140 °C reaction temperature does not lead to an elevated deuterium incorporation.

Next, we were interested in the applicability of this catalytic system for the labelling of nitrogen-containing heterocycles (Scheme 3). Under standard reaction conditions, complete deuterium incorporation occurred at the 2-position of imidazole (**2s**, **2t**) and benzimidazole (**2u**) moieties, while the other hydrogen atoms were left untouched. On the other hand, the labelling of indoles was significantly conditioned by ring substituents. For example, when 1-methyl-2-phenyl-1*H*-indole **1v** was subjected to our procedure, deuterium incorporation was exclusively de-



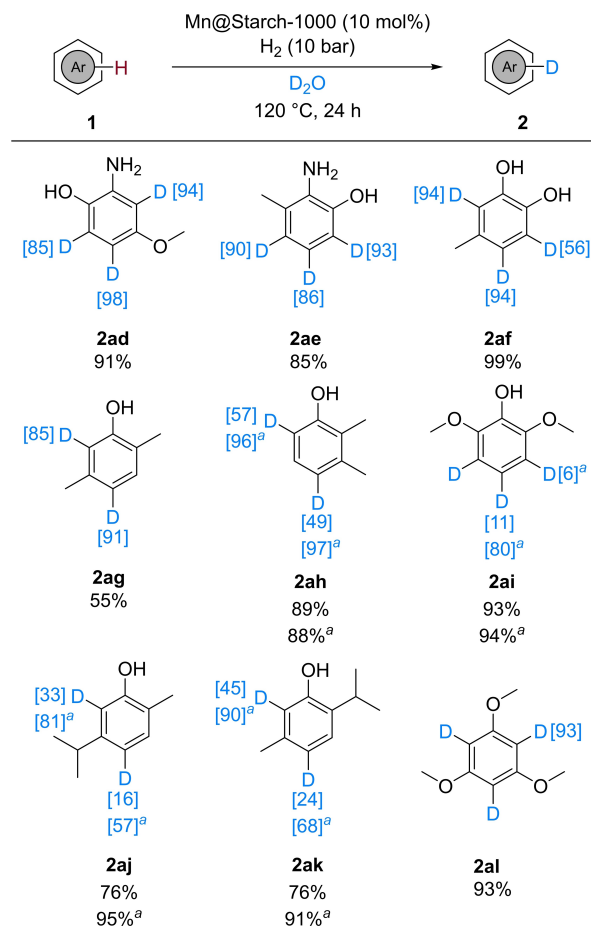
Scheme 3. Scope of N-containing heterocycles. Substrate (0.5 mmol), Mn@Starch-1000 (58 mg, 10 mol% Mn), H₂ (10 bar), D₂O (1.5 mL), 120 °C, 24 h. Isolated yields. The blue numbers between brackets represent the deuterium incorporation.

tected at the 3-position. However, 1-methyl-1*H*-indole **1w** also showed deuterium incorporation on the benzene ring. Naturally, an electron-donating substituent such as the methoxy group increases the deuterium incorporation (**2x**), whereas the methyl ester moiety present in **2y** limited the deuterium content. Indoline **1z** reacted smoothly and provided the deuterated analogue **2z** with 98% deuterium incorporation. The protons from the activated methyl group in 2,6-dimethylquinoline (**1aa**) smoothly underwent H/D exchange, however, the exchange took place to a limited extent with the aromatic protons, with merely 35% deuterium detected at the 3-position of the quinoline scaffold.

The introduction of deuterium atoms in drug candidates and marketed drugs is highly desirable, see above. To demonstrate the potential of the presented methodology, the 5-position of the triazole ring of fluconazole, a commercial antifungal medication, was efficiently labelled. Moreover, the 3-position of the phenyl ring neighbouring both fluorine atoms was concomitantly labelled, providing fluconazole-*d*₃ (**2ac**) in quantitative yield. Likewise, the imidazole ring of ketoconazole showed a comparable reactivity to more simple model substrates and afforded ketoconazole-*d*₁ (**2ab**) with a quantitative deuterium incorporation.^[45]

Furthermore, a variety of phenol substrates were labelled using our Mn@Starch-1000 catalyst (Scheme 4). In general, these substrates exhibit a poorer reactivity compared to anilines. Nevertheless, for most applied substrates good deuterium incorporation was observed, albeit at higher temperature. Electron-rich aminophenols (**2ad**, **2ae**) and a catechol derivative **2af** provided high D content at 120 °C. Mixed outcomes were obtained with dimethylphenols: while 2,5-dimethylphenol (**1ag**) is smoothly labelled under our standard reaction conditions, higher temperature was necessary to achieve a similar isotope incorporation in 2,3-dimethylphenol (**1ah**). Phenol **1ai** yielded a medium deuterium content. Deuterated analogues of monoterpenoids carvacrol and thymol (**2aj**, **2ak**) are produced using our manganese-catalysed methodology, underlining its applicability to natural products. Finally, electron-rich 1,3,5-trimethoxybenzene reacted efficiently and provided **2al** with 93% D.

To gain information on the reaction mechanism, we performed our model reaction in the presence of TEMPO as a radical scavenger (Scheme 5). In this case, the deuterium incorporation was drastically lowered to only 12%, strongly suggesting a radical mechanism. Additionally, performing the reaction using D₂ gas in water showed no deuterium incorporation, highlighting the importance of the D₂O/H₂ combination for efficient labelling. Besides, using D₂ as reductant instead of H₂ lowered the labelling of *p*-anisidine from 94% to 85%, providing a secondary kinetic isotope effect of 1.1. Due to the similarity in the catalysts' structures and reactivity, we propose a mechanism similar to the one discussed in our previous iron-mediated labelling methodology is likely to be taking place: homolytic D₂O cleavage by Mn@Starch-1000 generates D* and DO* radicals. A hydrogen atom from the substrate is abstracted by DO* providing

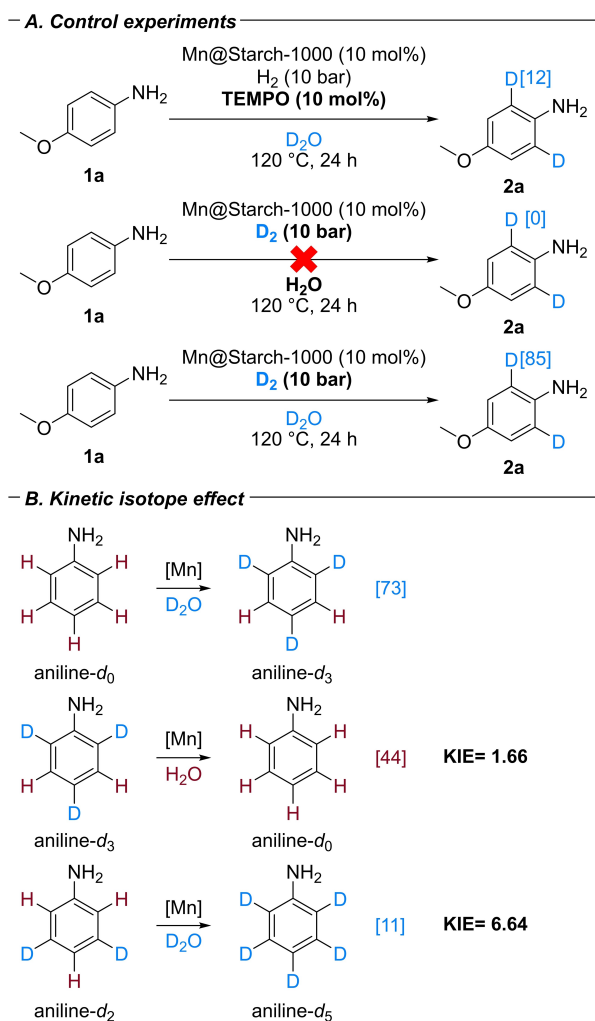


Scheme 4. Scope of phenols and electron-rich arenes. Substrate (0.5 mmol), Mn@Starch-1000 (58 mg, 10 mol% Mn), H₂ (10 bar), D₂O (1.5 mL), 120 °C, 24 h. Isolated yields. The blue numbers between brackets represent the deuterium incorporation. [a] 140 °C.

HDO and a phenyl radical which subsequently reacts with D* yielding the deuterated product.^[35] Interestingly, both de-deuteration of 2,4,6-trideuteroaniline and deuteration of 3,5-dideuteroaniline showed a positive kinetic isotope effect, the latter suggesting a different coordination of the aniline substrate on the catalyst's surface.

Conclusion

In conclusion, we report here the first example of a heterogeneous manganese catalyst, Mn@Starch-1000, for hydrogen isotope exchange reactions. The key to success for the deuterium incorporation is the formation of Mn/MnO_x core-shell particles supported on pyrolysed carbon. Notably, the concentration of manganese on the surface is rather low, demonstrating the high activity of these active centres. The presented practical methodology tolerates a range of functional groups and was successfully implemented for the labelling of electron-rich arenes and heteroarenes. Importantly, this strategy profits from the use of deuterium oxide as an easy-to-handle isotope source and is a competitive



Scheme 5. Control experiments – Kinetic isotope effect. Aniline substrate (0.5 mmol), Mn@Starch-1000 (30 mg, 5 mol% Mn), H_2 (10 bar), H_2O or D_2O (1.5 mL), 120 °C, 5 h.

alternative to more classical procedures relying on noble metals.

Acknowledgements

We thank the analytical staff of the LIKAT for their excellent service. Sara Kopf and Dr. Wu Li are thanked for valuable discussions with respect to deuterium incorporation. We thank Dr. Wolfgang Baumann for performing deuterium NMR experiments. We thank Dr. Peter McNeice for assistance during preparation of the manuscript. This project has received funding from the European Union's Horizon 2020 research and innovation program under grant agreement No 862179. We also acknowledge the European Research Council (EU project 670986-NoNaCat) and the State of Mecklenburg-Vorpommern for financial and general support. Open Access funding enabled and organized by Projekt DEAL.

Conflict of Interest

The authors declare no conflict of interest.

Data Availability Statement

The data that support the findings of this study are available in the Supporting Information of this article.

Keywords: Deuterium • Heterogeneous Catalysis • Hydrogen Isotope Exchange • Manganese • Starch

- [1] J. Atzrodt, V. Derdau, *J. Labelled Compd. Radiopharm.* **2010**, *53*, 674–685.
- [2] E. M. Simmons, J. F. Hartwig, *Angew. Chem. Int. Ed.* **2012**, *51*, 3066–3072; *Angew. Chem.* **2012**, *124*, 3120–3126.
- [3] M. Shao, J. Keum, J. Chen, Y. He, W. Chen, J. F. Browning, J. Jakowski, B. G. Sumpter, I. N. Ivanov, Y.-Z. Ma, C. M. Rouleau, S. C. Smith, D. B. Geohagan, K. Hong, K. Xiao, *Nat. Commun.* **2014**, *5*, 3180.
- [4] J. B. Grimm, L. Xie, J. C. Casler, R. Patel, A. N. Tkachuk, N. Falco, H. Choi, J. Lippincott-Schwartz, T. A. Brown, B. S. Glick, Z. Liu, L. D. Lavis, *JACS Au* **2021**, *1*, 690–696.
- [5] L. Konermann, J. Pan, Y.-H. Liu, *Chem. Soc. Rev.* **2011**, *40*, 1224–1234.
- [6] T. G. Gant, *J. Med. Chem.* **2014**, *57*, 3595–3611.
- [7] J. Atzrodt, V. Derdau, W. J. Kerr, M. Reid, *Angew. Chem. Int. Ed.* **2018**, *57*, 1758–1784; *Angew. Chem.* **2018**, *130*, 1774–1802.
- [8] T. Pirali, M. Serafini, S. Carginin, A. A. Genazzani, *J. Med. Chem.* **2019**, *62*, 5276–5297.
- [9] C. Schmidt, *Nat. Biotechnol.* **2017**, *35*, 493–494.
- [10] J. Atzrodt, V. Derdau, T. Fey, J. Zimmermann, *Angew. Chem. Int. Ed.* **2007**, *46*, 7744–7765; *Angew. Chem.* **2007**, *119*, 7890–7911.
- [11] J. Atzrodt, V. Derdau, W. J. Kerr, M. Reid, *Angew. Chem. Int. Ed.* **2018**, *57*, 3022–3047; *Angew. Chem.* **2018**, *130*, 3074–3101.
- [12] S. Kopf, F. Bourriquen, W. Li, H. Neumann, K. Junge, M. Beller, *Chem. Rev.* **2022**, *122*, 6634–6718.
- [13] C. Zarate, H. Yang, M. J. Bezdek, D. Hesk, P. J. Chirik, *J. Am. Chem. Soc.* **2019**, *141*, 5034–5044.
- [14] A. Palazzolo, S. Feuillastre, V. Pfeifer, S. Garcia-Argote, D. Bouzouita, S. Tricard, C. Chollet, E. Marcon, D.-A. Buisson, S. Cholet, F. Fenaille, G. Lippens, B. Chaudret, G. Pieters, *Angew. Chem. Int. Ed.* **2019**, *58*, 4891–4895; *Angew. Chem.* **2019**, *131*, 4945–4949.
- [15] V. Müller, R. Weck, V. Derdau, L. Ackermann, *ChemCatChem* **2020**, *12*, 100–104.
- [16] Q.-K. Kang, H. Shi, *Synlett* **2021**, *32*, A–J.
- [17] V. Pfeifer, T. Zeltner, C. Fackler, A. Kraemer, J. Thoma, A. Zeller, R. Kiesling, *Angew. Chem. Int. Ed.* **2021**, *60*, 26671–26676; *Angew. Chem.* **2021**, *133*, 26875–26880.
- [18] A. Tlahuext-Aca, J. F. Hartwig, *ACS Catal.* **2021**, *11*, 1119–1127.
- [19] A. Uttry, S. Mal, M. van Gemmeren, *J. Am. Chem. Soc.* **2021**, *143*, 10895–10901.
- [20] V. A. Schmidt, *Nature* **2020**, *584*, 46–47.
- [21] T. Junk, W. J. Catallo, L. D. Civils, *J. Labelled Compd. Radiopharm.* **1997**, *39*, 625–630.
- [22] A. Martins, M. Lautens, *Org. Lett.* **2008**, *10*, 4351–4353.
- [23] R. Giles, A. Lee, E. Jung, A. Kang, K. W. Jung, *Tetrahedron Lett.* **2015**, *56*, 747–749.
- [24] O. Fischer, A. Hubert, M. R. Heinrich, *J. Org. Chem.* **2020**, *85*, 11856–11866.

- [25] W. Li, M.-M. Wang, Y. Hu, T. Werner, *Org. Lett.* **2017**, *19*, 5768–5771.
- [26] W. Liu, L. Cao, Z. Zhang, G. Zhang, S. Huang, L. Huang, P. Zhao, X. Yan, *Org. Lett.* **2020**, *22*, 2210–2214.
- [27] B. Dong, X. Cong, N. Hao, *RSC Adv.* **2020**, *10*, 25475–25479.
- [28] M. Farizyan, A. Mondal, S. Mal, F. Deufel, M. van Gemmeren, *J. Am. Chem. Soc.* **2021**, *143*, 16370–16376.
- [29] H. Sajiki, N. Ito, H. Esaki, T. Maesawa, T. Maegawa, K. Hirota, *Tetrahedron Lett.* **2005**, *46*, 6995–6998.
- [30] I. Nobuhiro, E. Hiroyoshi, M. Tsuneaki, I. Eikoh, M. Tomohiro, S. Hironao, *Bull. Chem. Soc. Jpn.* **2008**, *81*, 278–286.
- [31] N. Ito, T. Watahiki, T. Maesawa, T. Maegawa, H. Sajiki, *Synthesis* **2008**, *2008*, 1467–1478.
- [32] G. Pieters, C. Taglang, E. Bonnefille, T. Gutmann, C. Puente, J.-C. Berthet, C. Dugave, B. Chaudret, B. Rousseau, *Angew. Chem. Int. Ed.* **2014**, *53*, 230–234; *Angew. Chem.* **2014**, *126*, 234–238.
- [33] M. Valero, D. Bouzouita, A. Palazzolo, J. Atzrodt, C. Dugave, S. Tricard, S. Feuillastre, G. Pieters, B. Chaudret, V. Derdau, *Angew. Chem. Int. Ed.* **2020**, *59*, 3517–3522; *Angew. Chem.* **2020**, *132*, 3545–3550.
- [34] C. G. Macdonald, J. S. Shannon, *Tetrahedron Lett.* **1964**, *5*, 3351–3354.
- [35] W. Li, J. Rabeah, F. Bourriquen, D. Yang, C. Kreyenschulte, N. Rockstroh, H. Lund, S. Bartling, A.-E. Surkus, K. Junge, A. Brückner, A. Lei, M. Beller, *Nat. Chem.* **2022**, *14*, 334–341.
- [36] J. R. Carney, B. R. Dillon, S. P. Thomas, *Eur. J. Org. Chem.* **2016**, 3912–3929.
- [37] Y. Wang, M. Wang, Y. Li, Q. Liu, *Chem* **2021**, *7*, 1180–1223.
- [38] J.-S. Lee, G. S. Park, H. I. Lee, S. T. Kim, R. Cao, M. Liu, J. Cho, *Nano Lett.* **2011**, *11*, 5362–5366.
- [39] C. Walter, P. W. Menezes, S. Orthmann, J. Schuch, P. Connor, B. Kaiser, M. Lerch, M. Driess, *Angew. Chem. Int. Ed.* **2018**, *57*, 698–702; *Angew. Chem.* **2018**, *130*, 706–710.
- [40] B. Zhang, J. Zhang, J. Shi, D. Tan, L. Liu, F. Zhang, C. Lu, Z. Su, X. Tan, X. Cheng, B. Han, L. Zheng, J. Zhang, *Nat. Commun.* **2019**, *10*, 2980.
- [41] These initial screening conditions correspond to the optimised reaction conditions from reference [35].
- [42] M. C. Biesinger, B. P. Payne, A. P. Grosvenor, L. W. M. Lau, A. R. Gerson, R. S. C. Smart, *Appl. Surf. Sci.* **2011**, *257*, 2717–2730.
- [43] E. S. Ilton, J. E. Post, P. J. Heaney, F. T. Ling, S. N. Kerisit, *Appl. Surf. Sci.* **2016**, *366*, 475–485.
- [44] S. Singh, K. K. Roy, S. R. Khan, V. K. Kashyap, A. Sharma, S. Jaiswal, S. K. Sharma, M. Y. Krishnan, V. Chaturvedi, J. Lal, S. Sinha, A. Dasgupta, R. Srivastava, A. K. Saxena, *Bioorg. Med. Chem.* **2015**, *23*, 742–752.
- [45] Absence of deuterium incorporation on the aniline scaffold can be attributed to the interaction of the amide moiety with the catalyst surface; thus, impeding coordination of the aniline.

Manuscript received: February 14, 2022

Accepted manuscript online: April 29, 2022

Version of record online: May 12, 2022

7. Appendix

7.1. Further publications

The following publications were prepared during my PhD. The review (chapter 3.1) contributed to the writing of the introduction of this thesis.

Catalytic Formal Hydroamination of Allylic Alcohols Using Manganese PNP-Pincer Complexes

L. Duarte de Almeida, F. Bourriquen, K. Junge, M. Beller.

Adv. Synth. Catal. **2021**, *363*, 4177–4181.

DOI: 10.1002/adsc.202100081.

Copper-catalysed low-temperature water–gas shift reaction for selective deuteration of aryl halides

W. Li, R. Qu, W. Liu, F. Bourriquen, S. Bartling, N. Rockstroh, K. Junge, M. Beller.

Chem. Sci. **2021**, *12*, 14033–14038.

DOI: 10.1039/d1sc04259a.

Recent Developments for the Deuterium and Tritium Labeling of Organic Molecules

S. Kopf,⁺ F. Bourriquen,⁺ W. Li, H. Neumann, K. Junge, M. Beller.

⁺contributed equally.

Chem. Rev. **2022**, *122*, 6634–6718.

DOI: 10.1021/acs.chemrev.1c00795

Diastereoselective hydrogenation of arenes and pyridines using supported ruthenium nanoparticles under mild conditions

F. Bourriquen, J. Hervochoon, R. Qu, S. Bartling, N. Rockstroh, K. Junge, C. Fischmeister, M. Beller.

Chem. Commun. **2022**, *58*, 8842–8845.

DOI: 10.1039/D2CC02928F.

7.2. List of publications

1. [F. Bourriquen](#), K. Junge, M. Beller. *Synlett* **2022**, in print. DOI: 10.1055/a-1992-6596.
2. [F. Bourriquen](#), J. Hervochon, R. Qu, S. Bartling, N. Rockstroh, K. Junge, C. Fischmeister, M. Beller, *Chem. Commun.* **2022**, 58, 8842–8845.
3. [F. Bourriquen](#), N. Rockstroh, S. Bartling, K. Junge, M. Beller, *Angew. Chem. Int. Ed.* **2022**, 61, e202202423. [Hot Paper]
4. S. Kopf[†], [F. Bourriquen](#)[†], W. Li, H. Neumann, K. Junge, M. Beller, *Chem. Rev.* **2022**, 122, 6634–6718.
5. W. Li, J. Rabeah, [F. Bourriquen](#), D. Yang, C. Kreyenschulte, N. Rockstroh, H. Lund, S. Bartling, A.-E. Surkus, K. Junge, A. Brückner, A. Lei, M. Beller, *Nat. Chem.* **2022**, 14, 334–341.
6. W. Li, R. Qu, W. Liu, [F. Bourriquen](#), S. Bartling, N. Rockstroh, K. Junge, M. Beller, *Chem. Sci.* **2021**, 12, 14033–14038.
7. L. Duarte de Almeida, [F. Bourriquen](#), K. Junge, M. Beller, *Adv. Synth. Catal.* **2021**, 363, 4177–4181.
8. [F. Bourriquen](#), A. Bruneau-Voisine, A. Jeandin, E. Stihle, S. Fantasia, *Chem. - Eur. J.* **2019**, 25, 9006–9011.

[†]contributed equally

7.3. Conference participations

- | | |
|--------------------|---|
| 16 – 19 March 2021 | 54. Jahrestreffen Deutscher Katalytiker, online, no contribution. |
| 24 February 2022 | LIKAT Workshop: Catalytic Hydrogenation of Renewables and Related Molecules, online oral presentation (Catalytic diastereoselective hydrogenation of arenes and pyridines). |
| 19 – 22 April 2022 | 4th International Green Catalysis Symposium, Rennes, France, poster presentation (Non-Noble Metal Nanoparticles for Hydrogen/Isotope Exchange). |
| 27 – 29 June 2022 | 55. Jahrestreffen Deutscher Katalytiker, Weimar, Germany, poster presentation (Non-Noble Metal Nanoparticles for Hydrogen/Isotope Exchange). |



FLORIAN BOURRIQUEN

PhD student with a strong interest in organic chemistry and catalysis

Born 3rd June 1995 in Paris, France

florian.bourriquen@catalysis.de

RESEACH EXPERIENCE

- Rostock, DE** **Leibniz-Institut für Katalyse e. V., Applied Homogeneous Catalysis department**
Jan. 2020 - present *Development and application of new methodologies for hydrogen/deuterium exchange reactions*
PhD Student under the supervision of Prof. Matthias Beller and Dr. Kathrin Junge. Synthesised homogeneous and heterogeneous catalysts and used them for various applications. Optimised the reaction conditions of diverse catalytic systems. Successfully completed research projects that lead to publications in academic journals. Analysed the scientific literature dealing with my main research project and co-authored a review on this topic (deuterium incorporation into organic molecules). Participated full time in a 4-month collaboration between LIKAT and the company Bayer to develop a synthetic process for an industrially relevant building block.
- Vitry-Sur-Seine, FR** **Sanofi, Integrated Drug Discovery department**
Feb. - Aug. 2019 *Synthesis of potential anticancer drug candidates*
Optimised the reaction conditions for the synthesis of building blocks of interest. Delivered and characterised compounds with therapeutic purposes after multi-step syntheses.
- Basel, CH** **F. Hoffmann-La Roche, Process Chemistry & Catalysis department**
Apr. - Aug. 2018 *Amination of chloropyridines with ammonia*
Screened pre-catalysts and optimised reaction conditions for the monoamination of pyridines *via* a cross-coupling reaction employing gaseous ammonia as *N*-coupling partner. Synthesised various amino-chloropyridines *via* a Buchwald-Hartwig reaction. Evaluated the scope and the limitations of this methodology on various substrates.
- Rennes, FR** **Ecole Nationale Supérieure de Chimie, Team Organic Chemistry and Interfaces**
Apr. - Jun. 2017 *Multi-step synthesis of galactofuranosides*
Supplied galactofuranosides with pharmaceutical applications *via* multi-step syntheses involving delective protection and deprotection of hydroxyl groups.
- Rennes, FR** **Institut des Sciences Chimiques de Rennes, Team Organometallics: Materials & Catalysis**
May - Jun. 2016 *Ruthenium complexes catalysis for C-H activation*
Synthesised ligands, zinc and ruthenium complexes and applied them for C-H bond activation.

EDUCATION

Rennes, FR **Université de Rennes 1**
2017 - 2019 *Master's degree in chemistry. High honours*
Specialisation in catalysis and organic chemistry

Rennes, FR **Université de Rennes 1**
2014 - 2017 *Bachelor's degree in chemistry. High honours*

SKILLS

Technical skills

Usual organic synthesis techniques

Development of diverse catalytic reactions and workups along with their monitoring

Synthesis of ligands and air sensitive organometallic complexes under inert atmosphere (Glove box, Schlenk line)

High-pressure reactions with compressed gases and autoclaves

Synthesis of heterogeneous catalysts and nanoparticles

Product analysis using 1D & 2D NMR, gas chromatography, liquid chromatography, mass spectrometry

Product purification with flash chromatography

IT skills

Scientific software including SciFinder, Reaxys, ChemInventory, Chemdraw, ISIS Draw, MestreNova, TopSpin, ACD/Spectrus, Zotero, Endnote

Microsoft Office including Word, Excel and PowerPoint

Communication

Oral communication skills developed by presenting at group seminars, conferences, and industrial board meetings

Written communication in preparing publications and reports for the European Union funding my PhD

Languages

French - Native speaker

English - Full professional proficiency, TOEIC 985/990 (2018)

German & Spanish - Basics, limited professional proficiency

PUBLICATIONS

1. **Bourriquen, F.**; Junge, K.; Beller, M. Homogenous iron-catalysed deuteration of electron-rich arenes and heteroarenes. *Synlett* **2023**, 34, 332-336.
2. **Bourriquen, F.**; Hervochon, J.; Qu, R.; Bartling, S.; Rockstroh, N.; Junge, K.; Fischmeister, C.; Beller, M. Diastereoselective Hydrogenation of Arenes and Pyridines Using Supported Ruthenium Nanoparticles under Mild Conditions. *Chem. Commun.* **2022**, 58, 8842-8845.
3. **Bourriquen, F.**; Rockstroh, N.; Bartling, S.; Junge, K.; Beller, M. Manganese-Catalysed Deuterium Labelling of Anilines and Electron-Rich (Hetero)Arenes. *Angew. Chem. Int. Ed.* **2022**, 61, e202202423. [Hot Paper]
4. Kopf, S.⁺; **Bourriquen, F.**⁺; Li, W.; Neumann, H.; Junge, K.; Beller, M. Recent Developments for the Deuterium and Tritium Labeling of Organic Molecules. *Chem. Rev.* **2022**, 122, 6634-6718.
5. Li, W.; Rabeah, J.; **Bourriquen, F.**; Yang, D.; Kreyenschulte, C.; Rockstroh, N.; Lund, H.; Bartling, S.; Surkus, A.-E.; Junge, K.; Brückner, A.; Lei, A.; Beller, M. Scalable and Selective Deuteration of (Hetero)Arenes. *Nat. Chem.* **2022**, 14, 334-341.
6. Li, W.; Qu, R.; Liu, W.; **Bourriquen, F.**; Bartling, S.; Rockstroh, N.; Junge, K.; Beller, M. Copper-Catalysed Low-Temperature Water-Gas Shift Reaction for Selective Deuteration of Aryl Halides. *Chem. Sci.* **2021**, 12, 14033-14038.
7. Duarte de Almeida, L.; **Bourriquen, F.**; Junge, K.; Beller, M. Catalytic Formal Hydroamination of Allylic Alcohols Using Manganese PNP-Pincer Complexes. *Adv. Synth. Catal.* **2021**, 363, 4177-4181.
8. **Bourriquen, F.**; Bruneau-Voisine, A.; Jeandin, A.; Stihle, E.; Fantasia, S. Streamlined Synthesis of Diaminopyridines by Pd-Catalyzed Ammonia Coupling with Deactivated Amino-Chloropyridines. *Chem. - Eur. J.* **2019**, 25, 9006-9011.

⁺ contributed equally

CONFERENCES

- 27 - 29 Jun. 2022 55. Jahrestreffen Deutscher Katalytiker, Weimar, Germany, poster presentation (Non-Noble Metal Nanoparticles for Hydrogen/Isotope Exchange)
- 19 - 22 Apr. 2022 4th International Green Catalysis Symposium, Rennes, France, poster presentation (Non-Noble Metal Nanoparticles for Hydrogen/Isotope Exchange)
- 24 Feb. 2022 LIKAT Workshop: Catalytic Hydrogenation of Renewables and Related Molecules, online oral presentation (Catalytic diastereoselective hydrogenation of arenes and pyridines)
- 16 - 19 Mar. 2021 54. Jahrestreffen Deutscher Katalytiker, online, no contribution